Investigating the role of *sufT* in *Mycobacterium abscessus* using CRISPRi

By

Nyaradzai Mitchell Chimukuche

Dissertation presented for the degree of Master of Science

Department of Molecular and Cell Biology

Faculty of Science

University of Cape Town

Date: 14 February 2022

Supervisor: Dr. Monique Williams

Acknowledgements

First and foremost, I would like to express my gratitude to the Lord Almighty for providing me with this opportunity.

I want to express my heartfelt gratitude to Dr. Monique Williams for overseeing my postgraduate (MSc) studies from start to finish. Thank you for your time and guidance during my work in the laboratory and during the writing up process. You have made a significant contribution to the research's success, and I truly appreciate you as my supervisor and mentor. I have learnt a lot from you, your patience and work ethic helped me become a better person and scientist.

I would like to thank the Building Research Academic Staff Grant (BRAAS) funding for the financial support.

I am grateful to my loving parents Tracey Chimukuche and Matthew Chimukuche, and my siblings, Rujeko Chimukuche, Clemence Chimukuche, Takudzwa Chimukuche and my Uncle Frank Chidawanyika, for their unwavering support and prayers.

To my amazing friends Desmond and Muki, thank you for your support, you have made this entire process worthwhile for me. I am proud of how far we have come, and I hope we can keep pushing forward.

Declaration

I confirm that the Dissertation submitted for the Master of Science Degree in the Department of Molecular and Cell Biology is my original work and has not been copied from another source (published or unpublished). It has not been submitted for any other university's degree examination.

I used referencing method for citations and references. Every contribution and quotation from other sources have been acknowledged, cited, and referenced in this dissertation.

Nyaradzai Mitchell Chimukuche

Signed by candidate

14/02/2022

Abstract

Mycobacterium abscessus (*M. abscessus*) is a rapidly growing non-tuberculous mycobacterium (NTM) that causes a wide range of infections including pulmonary *M. abscessus* disease. Treatment of *M. abscessus* infections is challenging because the mycobacterium is intrinsically resistant to different classes of antibiotics, including those used to treat tuberculosis. It is important to develop new and effective drugs for *M. abscessus* treatment, therefore acquiring knowledge on the unique vulnerabilities of *M. abscessus* which can be a targeted for future drug design is required.

The clustered routinely interspaced palindromic repeats interference (CRISPRi) system was recently optimized for transcription repression in mycobacteria. This study aimed to investigate the functionality of the mycobacterial CRISPRi in *M. abscessus*, specifically to investigate the role of the *sufT* homologue, *MAB_2744c*, in survival under iron limiting conditions and susceptibility to the metal chelator deferoxamine. To this end, 4 sgRNAs were designed, two targeting *MAB_2744c* (sg2744F1, sg2744F2) and two targeting the upstream gene *2745c* (sg2745F1 and sg2745F2) and used to generate 4 *M. abscessus sufT* knock-down strains (*M. abscessus attB::pLJR962-2744c*-a, *M. abscessus attB::pLJR962-2744c*-b, *M. abscessus attB::pLJR962-2745c*-a and *M. abscessus attB::pLJR962-2745c*-b. The CRISPRi strains all grew under standard conditions, reaching exponential phase between 24 and 48 hours and a maximum OD600 of 8 after 48 hours. Reduced growth for all CRISPR interference strains was observed when comparing iron limiting conditions to iron replete conditions (2 µM), while no difference was observed for any of the strains when comparing growth with and without sgRNA expression. Expression analysis revealed that no transcriptional silencing was achieved in any of the strains, and therefore no conclusions could be made about the role of *sufT* during growth under iron limitation. Similarly, while comparison of biofilm formation under iron limiting and iron replete conditions confirmed that biofilm formation is reduced when iron is limiting, the role of *sufT* in this process could not be investigated using the CRISPRi strains. The importance of iron for the growth of *M. abscessus* was further confirmed by investigating its susceptibility to the metal chelator deferoxamine.

This study demonstrates that the previously described mycobacterial CRISPRi system does not function optimally in *M. abscessus* when a single sgRNA is used and therefore the system requires further optimization for use in this organism.

List of Abbreviations

µg	Microgram(s)
µl	Microlitre(s)
µM	Micromolar
AE	Allelic exchange
AES	Allelic exchange substrate
Amp	Ampicillin
Anti-TNF-a	Anti-tumor necrosis factor alpha
Bp	Base pair(s)
CAF	Central analytical facility
$CaCl_2$	Calcium chloride
CRISPR	Clustered regularly interspaced palindromic repeats
CRISPRi	Clustered regularly interspaced palindromic repeats interference
CRISPR/Cas9	CRISPR– associated protein-9 endonuclease from *Streptococcus*
CFU	Colony forming units
cDNA	Complementary DNA
crRNA	CRISPR RNA
CRISPR-FnCpf1	A *Francissella novicida* Cas12a endonuclease
CT	Cycle Threshold
dCas9Sth1	Deactivated CRISPR-associated protein-9 endonuclease from (*Streptococcus thermophilus*)
DFO	Deferoxamine

DNA	Deoxyribonucleic acid
dNTP	Deoxyribonucleotide triphosphate(s)
dsDNA	Double stranded
DSB	Double stranded break
EDTA	Ethylenediamine tetra-acetic acid
E. coli	*Escherichia coli*
et al.,	et alia (and others)
EtBr	Ethidium bromide
FeS	Iron-sulfur clusters
GC	Guanine-cytosine
g	Gram(s)
x *g*	Times gravity
GPL	Glycopeptidolipid
HR	Homologous recombination
Hr	Hour(s)
HIV	Human immunodeficiency virus
Hyg	Hygromycin
IFN-γ	Interferon-gamma
IL-12	Interleukin-12
IS	Insertion sequences
i.e.	*id est* (that is (to say)

ISC	Iron–sulfur cluster
Kan	Kanamycin
kb	Kilobyte
KH_2PO_4	Potassium phosphate monobasic
LigD	Ligase D
LB	Luria Bertani broth
ml	Millilitre(s)
mM	Millimolar
min	Minute(s)
mRNA	Messenger RNA
M. abscessus	*Mycobacterium abscessus*
MABC	*Mycobacterium abscessus complex*
M. africanum	*Mycobacterium africanum*
M. aurum	*Mycobacterium aurum*
M. avium	*Mycobacterium avium*
MAC	*Mycobacterium avium complex*
MAH	*Mycobacterium avium subsp. hominissuis*
MAP	*Mycobacterium avium subsp. paratuberculosis*
M. bovis	*Mycobacterium bovis*
M. canetti	*Mycobacterium canetti*
M. caprae	*Mycobacterium caprae*

M. chelonae	*Mycobacterium chelonae*
M. fortuitum	*Mycobacterium fortuitum*
M. kansasii	*Mycobacterium kansasii*
M. leprae	*Mycobacterium leprae*
M. lepromatosis	*Mycobacterium lepromatosis*
M. malmoense	*Mycobacterium malmoense*
M. microti	*Mycobacterium microti*
M. mungi	*Mycobacterium mungi*
M. phlei	*Mycobacterium phlei*
M. pinnipedii	*Mycobacterium pinnipedii*
M. smegmatis	*Mycobacterium smegmatis*
M suricattae	*Mycobacterium suricattae*
M. szulgai	*Mycobacterium szulgai*
M. scrofulaceum	*Mycobacterium scrofulaceum*
M. tuberculosis	*Mycobacterium tuberculosis*
MTBC	*Mycobacterium tuberculosis complex*
M. vaccae	*Mycobacterium vaccae*
M. xenopi	*Mycobacterium xenopi*
M. intracellulare	*Mycobacterium intracellulare*
$MgCl_2$	*Magnesium chloride*
mAGP	mycolyl-arabinogalactan-peptidoglycan

MOPS	*3-(N-morpholino) propanesulfonic acid*
NaCl	Sodium Chloride
ND	NanoDrop
Ng	Nanogram(s)
NIF	Nitrogen fixation
Nm	Nanometer
nM	Nanomolar
NHEJ	Non-homologous end joining
NTM	Non-tuberculosis mycobacteria
NTM-PD	Non-tuberculousis mycobacterial pulmonary disease
n/a	Not applicable
OADC	Oleic Albumin Dextrose Catalase
Oligo	Oligonucleotide
ORFs	Open reading frames
ORBIT	Oligonucleotide-mediated recombineering followed by Bxb1 integrase targeting
OD_{600}	Optical density measured at 600 nanometres wavelength
PAM	Protospacer adjacent motif
PCR	Polymerase chain reaction
pH	Potential of hydrogen
qRT-PCR	Quantitative Real time Polymerase Chain Reaction

RbCl	Rubidium chloride
RNA	Ribonucleic acid
rDNA	Ribosomal DNA
RIN	RNA Integrity Number
s	Second (s)
Suc	Sucrose
sgRNA	Single guide RNA
sigA	Gene coding for RNA polymerase sigma factor A (σA)
ssDNA	Single stranded DNA
SufT	Sulfur utilization factor T
SUF	Sulfur utilization factor
SYBR	Synergy Brands Inc
TNF-α	Tumour necrosis factor α
TAE	Tris-acetate EDTA
TAG	Triacylglycerol
TIS	TraDIS-type
tgs	Triacylglycerol synthase
Tn	Transposons
TranscrRNA	Trans-activating crRNA
TrpD	Anthranilate phosphoribosyl transferase

ts-sacB system	Vector with thermo-sensitive origin of replication and the sacB selection marker
U	Units
UCT	University of Cape town
UV	Ultra-violet
V	Volt(s)
XP	5-Bromo-4-chloro-3-indolyl phosphate
zeo	Zeomycin
°C	Degrees celcius
%	Percentage
λ	Lamda
γδ-resolvase/res	Gamma-delta resolvase system
19Ag	19-kilodalton antigen
2-DOG	2-deoxygalactose
Φ	phi

List of Figures

List of Tables

Table of Contents

Chapter 1: Literature Review

1.1 Introduction

NTM are a diverse group of mycobacterial species apart from the *Mycobacterium tuberculosis* complex (MTBC; *Mycobacterium bovis* (*M. bovis*), *Mycobacterium africanum* (*M. africanum*), *Mycobacterium microti* (*M. microti*), *Mycobacterium canetti* (*M. canetti*), *Mycobacterium caprae* (*M. caprae*), *Mycobacterium pinnipedii* (*M. pinnipedii*), *Mycobacterium suricattae* (*M suricattae*) and *Mycobacterium mungi* (*M. mungi*) and organisms causing leprosy *Mycobacterium leprae* (*M. leprae*) and *Mycobacterium lepromatosis* (*M. lepromatosis*) [1]. NTM can be referred to as environmental mycobacteria, atypical mycobacteria and mycobacteria other than tuberculosis [2], [3]. The diversity of NTM vary worldwide and there are approximately 160 known species naturally found in the environment, and most of the NTM are not associated with disease whilst approximately 20 – 30 are clinically relevant. NTMpathogenesis varies extensively with some species being clinically relevant. The clinically relevant pathogens include slow growing bacteria such *as Mycobacterium avium (M. avium) complex, Mycobacterium malmoense* (*M. malmoense*), *Mycobacterium kansasii* (*M. kansasii*) *and Mycobacterium xenopi* (*M. xenopi*) [2] and rapid growing mycobacteria such as *Mycobacterium abscessus* complex (*M. abscessus* complex) (MABC) [2]. Examples of highly pathogenic NTM are *M. malmoense, M. szulgai, M. kansasii, M. abscessus, M.xenopi* and *Mycobacterium avium* (*M. avium*) [2], while *Mycobacterium simiae* (*M.simiae*), *Mycobacterium chelonae* (*M. chelonae*) and *Mycobacterium intracellulare* (*M. intracellulare*) have relatively low pathogenicity [2].

The NTM species most associated with disease are the three subspecies of the *M. abscessus* complex (MABC) (*M. abscessus* subsp. *abscessus*, *M. abscessus* subsp. *massiliense*, and *M. abscessus* subsp. *bolletii*) [4], the 3 major subspecies of the *Mycobacterium avium* complex (MAC) (*M. avium* subsp. *paratuberculosis*, *M. avium* subsp. *avium*, and *M. avium* subsp. *hominissuis*) and *M. intracellulare* [5]. *M. abscessus* has increased in frequency and is becoming difficult to treat. The MAC is predominant in North America and East Asia, whereas in regions within Europe, *M. kansasii*, *M. xenopi*, and *M. malmoense* are more common [3]. The disease-causing

species vary with geographic location such that *M. avium* and *M. abscessus* species are implicated worldwide whereas *M. malmoense* and *M. xenopi* are regionally important [3]. Advances in molecular, microbiological and imaging techniques have extensively enhanced chronic pulmonary infection knowledge [3] but there are still uncertainties about their clinical relevance and epidemiology.

NTM are ubiquitous organisms found in water reservoirs, soil and dust [4], and can enter the body through inhalation as aerosols or fomites [6]. These organisms are known to be resistant to chlorine thus remain persistent in water sources thereby increasing their prevalence. NTM species affect the human body in different ways. The disease severity, treatment, and disease recovery vary widely amongst individuals [4]. The pulmonary disease outcome is highly dependent on various factors such as virulence of organism, organism particle size, amount of exposure the individual had, overall individual health and bacterial genetic background [4].

NTM are opportunistic pathogens that are prevalent in older individuals and notably in individuals that smoke [5]. Individuals with immune deficiency, hereditary lung diseases are also susceptible to NTM. The immuno-suppressive conditions related to NTM pulmonary disease (NTM-PD) include human immunodeficiency virus (HIV), inflammatory disorders and anti-tumor necrosis factor alpha (anti-TNF-a) agents [5]. Chronic pulmonary disease caused by NTM is mostly associated with lung diseases such as cystic fibrosis and bronchiectasis, which can be worsened by co-infection with other bacteria or fungi like *aspergillus* [7] . Macrophages have been found to have a key role in the control pathogenesis of NTM [8] and cytokines;Interleukin-12 (IL-12), tumour necrosis factor α (TNF-α), and interferon-gamma (IFN-γ) are vital in the anti-mycobacterial regulation and immune response [8]. Any defect in these cytokine pathways increases the susceptibility to NTM [8].

NTM pulmonary disease (NTM-PD) epidemiology is affected by two major factors. First, NTM-PD is a condition that is not reportable in most countries [9], the burden, trend, and risk of acquiring NTM-PD is highly dependent on several studies and surveys [9]. Secondly, the use of uncontaminated clinical specimens for the isolation of NTM-PD is not enough to diagnose the disease, because patients may have respiratory secretions

colonized with NTM but not show any symptoms. This is why clinical information and microbiological data are required together to determine disease certainty in an individual [9]. Recently, relying on microbiological data alone has been shown to give reasonable approximation. There is insufficient evidence on disease distinctness and usually the disease reports are not stated [9].

The diagnostic criteria that have been established for NTM comprise microbiological, radiographic, and clinical criteria [9], [2]. The criteria require symptomatic patients to seek medical health care and diagnosis requires more than one positive sputum, or one positive bronchial wash or lavage, or lung biopsy with mycobacterial histopathology and one positive culture. NTM-PD is slowly progressive and chronic [4], and the limitation is that some patients may have a problem in producing sputum samples. Radiography imaging should be done using chest radiography or a high-resolution computed tomography scan. Two positive sputum cultures and bronchial wash are used in mycobacterial criteria, as are mycobacterial histological findings such as positive acid-fast bacilli lung biopsy, granulomatous inflammation, positive lung biopsy culture, and multiple positive sputum cultures and bronchial wash [10]. NTM cannot be visualized on Gram stain and either the Ziehl-Neelsen (ZN) staining (acid fast bacilli) or auramine staining is used [2]. Because multidrug-resistant tuberculosis is so severe, getting an accurate diagnosis is crucial. It is a major error to mistake people with NTM for people with multidrug-resistant tuberculosis [11]. However, all mycobacteria are acid-fast; many environmental species cause lung disease that is often indistinguishable from tuberculosis; tuberculosis is diagnosed by the clinical presentation and laboratory findings of sputum smear microscopy in countries with a high prevalence [11]. Disease caused by NTM does not usually respond to anti-tuberculous medication. One study discovered that individuals diagnosed with multidrug-resistant tuberculosis frequently had infections with environmental mycobacteria; 30% of suspected multi drug resistant tuberculosis patients really had NTM, and 27% fit the current ATS/IDSA criteria for NTM illness [11]. *M. kansasii* and *M. abscessus* were the major organisms. NTM diseases have clinical and radiological characteristics that are comparable to tuberculosis.

Underlying pulmonary disease, immunosuppression, organ transplantation, HIV infection, and advanced age are all risk factors for NTM patients. Expert consultation is often required for diagnosis and suspected NTM lung disease patients should be followed until the diagnosis is fully established [11], [12], [13].

Genetic manipulation of bacteria is important because it provides insights into the pathogenesis of infectious agents and facilitates the development of new drugs and vaccines. These techniques increase our understanding of the mechanisms implicated in virulence, cellular growth, metabolism anti-mycobacterial drug action and resistance, and provided clues for new vaccine development, such as generation of potential recombinant live vaccines [14]. There are several genetic engineering approaches for the mycobacterial genus that have been developed. The techniques canfunction by mutation, insertion and deletion of genes in the mycobacterial genome for thegeneration of mutants [14]. This chapter will review these techniques and their applicationto NTM.

1.2 Methods for delivery of deoxyribonucleic acid (DNA) into mycobacterial cells

The delivery of DNA into mycobacterial cells is the critical first step for all genetic manipulation techniques. Mycobacteria have cell envelopes that are complex [15]. The multi-layered cell envelope consists of a phospholipid bilayer forming the plasma membrane, a peptidoglycan layer, an outer myco-membrane and a capsule, providing structure, rigidity and osmotic stability. Within the cell envelope structure, the mycolyl-arabinogalactan-peptidoglycan (mAGP) complex contributes to the integrity of the cell wall and is essential for the viability of cells. It consists of a myco-membrane, that includes mycolic acids, arabinogalactan and peptidoglycan [16]. Peptidoglycan is a macromolecular structure that has a backbone of glycan and the complex structure consists of β (1,4)-connected N-acetylglucosamine and N-acetylmuramic acid links .The *N*-acetylmuramic acid can be oxidized to form *N*-glycolyl-muramic acid and this increases the peptidoglycan strength through hydrogen bond formation. N-acetylmuramic acid is important in the growth of cells, communication between cells and initiation of host response.

The arabinogalactan is a polysaccharide that is highly branched, mainly consisting of galactose and arabinose residues in the furanose ring form. Arabinogalactan links peptidoglycan with the mycolic acid layer via a phosphodiester bond. The galactan component has an alternating linear chain of about 30 β(1-5) and β (1-6) Gal*f* residues; these are linked via a C-5 β (1-6) linkage to the strongly branched arabinose chains. Mycolic acids, 2-alkyl, 3-hydroxy long-chain fatty acids, are characteristic of the cell envelope of mycobacteria [17]. They can be found either unbound or esterifying the terminal penta-arabinofuranosyl components of arabinogalactan. The different forms of mycolic acid are presumed to have a key role in the cell envelope's structure and impermeability, as they are involved in myco-membrane function and structure [17]. They also contribute to the permeability and fluidity of cell wall. Due to the thick layer of mycolic acids in mycobacterial cell walls, mycobacteria are very difficult to transform [17]. In mycobacteria, transformation is a natural method of DNA uptake, but not all the mycobacterial species are naturally competent [18]. Due to these drawbacks, inducing artificial competence has become the widely used method to transform mycobacteria.

The two main methods used for mycobacterial transformation are electroporation and transduction.

1.2.1 Electroporation

Electroporation is a method of subjecting living cells to a brief high electrical impulse to increase cell membrane permeabilization [19]. The mechanical method is affected by washing cells before electroporation, cell number, DNA amount and cell growth phase [20]. It was previously demonstrated that the electroporation efficiency of *Escherichia coli* (*E. coli*) DH10B was improved by pre-washing the cells with glycerol, which enhances cell resistance ensuring minimal level of conductivity [21]. When compared to *E.coli*, the wild type *M. smegmatis* (mc²155) had a limited capability of being transformed by electroporation whereby 6 independent experiments yielded 1-10 kanamycin resistant transformants per 1 µg of DNA, with an electroporation efficiency of <10 colony forming units (CFU) / µg of DNA [22]. To overcome this, the authors isolated and characterized *M. smegmatis* (mc²155, mc²230, mc²235) mutants that could easily be transformed by electroporation. These yielded 10^4 to 10^5 transformants/ µg of DNA with electroporation efficiencies of 10^4 to 10^5 higher than the wild type [18], with the mc²155 strain displaying the greatest transformation efficiency of $> 10^5$ colonies / µg of DNA [22]**.**

In one study, authors compared the electroporation efficiencies of *M. smegmatis* (mc²155) with *MAP* (ATCC19698, K-10 and S-23) and *M. avium* complex strains. They showed that *M. avium* (mc²76 and 8627-86) had an efficiency of 1×10^4 CFU / µg of DNA and 2.1×10^4 CFU / µg of DNA respectively, which is 10 to 50-fold higher than *MAP* and other *M. avium* strains [23]. *M. smegmatis* (mc²155) had an electroporation efficiency of 3.1×10^5 CFU / µg of DNA which is 10-fold higher than the *M. avium* (mc²76 and 8627-86) strains, suggesting that the *M. smegmatis* (mc²155) mutant has a more permeable cell wall compared to *M. avium* and *MAP* strains [23]. Also, the transformation efficiency was found to be largely determined by host strain properties rather than the plasmid DNA used. In addition, the *M. avium* complex strains were found to contain indigenous plasmids, that were suspected to decrease efficiency by mechanisms of incompatibility, replication competition and partitioning [24].

In a different study, electroporation of 11 *M. avium* strains resulted in transformation of 4

M. avium (A5, 920A-6, 927A-46 and 950A-48) strains, with *M. avium* (A5) displaying a high transformation efficiency of 10^5 transformants per µg of DNA [20]. The *M. avium* (A5 and 920A-6) strains both had an electroporation efficiency of 1-8 × 10^3 CFU / µg of DNA [20]. This suggests that *M. avium* complex strains vary in their cell wall composition therefore explaining the different efficiencies obtained by the different strains.

Interestingly, the electroporation of *M. smegmatis* (mc^2155) and *M. intracellulare* (96 and 613) at different temperatures yielded different transformation efficiencies [19]. *M. smegmatis* had the highest transformation efficiency at 0 degrees celsius (°C) with 10^4 CFU / µg of DNA whilst *M. intracellulare* had a transformation efficiency < 10 CFU / µg of DNA. A 50-fold drop in efficiency of 10^2 CFU / µg of DNA was observed at 37 °C in *M. smegmatis*, whereas for *M. intracellulare* it was 10^3 CFU / µg of DNA, increasing markedly with an increase in temperature. This suggests that a temperature increase alters the cell wall of fast-growing mycobacteria *M. smegmatis* therefore increasing permeability [19].

Addition of compounds to growth media or wash solutions can also impact electroporation efficiency. A 2-4-fold increase in transformation efficiency was observed following pretreatment with glycine [19]. In a study of optimizing *M. avium* electroporation conditions, the authors found out that an 18-hour pretreatment of mycobacteria with glycine during the final growth stage resulted in a 41000-fold increase in transformation frequency, and a 48-hour pretreatment resulted in a 44000-fold increase [20]. This implies that the increase in transformation efficiency was caused by reduction of viable bacteria in relation to the time of glycine treatment [19]. The authors also observed that there was a (734-fold) increase in transformation frequency as plasmid DNA amount increased from 1.5 to 3 µg. A further 6.4-fold rise was obtained by doubling the DNA quantity to 6 µg [20]. *M. avium* strain A5 had a plasmid DNA electroporation efficiency of 10^5 per µg usinga vector generated from *M. avium* plasmid pLR7, under the same electroporationconditions as used in *M. smegmatis* protocol. In *M. abscessus*, the electroporation efficiency increased to 2-5 × 10^4 CFU / µg of DNA, by increasing the plasmid DNA concentration from 1 to 10 µg [25], the addition of oleic albumin dextrose catalase (OADC) and tyloxapol supplements to the Sauton's growth medium, as well as increasing the number of cell washes [25]. Similarly, in *M. aurum* optimizing the glycine, sucrose and plasmid DNA concentration parameters led to an increase in the electroporation efficiency[26].

1.2.2 Specialized transduction

The transfer of DNA into mycobacteria by a mycobacteriophage is referred to as transduction. The use of mycobacteriophages to transform mycobacterial cells has been exploited for efficient DNA delivery. The formation of 'shuttle phasmids', consisting of an *E. coli*-mycobacterial shuttle cosmid and the essential regions of the genome of a mycobacteriophage, facilitates manipulation and amplification of DNA in *E. coli* and effective mycobacterial transformation through transduction. Furthermore, mycobacteriophages D29 and TM4 have been used to create conditionally replicating shuttle phasmids that are thermosensitive and thus permit replication in mycobacteria at 30 °C but restrict replication at 37 °C [27]. The ability to prevent replication facilitates subsequent mutagenesis via transposons or allelic exchange.

The specialized transduction of *M. avium* (mc 2501 and mc 2500) using a temperature sensitive derivative of TM4 (phAE87) found that transformation could be achieved, but that it was 2 orders of magnitude lower when compared to *M. bovis* [28]. In *M. avium* subsp. *hominissuis* (MAH) [29], seven clinical isolates were screened and transduced by the phagemid MycoMarT7, which contained the Himar1 transposon inserted with a kanamycin selectable marker [29]. The transduction efficiency was very high especially in the strain MAH 11, whose transformation was 100-fold more susceptible to plasmid transformation by specialized transduction than the MAH 104 strain [29]. This suggests that the MAH 11 strain has a more penetrable cell wall and most probably the different cell wall compositions could have made it more susceptible to transformation by transduction.

Investigation of *M. avium* subsp. *paratuberculosis* (K10 and K10- green fluorescent protein (gfp)) strains transduction efficiency used 2 methods [30]. In method A, strains were cultured to an optical density of 0.6 at 600 nm (OD_{600}), centrifuged at 12 000 x g and the pellet was re-suspended in broth medium without tween 80, then incubated in the

MP buffer at 37 °C. They observed a transduction efficiency between 0 - 2.3 % for both *M. avium subsp. paratuberculosis* (K10 and K10-gfp) strains [30]. In contrast, when the authors used method B in the transduction of the strains, they reduced bacterial clumps by gravity sedimentation cycles and low speed centrifugation [30]. The (K10 and K10-gfp) strains were cultured to an OD_{600} of 0.6 then vigorously shaken and sedimented [30]. The hygromycin concentration was increased to 75 µg/ ml for selection. *M. avium* (K10) transduction efficiency of 1.1×10^{-8}, 11×10^{-7} and 2.9×10^{-7} in was achieved 3 independent transductions [30], whilst the *M. avium* (K10-gfp) transduction efficiency was 2×10^{-7}, 1.8×10^{-7} and 1.7×10^{-7}. Comparison with the first method showed that the transduction frequency had increased from (0 - 2.3 to 78 - 96 %) [30]. This suggests that the improvements increased the dispersion of bacterial cells, thereby increasing the selection by antibiotics.

The transformation of fast-growing *M. phlei, M. smegmatis, M. aurum, M. fortuitum, M. chelonae,* and *M. vaccae* using D29 phage derivatives yielded 3 *M. smegmatis* strains and 1 *M. phlei* ($mc^2$19) strain that were efficiently transduced [31]. phAE78 had transformation efficiencies of 10^6 CFU/ µl in $mc^2$155 compared to phAE70 [32], and authors observed that phAE77 and phAE94 did not transform all the strains, whilst TM4 derivative PH101 had a reversion frequency of 10^7 CFU/ µl in *M. smegmatis* at 37 °C. This study showed that different phages have different transformation efficiencies within a species [32].

In addition, the *M. smegmatis* and *MAP* (ATCC 19698, K-10 and S-23) strains had plaques/ ml efficiencies of 9×10^1, 7×10^1 and 6×10^1 respectively [23]. ThephA6O had reduced plaque efficiency with ATCC 19698 strain but had varied efficienciesof 4×10^8 and 3×10^5 with K-10 and S-23 strains [23]. The TM4 achieved a transformationefficiency 1000-fold lower in *MAP* than in *M. smegmatis* ($mc^2$155), indicating that *MAP* has much lower transduction efficiency [23]. This studysuggests that different phages transduce different mycobacteria differently. In *M. scrofulaceum, M. marinum, M. avium* (701, 702 and 3746/02) strains they tested the transduction efficiency using a group of similar phages (cluster) phages [31]. TM4 could not transform *M. scrofulaceum* and *M. avium* (701, 702, 3746 /02) strains, however it could effectively transform *M. bovis* 5 to 6 magnitudes less than *M. smegmatis* [31]. D29achieved transformation of *M. scrofulaceum* at different

host efficiencies.

1.3 Mutagenesis methods for mycobacteria

Site specific mutagenesis is a process used to change a gene or DNA sequence at a targeted position to create point mutations, insertions and deletions. Various methods have been developed to undertake this process in mycobacteria and these are discussed below.

1.3.1 Targeted mutagenesis by one-step and-two-step allelic exchange using vectors.

Allelic exchange mutagenesis is a technique that allows the replacement of a specific region of DNA by a similar piece of DNA using the cellular process of homologous recombination [33]. The initial mutagenesis systems used one-step allelic exchange (AE). In one-step allelic exchange, suicide vectors with no origin of replication or conditionally replicating vectors are used. Vectors contain flanking sequences of gene locus to be deleted separated by an antibiotic resistance marker [14]. Antibiotic selection follows the transformation of a host bacterial cell with a suicide vector, and thebacteria will only survive if homologous recombination with the host chromosome occurs. A double cross-over between the homologous region of the mycobacterial genome and the allelic exchange substrate results in the replacement of the original gene with the antibiotic resistance marker and the formation of a marked mutant [14]. Intwo-step allelic exchange, the allelic exchange substrates also contain a counter selection marker. In the first step of the process, positive selection is used to select clones that have undergone a single cross-over event between a region of mycobacterial genome and the homologous region on the suicide vector, resulting in integration of the suicide vector into the host genome [14]. In the second step, the second cross-over event is selected for using a negative selection marker, such as the *sacB* gene, which induces sucrose sensitivity. This step removes the integrated vector backbone, therefore creating a wildtype strain or an unmarked mutant strain, in which the region of the chromosome is replaced by the homologous region (harboring thedesired mutation) that was originally present on the plasmid [14].

1.3.2 One-step allelic exchange

Selective gene disruption enables the study of specific genes and has improved our understanding of mycobacterial virulence. Specialized transduction was initially used in fast and slow growing mycobacteria, namely *M. smegmatis*, *M. bovis* and *M. tuberculosis,* for thegeneration of AE mutants through delivery of homologous DNA substrates [33]. This study used conditionally replicating thermo-sensitive mycobacteriophages that allow replication at 30 ºC but do not replicate at non-permissive temperature of 37 ºC. The authors observed an efficient substrate delivery to nearly all recipient cells at 30 ºC by transduction, and subsequent incubation at 37 ºC to facilitate the generation of isogenic auxotrophic strains by one-step allelic exchange. This transduction protocol has been adapted and applied in *M. smegmatis, M. avium* and *M. abscessus*. In *M*. *smegmatis,* using constructs targeting *lysA* and *panC* yielded 95% hygromycin (hyg) resistant mutants that were lysine auxotrophs. The homologous DNA substrates were introduced into the mycobacterial cells via transduction, and the recombination frequency was around 10^{-6}, similar to those produced from electroporation of mc²155 [33], therefore the transduction protocol was effective for gene replacement. In a different study, investigation of functions of *relA, pknG* and the *lsr2* genes *M. smegmatis* using specialized transduction, an allelic exchange efficiencies of 90 – 100 % were achieved [30].

Specialised transduction was used to deliver an AE substrate targeting the *leuD* gene, with hygromycin selection marker, to transparent and opaque *M. avium* clinical strains (mc22500 and 22501) [28]. Screening for leucine auxotrophy revealed 200 colonies with spontaneous hygromycin resistance and only 1 opaque *M. avium* (mgm93) with a successful allelic exchange, suggesting that there was a chance of allelic exchange in *M. avium*, but at very low efficiency [28]. To overcome the high rate of spontaneous antibiotic resistance, the authors used the *M. avium* leucine auxotroph (Δ*leuD*) strain as a genetic manipulation host with the *Streptomyces ceolicolor leuD* as the selection marker on the AE substrate. This produced 7 leucine prototrophs [5], and southern hybridization screening revealed that 4 of the 7 leucine prototrophs contained the desired *pcaA* locus disruption.

The remaining 3 leucine prototrophs were illegitimate recombinants as demonstrated by the existence of the wild type *pcaA* locus and random integration of theconstruct on the

chromosome DNA. These findings suggest that allelic exchange is feasible in *M. avium* when not limited by spontaneous antibiotic resistance.

Evaluation of specialized transduction and allelic exchange in *M*. *avium* subsp *paratuberculosis* (K10) using a hygromycin selection marker, revealed that it was extremely difficult to disrupt genes in this strain. A high rate of spontaneous hygromycin resistance was shown by screening 300 of the 1000 transformants; a 0 - 2.3% allelic exchange efficiency for 7 *pknG* mutations was observed and none for *relA* in both the K10 and K10 - gfp strains [7]. In comparison to *relA*, which was smaller (873bp), the *pknG* mutant was proposed to have undergone AE replacement because the insertion size was comparable to the deletion size (1,915 bp vs. 1,737 bp). Therefore, a phage containing an AE substrate designed for *relA* (1737) deletion was used to determine the effect of insertion and deletion sizes on recombination at different loci. No mutants were identified after screening of the 150 colonies suggesting, that deletion size was not a limitation in this case, and therefore appears to be affected by the locus itself [30]. The authors altered the system to enhance allelic exchange efficiency. They hypothesized that the low AE efficiency was partly caused by aggregation of the cells and therefore decreased probability of plating clumped bacteria by repeated gravity sedimentations and centrifugation and increasing the hygromycin concentration from 50 to 75 µg/ ml [30]. This improved the efficiency of AE with a 10-fold increase (78 % - 100 %) observed [30].The K10 - gfp strain expresses gfp and allows simple tracking of mutants in assays, such as macrophage infections [30]. Mutants from wild-type K10 and K10 - gfp strains were similar, and therefore the K10 - gfp strain can be used in phenotyping of the mutants [30].

A subsequent study of *MAP* (K10) demonstrated one-step allelic exchangeusing phAE87 mediated transduction and a kanamycin selection marker [34]. The AE substrate targeted the mce4 operon and 3 separate transduction experiments yielded 50 kanamycin resistant colonies [34]. Analysis of 15 colonies showed increased resistance to kanamycin, with only 3 colonies undergoing allelic exchange. In this study, the difficulty of in-vitro packaging for recombinant mycobacteriophage was overcome by the implementation of an optimized method to incorporate the allelic exchange substrate (AES) into the phAE87 phasmid [34]. The linear *mce4* substrate is electroporated into the *E. coli* (DY380) strain, containing inducible lamda (λ) recombination genes and

circularized phAE87 DNA. Antibiotic selection facilitates the isolation of the recombinant *mce4* - phAE87 phasmid without the need for multiple cloning steps.

One approach to overcome high spontaneous antibiotic resistance during selection is to use markers in combination. A system that combined fluorescent and antibiotic selection to target *mmpL4a*, a gene involved in glycopeptidolipid (GPL) biosynthesis, was employed in the *M. abscessus* (CIP104526) strain using 1500, 500 and 100 bp of homologous DNA [25]. Gene disruption was facilitated by the vectors expressing fluorescence proteins (td tomato and mWasabi) under the control of an acetamidase promoter, because the fluorescence proteins would permit filtering out a large population of spontaneous antibiotic resistant mutants [25]. The *M. abscessus* colonies had high spontaneous antibiotic resistance, identified by colonies that were not fluorescent [25]. The plasmid transformation efficiency was 1.45×10^4 CFU/ µg DNA. The roughphenotype resulting from loss of GPL was observed in 100 % of the red fluorescent colonies suggesting that most of the red fluorescent colonies observed were a result of plasmid uptake into the *M. abscessus* chromosome via homologous recombination [25]. The number of red fluorescent colonies resulting from the 1 500 bp substrate was much higher than of the 500 bp substrate, and no red fluorescent colonies were obtained for the 100 bp AES, indicating that large fragments are more prone to homologous recombination. Double homologous recombination events between the plasmid and host chromosome *mmpL4a* locus were confirmed by polymerase chain reaction (PCR screening) [25]. The wasabi protein was also used for selection, and it yielded comparable results.

The authors of another study on *M. chelonae* investigated transformation efficiency and using various antibiotic selection markers (gen, zeo, and kan) [35]. The plasmids pOMK-zeo and pJV53-xylE conferring resistance to zeo and kan respectively, were used to transform *M. chelonae* ATCC 35752 and *M. chelonae* 9917 [35]. Furthermore, other pPR27- derived plasmids were used to carry zeo or kan-disrupted alleles of the porin genes. *M. chelonae* ATCC 35752 transformation efficiencies were two orders of magnitude higher with pOMK-zeo than what was previously observed with *M. abscessus* ATCC 19977 (previously reported transformation efficiency of 10^3 transformants / µg of DNA [36]), and significantly higher (400-fold) with pOMKzeo and pJV53-xylE than with

the pPR27-derived constructs [35]. The 9917 strain had transformation efficiencies that were 70 to 500-fold lower than the ATCC 35752 strain, indicating that different *M. chelonae* strains have significant variations in transformation efficiency [35]. The *M. chelonae* transformants with xylE-containing plasmids (pJV53-xylE; pPR27-derived plasmids) all stained yellow with catechol spraying, however, depending on the plasmid used, the transformations exhibited variable selection efficiency for the kanamycin cassette [35]. Kanamycin selection was efficient in *M. abscessus* ATCC 19977, *M. chelonae* ATCC 35752 and *M. chelonae* 9917 using pOMK-zeo and pJV53-xylE with 56 to 100 % kanamycin resistant colonies had the plasmid [35]. The pPR27-derived plasmids had less than 1 % CFUs. The findings show that *M. chelonae* transformation efficiencies vary depending on the strain and the plasmid transformed and are approximately 100 times higher than *M. abscessus* ATCC 19977 [35].

Site specific mutagenesis was initially demonstrated in *M. intacellulare* (1403) avirulent strain in a study that determined the role of 19-kilodalton antigen (19Ag) in virulence by utilizing suicide vector approach [36]. In the previous model system designed to test allelic exchange efficiency, a chromosomally integrated *aacC1* gene (encoding gentamicin resistance) was replaced by a suicide vector carrying an *aacC1* allele disrupted by a kanamycin resistance cassette. PCR analysis revealed 2 *M. intacellulare* (1403) derivatives with complete AE replacement of the *aacC1* gene. In the disruption of 19Ag, a gentamycin cassette was used for selection and *M. intacellulare* (1403) electroporation using 1 µg of the suicide vector (p19K5) yielded 12 gentamycin resistant isolates. In addition, the authors performed another 4 similar transformations and they yielded 8 - 15 transformants per electroporation [36]. PCR screening revealed that 11 out of the 12 gentamycin-resistant transformants were single step crossovers or had undergone illegitimate recombination, while the remaining transformant had undergone allelic exchange replacement [36]. In the mouse-virulent strain D673, an isogenic 19Ag mutant could not be generated by AE, and therefore a chemically mutagenized *M*. *intracellulare* (FM1) strain, which is a derivative of D673 was used. In comparison tothe D673 parental strain, which had a clear and smooth colony morphology, FM1 had a stable flat and crenate morphology. FM1 was highly susceptibility to antibiotics and could be easily transformed, with 29 gentamycin resistant transformants observed from a single

electroporation of FM1 strain with 2 µg of the allelic exchange substrate. Of these transformants, 2 had PCR amplification characteristic of a 19Ag mutant [36]. Low transformation efficiency is therefore a major limitation in generating mutants by one-step allelic exchange.

Another limitation of one-step allelic exchange is that mutants are marked, which can have polar effects and limit downstream genetic manipulation due to the limited number of marker genes available. In mycobacteria, several site-specific recombination systems have been used to allow the removal of antibiotic resistance cassette following one-step allelic exchange, including: the gamma-delta resolvase (γδ - resolvase/ res) [33], [37], the Cre/ *loxP* [38], the *Xer/ dif* or the *FlpE/ FRT* system [39]. The recombination sites are direct repeats and placing the marker sequence between the repeats allows removal in one-step after site-specific recombination [39]. A study in *M. smegmatis* (mc²155) demonstrated the successful removal of a hygromycin cassette flanked with (res) sites specific for resolvase *cd*- TnpR. When a resolvase gene (*tnpR*) is supplied by a plasmid and transiently expressed in the host mutant strain, the product of site-specific recombination between res sites is a precise removal of the hygromycin gene cassette, unmarking the deletion [33]. Following TnpR expression, 20 - 30 kanamycin resistant colonies were observed, and these were screened for hyg sensitivity. Using Southern blot analysis, the hygromycin-sensitive colonies were further screened for loss of the hygromycin cassette, and they showed that the gene had been deleted [33]. In another study of *M. smegmatis*, the *Flp/ FRT* system was used in creating unmarked deletions using a plasmid with selectable *rpsL* gene and a *FRT*- hyg -*FRT* cassette [40].

1.3.3 Two-step allelic exchange

Two-step allelic exchange process is efficient because it does not require heterologous recombinases to insert or excise selection markers from the target chromosome. Instead,

suicide vector properties and host cell proteins are the only things that allow positive and negative selection to occur. Mutant alleles flanked with homologous regions are created in vitro and then cloned into allelic exchange vectors. Following transformation of the recipient cells, antibiotic-resistant single-crossover mutants emerge via homologous recombination. Two-step allelic exchange is efficient because it uses counter-selection (usually sucrase-mediated) to isolate unmarked double-crossover mutants directly.It produces alterations that are seamless and accurate to a single base pair of DNA.

In *M. avium* (104), two-step allelic exchange was used to inactivate methyl-transferase D (*mtfD*) using the antibiotic selection marker kanamycin (kan). The plasmid contained the counter-selection markers, *sacB*, that confers sucrose susceptibility when expressed by mycobacteria, and a temperature-sensitive mycobacterial replication origin, that is non-functional at a 39 °C [41]. *M. avium* (104) electroporation with the pPR27:*mtfD:*Kan vector and selection on kanamycin-containing medium at 32 ºC resulted in a single crossover event. PCR analysis revealed only 2 out of 10 kanamycin resistant *M. avium* (104) possessed the plasmid, indicating a high rate of spontaneous kanamycin resistance [41]. *M. avium* (104) selection at 39 ºC and in sucrose medium revealed that the second crossover event had occurred in 8 % (4 out of 50) of the colonies. Most of the remaining clones had illegitimate recombination, lost the positive selection marker and had simple background due to loss of counter-selection [41].

In *M. avium* (920A6) strain the authors deleted the rhamnosyl-transferase (*rtfA*) gene [42], by combining hygromycin selection marker and the *xylE* marker to differentiate recombinants from spontaneous mutants. Catechol spraying of transformants harboring *xylE* plasmids resulted in yellow staining revealing that *xylE* is an acceptable marker. *M. avium* (920A6) electroporation yielded 25 – 40 % yellow colonies upon catechol spraying, indicating high spontaneous hygromycin resistance and a transformation efficiency of 1-8 × 10^2 transformants per µg of DNA [42]. Selection of *M. avium* (920A6) at 39 °C, to prevent plasmid replication, and on sucrose medium, to select for the second cross-over event, [42], resulted in a high background of *xylE*-positive and sucrose-resistant colonies. This suggests either a high frequency of illegitimate recombination, single crossover events, an increase in *sacB* spontaneous mutation or the inability of *sacB* to provide

effective counter selection. Hygromycin resistant colonies that lost plasmid DNA, ie. the double crossover mutants, were reflected by *xylE*-negative colonies. Further screening of the 10^4 colonies yielded only one isolate with complete AE of the *rtfA* gene [42].

A recent evaluation of two-step allelic exchange in the generation of unmarked alleles was done in *M. abscessus* (*MAB_2875* and *MAB_2833*) [43], similar to the prior work in *M. smegmatis* and *M. avium*. The authors used *galK,* which encodes a galactokinase, as the counter selection marker. This is because in previous studies, *sacB* could not function in *M. abcessus*. The authors also found it difficult to use the counterselection marker (*rspl*) gene which confers streptomycin susceptibility [44], due to the high level of intrinsic resistance and large streptomycin doses required [44]. Electroporation of *M. abscessus* with *galK* vectors yielded primary recombinants that were kanamycin resistant and sensitive to 2-deoxygalactose (2-DOG). Screening of 64 kanamycin resistant mutants revealed 2 that were 2-DOG susceptible. Subsequent culture and selection of one of the susceptible clones on 2-DOG yielded 2-DOG resistant clones with a 6×10^{-5} mutation frequency. Of the 2-DOG resistant clones, 90 % were susceptible to kanamycin, which represents true double cross-over AE mutants [43].

A vector consisting of a temperature sensitive mycobacterial origin of replication and sacB gene (ts- sacB) system was successfully applied in *M. chelonae* ATCC 35752, having a counterselection efficiency of 3.38×10^{-4}. The counter selection at 37 °C and in sucrose media was effective in reducing the frequency of CFU by 3-4 orders of magnitude, however 10 times less effective than in *M. smegmatis*, and when compared to *M. abscessus* the ts- sacB was not effective due to lack of sacB counterselection [35][31]. Transformation of the knock-out transformants (T1, T2 and T3) revealed 3-8 double crossover mutants that had undergone complete AE. For example, 50 - 100 % sucrose and zeo resistant *xylE* mutants$^-$ isolated on the last step of selection were most probably from kanamycin resistant clones that emerged in the various culturing steps [35]. The authors conclude that genes in *M. chelonae* can be inactivated by both ts-sacB and recombineering systems if appropriate antibiotic selection markers are used and zeo was more efficient in both systems [35].

Application of the ts-sacB system revealed *M. smegmatis* to have a counterselection

efficiency of 6 × 10^{-5} whilst *M. abscessus* had 0, suggesting that either *sacB* or the temperature sensitive origin of replication (ori-ts) are not functional in *M. abscessus*. The authors revealed that when using the ts-sacB, *M. smegmatis* had 100 % allelic exchange efficiency compared to *M. abscessus* which had no AE efficiency [45]. The use of the specialized transduction system to disrupt *mmpL4b* in *M. abscessus* (CIP104536T) was significantly less efficient, 100 ng linear DNA yielded a mean of 50 transductants in both *M. abscessus* and *M. smegmatis* however, none had undergone allelic exchange in contrast to *M. smegmatis* which had a 100 % AE efficiency [45].

Table 1: Summary of the one- and two-step allelic exchange systems applied in mycobacteria (slow- and fast growing).

Mycobacterial species	**DNA delivery method**	**Target gene(s)**	**Allelic exchange substrate**	**Positive selection markers**	**Negati ve selection markers**	**References**
One-step Allelic Exchange						
M. intracellulare (TMC1403, D673, FM1)	Electroporation	*19Ag*	Suicide vector	Gm^r	n/a	[36]
M.avium subsp. paratuberculosis (K10, K10-GFP)	Transduction	*relA, pknG lsr2*	Phasmid derived from pHAE87	Km^r Hyg^r	n/a	[30]
M.avium subsp. paratuberculosis (K10)	Transduction	*mce4*	Phasmid derived from pHAE87	Km^r	n/a	[34]
M. abscessus subsp. abscessus (CIP104526)	Electroporation	*mmpL4a mmpS4*	Suicide vector	Km^r mWasabi tdTomato	n/a	[25]
M. avium (JCM34) (Leucine auxotroph)	Transduction	*pcaA*	Phasmid derived from pHAE87	Hyg^r leuD	n/a	[28]

Mycobacterial species	DNA delivery method	Target gene(s)	Allelic exchange substrate	Positive selection markers	Negative selection markers	References
Two-step Allelic Exchange						
M. avium (920A6)	Electroporation	*rtfA*	Conditionally replicating vector (ts-oriM)	Hyg^r xylE	sacB	[42]
M. avium (104)	Electroporation	*mtfD*	Conditionally replicating vector (ts-oriM)	Km^r	sacB	[41]
M. chelonae (ATCC 35752)	Electroporation	*MCH_4689c MCH_4690c MCH_4691c*	Conditionally replicating Vector (ts-oriM)	Km^r or Zeo^r xylE	sacB	[35]
M. marinum	Electroporation	*esxB-esxA*	Suicide vector	Hyg^r lacZ	sacB	[46]
M. abscessus (ATCC19977)	Electroporation	*MAB_435 [aac(2')]*	Suicide vector	Apr^r	katG	[47]
M. abscessus (ATCC19977)	Electroporation	*mmpL4b mbtH MAB_2875 MAB_2833*	Suicide vector	Km^r lacZ	galK	[43]

The table shows a summary of the studies done using one step and two-step allelic exchange systems in fast and slow growing mycobacteria. It shows the targeted genes, positive and negative selection markers (Kanamycin abbreviated as “km”, and zeomycin abbreviated as “zeo” and hygromycin abbreviated as “hyg”. The references are also indicated in the table.

1.3.4 Double and single-stranded DNA recombineering

Recombineering is an in vivo homologous recombination process that involves the introduction of linear DNA substrates, either as double stranded (dsDNA) or single stranded DNA (ssDNA) oligonucleotides into cells that are expressing bacteriophage encoded recombination enzymes [48]. The DNA substrates contain the desired deleted or mutated genes flanked with homologous regions of the target gene [48]. Recombination enzymes recombine the linear and target DNA to introduce the deletion or mutation into the chromosome [49]. Two recombineering system commonly used in *E. coli* are the lambda (λ) Red system, which involves three phage encoded proteins namely Exo, Beta and Gam, and the Rac prophage system which encodes RecE and RecT [49]. The Exo and RecE exonucleases cleave DNA from the 5’ to 3’ direction to generate a (ssDNA) tail or overhangs from a linear dsDNA; thereafter, the (RecT or Beta)binds to ssDNA promoting ssDNA annealing. The (λ) Red Gam inhibits RecBCD to protect the dsDNA from degradation [49]. The introduction of phage encoded recombineering systems in *E. coli* increased recombination efficiency from 10 to 100-fold [50].To overcome the low efficiency of the (λ) Red and Rac systems in mycobacteria, Van Kessel *et. al.* developed a homologous system derived from the mycobacterial Che9c phage. The system has been applied to genetically engineer fast and slow mycobacteriausing dsDNA and ssDNA substrates [49], [51]. The most commonly used plasmids for recombineering are pJV53 (expressing Che9c gene *gp60* (RecE homologue) and *gp61* (RecT homologue)), which is used with dsDNA, and the pJV63 (expressing Che9c *gp61*) which is used with ssDNA [49]. The inducible acetamidase promoter has been used to reduce the toxicity observed with Che9c *gp60* expression, and although induction of the system is required for function in *M. tuberculosis*, higher expression does not necessarily cause high recombineering levels [52]. There are a few reports of recombineering in NTM that are currently found in literature. dsDNA recombineering of *M. smegmatis* showed that efficiency was improved by using larger homology regions (between 50 bp and 500 bp) and that the absolute number of recovered transformants was largely dependent on the

competence of the cell. Recombineering with an AES substrate containing 500 bp of homology on either side of a hygromycin gene yielded recombination frequencies of between 2.4 x 10^{-5} and 2.8 x 10^{-4} with > 90 % of the colonies being recombinants [52]. Similar frequencies were observed in *M. tuberculosis* [52], [53], and thermo-sensitive plasmids and counter selection markers (SacB) have been used to curethe recombinant strain from the recombinant protein expressing plasmid [49].

Recombineering using short ssDNA (50 – 100 bp) is considerably more efficient than dsDNA recombineering (10 – 100-fold), although this is also largely influenced by cell competence. Substrates that target different strands have different recombinant efficiencies, with oligonucleotides targeting the lagging strand being more efficient. The degree of bias depends on chromosomal location, with up to a 10 000-fold difference observed in some loci [49]. ssDNA recombineering in slow growing mycobacteria had a recombineering efficiency of 5 to 10-fold lower than *M. smegmatis* (fast growing mycobacteria) and was highly dependent on ssDNA sequence and gene locus. In the absence of a selectable phenotype, such as antibiotic resistance, screening of up to 1000 single clones for mutant identification is required, and this is a major drawback of this technique [52].

Initial application of the mycobacteriophage Che9c system in *M. chelonae* was for the creation of knock-out mutants from the disruption of 3 porin genes, (*MCH_4689c*, *MCH_4690c* and *MCH_4691c*) using a *gp60* and *gp61* expressing plasmid. In the recombineering system, 3 independent electroporations of *M. chelonae* using 300 ng of linear AE substrate yielded between 29 and 65 zeomycin resistant colonies. Increasing the DNA to 1 µg raised the efficiency 3-fold demonstrating that saturation levels had not been attained [35]. PCR analysis of these colonies revealed 30 – 80 % that had undergone allelic exchange and direct selection of recombineering mutants on zeomycin plates without kanamycin resulted in zeomycin^r colonies, of which 15 to 26 % of these colonies were susceptible to *xylE* and kanamycin, and this suggests loss of the recombineering plasmid [35]. The authors showed that if there is lack of kanamycin selective pressure, the recombineering plasmid can be effectively cured either during the mutant selection process or by 2 passages of the chosen knock-out mutants in medium lacking kanamycin [35].

Double stranded recombineering was applied in *M. abscessus* (CIP104536T) in the disruption of the *mmpL4b* gene of the glycopeptidolipid pathway, using *M. smegmatis* for comparison [45]. Using a plasmid expressing the recombineering proteins Gp60 and Gp61, recombinant strains were generated by transformation, however the double stranded recombineering was substantially less effective, with only 7 % of clones undergoing allelicexchange [45]. Several single cross-over events were observed in M. abscessus, and therefore the authors hypothesized that recircularization had occurred since the construct that had compatible ends. Redesigning a new AE substrate with incompatible ends yielded an allelic exchange frequency of 7 mutants having undergone a double crossover event. While this was an improvement, the recombineering system was still significantly less efficient in *M. abscessus* when compared to *M. smegmatis* [45]. They also revealed that *M. abscessus* transformation efficiency was 2 orders of magnitude less efficient when compared to *M. smegmatis* and *M. tuberculosis*, but this does not fully explain the low recombineering efficiency [45]. A possibility is that the expression levels of the recombineering enzymes could be higher in *M. smegmatis*, since they were obtained frommycobacteriophage (Che9c) that infects *M. smegmatis* [45].

Double stranded recombineering was applied in *M. abscessus* to disrupt the triacylglycerol synthase (*tgs1* and *tgs2*) genes which have the highest percentage identity to *M. tuberculosis* Rv3130 (*tgs1*), using an AE substrate containing a hygromycin cassette. *M. abscessus* was electroporated with *gp60* and *gp61* expressing plasmid and their expression induced by 0.02 % acetamide, however the authors do not clearly state the transformation efficiency. The *M. abscessus tgs*1 mutants had an 80 % reduction in (triacylglycerol) TAG production efficiency indicating the loss of functionality of the *tgs*1 gene, whereas the *tgs2* mutants had no effect in the TAG production efficiency [54]. The reduction in TAG production suggest that complete AE had occurred on the *tgs1* locus of the *M. abscessus* chromosome. An illustration of ds and ssDNA recombineering is shown in Figure 1.

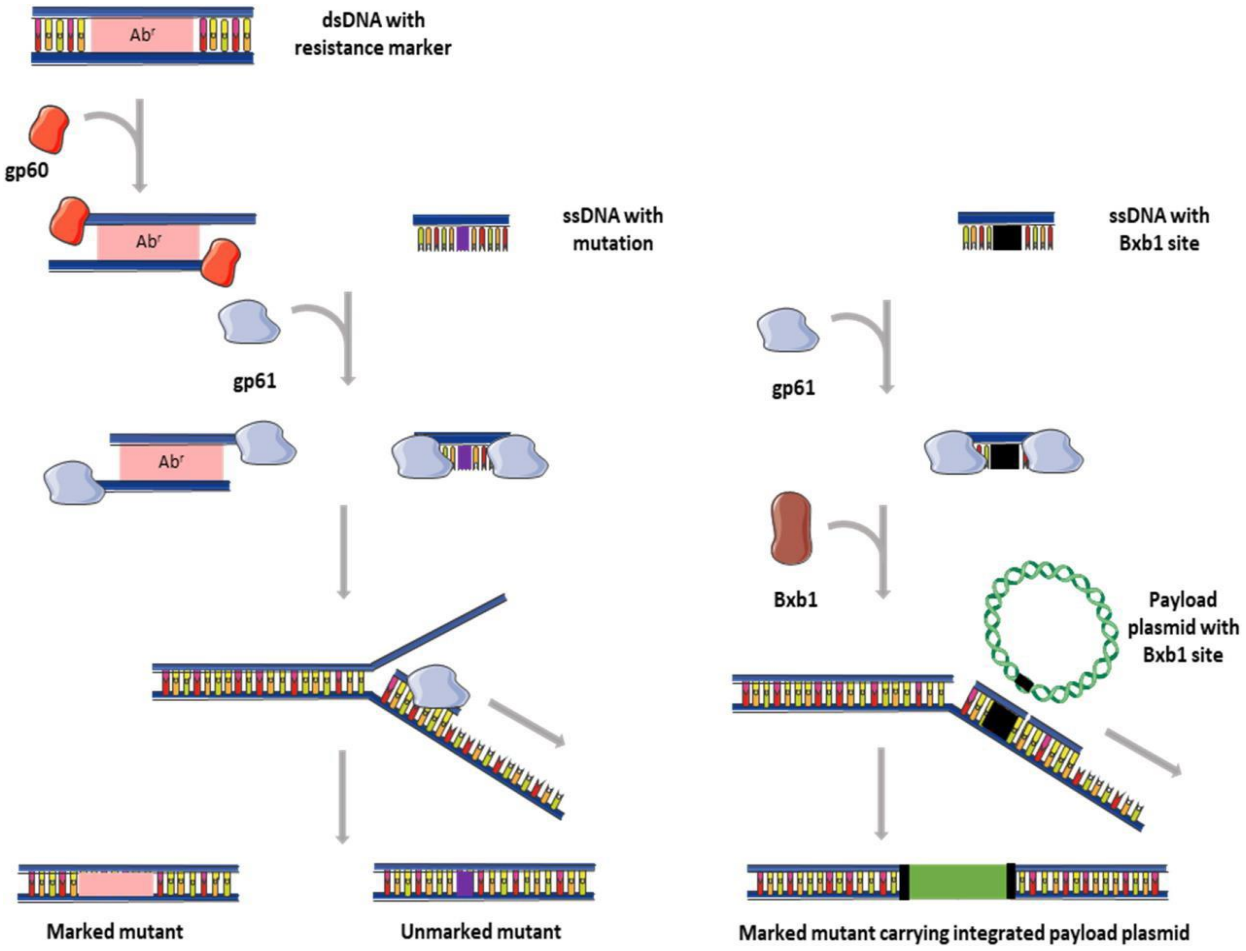

Figure 1: Showing recombineering with ds ssDNA and ORBIT.

dsDNA substrates (left) usually contain an antibiotic resistance marker for selection, while ssDNA substrates (middle) carry only the desired mutation flanked by short regions (25–50 bp) of homology. In ORBIT (right), the ssDNA substrate contains a Bxb1integration site flanked by short regions (25–50 bp) of homology. The gp60 exonuclease(RecE homolog) generates single stranded overhangs from the dsDNA fragments, whilegp61 (RecT homolog) promotes annealing of ssDNA to homologous regions in the chromosome. Recombineering is more efficient when oligonucleotides are targeted to the lagging strand (indicated in diagram). In ORBIT, Bxb1 facilitates concomitant integration of the payload plasmid. Taken from review article by (*Chimukuche* and *Williams.*, *2021*) [55]

1.3.5 ORBIT, oligonucleotide-mediated recombineering followed by Bxb1 integrase targeting.

Oligonucleotide-mediated recombineering followed by Bxb1 integrase targeting (ORBIT) was developed by combining of two efficient recombination systems, namely homologous recombination and site-specific integration [56]. The technique is mediated by the co-expression of the phage Chec9 Gp61 annealase and site-specific Bxb1 integrase from an episomal plasmid, which may be cured from the strain after mutagenesis. The Chec9 Gp61 annealase mediates the homologous recombination of a synthetic oligonucleotide that contains a recombination site that is specific for the Bxb1 integrase into the mycobacterial chromosome [56]. Co-transformation of the payload plasmid (containing an antibiotic selectable marker and a Bxb1 recombination site) with the targeting oligonucleotide into a strain that expresses the annealase and integrase permits one-step selection of antibiotic resistant homologous recombinants [56].

Bxb1 expression facilitates directional integration of the payload plasmid into the site by site-specific integration and antibiotic selection is used to identify the drug resistant homologous recombinants [56]. The *attP* (45 - 70 bp) homologous sites generated for subsequent Bxb1-mediated integration of the payload plasmid on target through (*attP* - *attB)* site-specific recombination, forming an *attL* and *attR* locus that flanks the payload plasmid [57]. A library of payload plasmids was generated and used for promoter replacements, deletions and addition of N and C-terminal tags [56].

Application of ORBIT in *M. smegmatis* and *M. tuberculosis* yielded 20 - 200 clones for each transformation (using 1 lg oligonucleotide and 200 ng payload plasmid). The Bxb1 integration system is independent of host factors because ORBIT provides both the Bxb1 and recombination site, therefore given that Che9c Gp61 function has been demonstrated in several NTM ORBIT should be feasible in these organisms [53]. An illustration of ORBIT is shown in Figure 1.

1.3.6 Random mutagenesis using transposons

Transposable elements are jumping genes that move from one position in the genome to

another or between DNA molecules [44]. Bacteria have two types of transposable elements namely, insertion sequences (IS) and transposons [58]. IS are generally less than 2 kilobytes (kb) with 10 - 40 bp terminal repeats and have a transposase gene encoding the DNA-binding enzyme involved in transposition. In contrast, transposons (tn) also have genes encoding a phenotypic trait, such as antibiotic resistance genes, in addition to the genes essential for transposition. The mariner transposons have been extensively used in random transposon mutagenesis since they require no host-species specific factors and require only a TA dinucleotide for insertion [45].

Transposition generates repetitive DNA sequences on the chromosomal DNA, and two types of transposition events exist. Replicative transposition is when co-integration occurs between the delivery transposon vector and the target replicon to form concomitant transposon duplication [58]. A site-specific recombinase resolves the co-integration and reforms the delivery replicon and target molecule such that the target host will only have one transposon copy. In cut-and-paste transposition, a transposase binds to a transposon creating a synaptic complex, cleaves it from the donor molecule and inserts into the target site without duplication [58]. The transposase is cleaved by host proteins which also complete the gaps on the insertion site. Cut-and-paste transposition is typical for Tn5, Tn10 and mariner transposons [59]. Transposon mutagenesis has been extensively used in the mycobacterial species, including *M. tuberculosis, M. smegmatis, M. avium, M. avium subsp. paratuberculosis, M. kansasii, M. smegmatis* and *M. marinum*.

The first insertional mutant libraries in *M. smegmatis* (mc^2155) were created using the Tn*611* transposon, a derivative of the *M. fortuitum* transposon Tn*610*, in which the antibiotic resistance gene *sul3* had been replaced by a kanamycin resistance gene [60]. Initially the transposon was used with non-replicating plasmids, but this resulted in low

transposition efficiency. To overcome this limitation, Tn*611* was subsequently combined with thermo-sensitive plasmids, allowing initial selection of transformants at 30 ^{o}C, and subsequent selection of mutants that had undergone transposition at 39 ^{o}C (non-permissive temperature). Transposition of Tn*611* occurs by the replicative mechanism, resulting in three IS6100 copies at the insertion site, with 2 insertion sequences located in the same orientation [61]. In *M. smegmatis* no insertion hotspots were observed, and many unique mutants could be recovered. Culturing mutants in medium without antibiotic until saturation revealed that the reversion frequency was low; indicating that Tn*611* stabilizes upon host chromosome integration [61].

The transposons Tn*5367*, Tn*5368* and Tn*5370* are derived from the *M. smegmatis* IS*1096* insertion sequence and have been combined with conditionally replicating plasmids to construct mutant libraries in several mycobacterial species [47], [62]. Thesetransposons differ from Tn*611* in that the mechanism of transposition is cut and paste, rather than replicative [63]. Transposon insertion is random, and analysis of the insertion sites identified a weak consensus sequence for insertion (5'-NNP y(A/T)A(A/T)NN-3'), showing a preference for an adenine - thyamine (AT)-rich centre. To overcome the low efficiency of plasmid delivery by electroporation, transposons were combined with temperature sensitive phages such as phAE77 and phAE94. In *M. marinum* transductionwith phAE94 carrying Tn*5367* yielded 10^5 Kan^r colonies per ml of the transduction mixture.This was significantly more efficient than the phAE77 derivative [64], [65], which yielded only 10^3 per ml, demonstrating that phage choice influences efficiency. Transposition efficiency also differs between species and is influenced by experimental conditions. Forexample, in *MAP* (K-10) strain a transposition frequency of 10^{-6} to 10^{-7}per recipient cell was observed with Tn*5367*, which is 10-fold lower than thefrequency observed for *M. bovis*. Optimal transposition frequencies for *M. avium* were obtained after 4 hours of co-incubation of bacteria and phages, while the frequency dropped 10-fold with longer incubation times [65]. Tn*5367* mutagenesis in both *M. marinum* and *MAP* (K-10*)* revealed that insertions were flanked with 8bp target duplication, and in *M. marinum* insertion of small parts of the phage DNA was observed in some mutants. Use of the phAE94/ Tn*5367* system in *M.*

ulcerans resulted in a high number of mutants with slow growth, limiting DNA isolation for Southern blot hybridization [64]. Sequencing of random PCR primed products suggested transposon insertion; however, plaque formation at 32 ^{o}C led the authors to speculate that integration of the prophage had occurred. phAE94 may therefore be functioning as a temperate phage in *M.* ulcerans, highlighting the need to confirm temperature-sensitive replication in different species.

Mariner transposons have recently been developed as genetic tools for use in bacteria and the most commonly used are *Mos1* and *Himar1* [57]. One of the major advantages of the mariner transposons are their reduced recognition sequence (5'-TA-3'), which compared to the recognition sequence of IS*1096*-derived transposons (5'-NNPy(A/T)A(A/T)NN-3') is less restrictive. The first mariner transposon used for mutagenesis in *M. marinum* was *Mos1* isolated from *Drosophila melanogaster*. A delivery vector, pM272B, was engineered to contain the transposon with a kanamycin resistance gene, a thermosensitive origin of replication and a *sacB* gene used for counter selection [66]. Following initial selection of Kan^{r} transformants after electroporation, transposition was observed at a rate of approximately 3 x 10^{2} Kan^{r} sucrose (Suc)^{r} bacteria per 10^{5} Kan^{r} bacteria. Analysis of the transposon junctions revealed a TA dinucleotide insertion site followed by guanine - cytosine (GC)-rich genomic sequences. Furthermore, the mariner transposon inserted randomly, usually with one transposon copy per genome, and the delivery vector was lost upon transposition.

The most-commonly used transposon in mycobacterial research is the *Himar-1*-derived MycomarT7 mariner transposon. This transposon has been engineered to contain a kanamycin selection marker and a T7 promoter, for insertion site identification, and is usually delivered using a temperature-sensitive phage. A comparison of Tn*5367* and the MycoMarT7 mariner transposon in *M. avium* subsp*. paratuberculosis* revealed more than a 3-fold higher number of insertions for MycoMarT7, and a higher percentageof insertions occurring within genes (83 % vs. 74 %) [67], demonstrating that the MycoMarT7 transposon is superior at creating a comprehensive library. Despite the reduced recognition sequence, transposition bias was detected for MycoMarT7, and it

was estimated that 400 000 MAP mutants would be required for a representative MAP library. This is 4- times higher than the estimate for *M. tuberculosis* and such biases could result in an overestimated of actual number of essential genes [67].

Evaluation of ΦMycoMarT7 in *M. kansasii* revealed that the temperature sensitivity was maintained, although compared to *M. smegmatis*, plaque formation in *M. kansasii* at the permissive temperature (30 ºC) was 800-fold less efficient. Using the TraDIS-type TIS method, 12 071 different TA insertion sites were mapped for 14700 mutants in the *M. kansasii* transposon library. Analysis of the insertion sites revealed that 82 % of the insertions in the chromosome were in open reading frames (ORFs), while a similar percentage (83 %) was observed for the pMK12478 plasmid present in the strain [68]. When comparing the number of hits in annotated genes, the slightly higher percentage in the plasmid (74 % vs 62 %) could be due to the non-essential nature of genes present extra-chromosomally, however since the library is not saturated this data is not conclusive. Transposon mutagenesis is a powerful tool for the genome-wide identification of essential genes; however, this requires the generation of very large saturating transposon mutant libraries (hundreds of thousands of mutants). By comparing the frequency of insertions observed within a gene, and the abundance of mutants within the pool, essential genes and mutations conferring a growth advantage or defect can be identified. This method has been used to identify essential genes in *M. marinum*, *Mycobacterium avium* subsp. *hominissuis* and *Mycobacterium intracellulare* [69], [70], [29].

Since non-saturated transposon mutant libraries are easier to generate, most studies in non-tuberculosis mycobacteria have used transposon mutagenesis to select for mutants with specific phenotypes. Examples include pigmentation variants in *M. marinum* [66], *M. kansasii* mutants with altered colony morphology [68] and *M. avium* mutants with altered antibiotic susceptibility [71]. A more targeted screen, aimed at identifying mutants with insertions in membrane or secreted proteins [72], was developed using the Tn*phoA* transposon. The Tn*phoA* transposon contains a partial *phoA* gene, that codes an alkaline phosphatase enzyme, lacking a signal sequence [73]. The transposon insertion into

membrane or secreted protein genes via replicative transposition promotes alkaline phosphatase expression, facilitating selection on 5-Bromo-4-chloro-3-indolyl phosphate (XP). A 450-mutant library was created by electroporating the delivery vector, pRT291, carrying the Tn*phoA transposon* into *M. fortuitum*. Of the 450 mutants, 42 mutants showed alkaline phosphatase activity, reflected by the presence of blue colonies on XP plates [73]. Analysis of a mutant (MT721) with a biofilm formation defect identified a deletion in the membrane protein anthranilate phosphoribosyl transferase (TrpD) [73].

One of the limitations of using transposons for mutagenesis is that a functional transposase must be produced within the host. The use of transposomes, which is a stable complex between a purified transposase enzyme and the transposon, overcomes this limitation [74]. A commercial transposome system derived from *Tn*903, EZ-Tn (Epicentre), has been developed for use in a broad host range, and was used to generate a mutant library of 3500 mutants in the *M. avium subsp. avium HMC02* [62]. *M. avium* exists as different colony morphotypes, due to differences in cell wall composition. The efficiency of transposition efficiency of EZ-Tn in certain morphotypes was significantly lower than others, presumably due to impaired transposome delivery. Low transformation efficiency is therefore a major limitation of this system.

1.3.7 Random mutagenesis by illegitimate recombination

Although high levels illegitimate recombination is undesirable when introducing site-specific mutations, its non-specific nature can be harnessed to introduce random mutations. The high levels of illegitimate recombination in slow-growing mycobacteria were exploited to generate mutants in *M. bovis* and *M. avium* [75], [76], [24]. The initial study in *M. bovis* was aimed at investigating the role of the *aphC* gene, and therefore used a kanamycin resistance gene (aph) flanked by sequences from the *M. bovis aphC* gene. Of the 440 transformants containing an insertion, none of these had disrupted the *aphC* gene, indicating that allelic exchange had not occurred [76]. Since the flanking regions do not appear to confer any specificity, the study in *M. avium subsp. Hominissius* used a linear DNA fragment containing a hygromycin resistance gene flanked by vector (pYUB854) sequences. Electroporation of 3 – 6 µg of this linear DNA fragment yielded

about 1 000 hyg^r colonies [24]. Analysis of 13 randomly chosen mutants revealed that the resulting deletions ranged between 2 and 669 bp, and 12 of the 13 deletions had disrupted a single gene. While this method is much easier to perform that transposon mutagenesis, it is significantly less efficient.

Table 2: Showing random mutagenesis systems in mycobacteria. The delivery vectors are phages that use specialized transduction and plasmids which use electroporation as methods to enter DNA into the mycobacterial cells facilitating random transposon mutagenesis in NTM. Most of the phages used are derivatives of the mycobacteriophage TM4.

Mycobacterial species	**Transposon**	**Plasmid/ phage**	**Selection marker(s)**	**Purpose/ selection**	**References**
M. marinum	IS1096 IS6110	pYUB285 pUS252 (suicide plasmids)	Km^r	Insertional library	[77]
M. marinum	Tn5367	phAE94 (TM4) phAE77(D29) (ts phasmids)	Km^r	Insertional library	[64]
M. marinum	Mos1	pM272B (ts-oriM)	Km^r sacB	Insertinal library pigmentation mutants	[66]
M. marinum	MycoMarT7	phAE94 (TM4)	Km^r	Essentiality Screen	[69]
M. avium subsp. paratuberculosis	Tn5367	phAE94(TM4)	Km^r	Insertional library	[65]
M. avium subsp. paratuberculosis	Tn5367 MycoMarT7	phAE94 (TM4) phAE94 (TM4)	Km^r	Insertional library	[65], [73]
M. avium	MycoMarT7	phAE94(TM4)	Km^r	Insertional library, antibiotic susceptibility	[71]
M. avium subsp. hominissuis	MycoMarT7	phAE94(TM4)	Km^r	Essentiality screen	[25]
M. avium subsp. avium (HMC02)	EZ::TN	n/a	Km^r	Insertional library Ciprofloxacin^S	[71]
M. kansasii	MycoMarT7	phAE94(TM4)	Km^r	Insertional library, colony morphology	[68]

Mycobacterial species	**Transposon**	**Plasmid/ phage**	**Selection marker(s)**	**Purpose/ selection**	**References**
M. intracellulare	MycoMarT7	phAE94 (TM4)	Km^r	Essentiality screen	[70]
M. fortuitum	TnphoA	pRT291 (suicide vector)	Km^r phoA	Library with insertions in secreted/ membrane proteins, resistance to acid stress biofilm defect	[73]
M. ulcerans	Tn5367	phAE94 (TM4)		Unsuccessful	[64]

1.3.8 Gene editing with CRISPR Cas

Clustered Regularly Interspaced Palindromic Repeats (CRISPR)/ associated protein-9 endonuclease from *Streptococcus* (Cas9) system, has been employed in genetic engineering tools for microbes, plants, animal, and proposed for use in of the treatment of human diseases [78]. The CRISPR/Cas9 system in prokaryotes functions to destroy foreign DNA and consists of a DNA binding Cas9 nuclease and a guide RNA. Foreign DNA, such as phages or plasmids are digested and integrated into the CRISPR locus of the bacterial genome as short sequences termed spacers [44]. The integrated DNA is transcribed to produce a mature transcript, crRNA, which forms a duplex with the trans-activating crRNA (tracrRNA), and the duplex associates with the Cas9 nuclease to form a CRISPR/ Cas9 complex. The complex functions by recognizing invading DNA that is complementary to the crRNA and cleaves it to form a blunt double stranded break (DSB) [79]. Cas9 target DNA binding is dependent on a protospacer adjacent motif (PAM). The PAM is a short-conserved sequence of 2 - 5 bp located downstream of the target DNA, but is not included in the CRISPR locus, therefore preventing the CRISPR locus being cleaved [79].

The CRISPR-Cas9 system (from *Streptococcus pyogenes*) is has been widely and successfully implemented in genome editing of various organisms. CrRNA and tracrRNA exist in nature as a duplex but can be combined synthetically to form one fusion sequence known as single - guide RNA (sgRNA). This facilitates site-specific Cas9 endonuclease cleavage of DNA under the guidance of sgRNA [80]. The Cas12a type V-A endonuclease from the class 2 CRISPR-Cas system, has also been harnessed for genome editing, and unlike Cas9 is guided by a single crRNA only and functions in crRNA processing.

When CRISPR-Cas9 is used in genome editing, the host needs to repair the DSB introduced into the chromosome, and it is this process that results in mutations at the

cleavage site. The DSB repair is either performed by homologous recombination (HR) using a corresponding homologous template or by non-homologous end joining (NHEJ), in absence of a homologous template [81]. NHEJ repair system can maintain genomic stability and easily manage DSB since it requires no sequence for the dsDNA ends ligation. NHEJ is prone to insertions and deletions; and can generate frame-shift mutations that mutate the target gene [81]. The NHEJ pathway eukaryotic key components; Ku protein, ligase D (LigD) and NrgA (conserved region between the Ku and lig D) have homologs that exist and are functional in mycobacteria [81]. Following CRISPR cleavage, Ku protein binds to dsDNA ends, then recruits LigD which promotes DNA processing and ligation [81].

The first reported use of the CRISPR/ Cas9 system in mycobacteria was for gene silencing [82]. Genes can be silenced by mutating the endonuclease domain of the Cas9 to make it catalytically inactive to prevent DNA cleavage [79]. Binding of the inactive causes transcriptional repression and this is known as CRISPR interference (CRISPRi) [80]. Evaluation of 11 Cas9 proteins in mycobacteria revealed that the enzyme from *Streptococcus thermophilus* ($dCas9_{Sth1}$) was most efficacious in the knock-down of endogenous gene expression and is robust even when targeted far from the transcriptional start site [44].

In *M. smegmatis,* the first application of CRISPR-Cas12a was to increase recombineering efficiency. The two-plasmid system, also demonstrated to function in *E. coli* and *Yersinia pestis*, coupled the CRISPR-FnCpf1 (a *Francissella novicida* Cas12a endonuclease) and the recombineering proteins (Chec9c Gp60 and Gp61) to create markerless and scarless mutations. Authors used short oligonucleotides (ssDNA) to target a *gfp* gene previously inserted in the chromosome. As expected, the strands bias associated with recombineering was observed, with a recombination efficiency of 80 % and 69 % obtained for oligonucleotides targeted to the lagging strand whereas the leading-strand oligonucleotide had a 5-fold lower efficiency [86]. Most notably, recombineering was 50-times more efficient when the CRISPR-FnCpf1system was present. The CRISPR-FnCpf1-enhanced recombineering was able to efficiently introduce point mutations, while

deletion and insertion efficiency were dependent on the size. For insertions, 27 % of transformants had 5 bp insertions, 10 % had 10 bp insertions, while only 3.1 % had 20 bp insertions [83]. Similarly, for deletions the efficiency analysis of small deletions (5, 10, 20 bp) ranged between 70 % and 90 %, which drastically reduced to 17.4 % and 8.2 % for 418 bp and 1000 bp deletions, respectively. Using 1 kb double-stranded DNA fragments instead of short ssDNA with this system facilitated the introduction of marker lessdeletions of up to 4000 kb with an efficiency of more than [83], [84].

The CRISPR-FnCpf1 system was unable to generate mutants in *M. smegmatis* in the absence of recombineering substrates, suggested that NHEJ was not functioning to repair DSB generated by the nuclease. In contrast, expression of the CRISPR-FnCpf1 nuclease and crRNA targeting a non-essential gene in *M. marinum* resulted in deletions ranging from 2 bp to 10 179 bp. Furthermore, the deletion of *ku* and *ligD* genes in *M. marinum* reduced genome editing efficiency to below 10 %, while complementation increased NHEJ editing efficiency to 90 % [81]. Expression of the *M. marinum* NHEJ (MmNHEJ) locus with the CRISPR-FnCpf1 system in *M. smegmatis* resulted mutations in 0.75 % of transformants [81]. This efficiency was increased to 90 % when the experiment was performed in a recA null mutant, suggesting that inhibiting HR is required for the NHEJ system to efficiently introduce mutations following nuclease cleavage in *M. smegmatis*.

To facilitate efficient CRISPR-FnCpf1-assisted non homologous end-joining (NHEJ) genome editing in mycobacteria a two-plasmid system was subsequently developed; one plasmid consists of $RecA_{mu}$ (dominant RecA negative mutant), RecX (RecA regulator), MmNHEJ (*M. marinum* NHEJ) and the other of FnCpf1 and the crRNA. These promoted the NHEJ genome editing in *M. smegmatis* with high efficiency (80 % - 90 %). Moreover, comparison of FnCpf1 and $Cas9_{Sth1}$ (Cas9 from *Streptococcus thermophilus*) assisted NHEJ revealed about 20 % transformants survived, with a very high genome editing efficiency above 80 % occurring with both nucleases [81]. Analysis of the cleavage sites in the recovered mutants revealed random deletions between 1 kb and 10 kb. The CRISPR-assisted NHEJ repairing system was further enhanced for use in *M. tuberculosis* by adding a *sacB* gene, to facilitate plasmid curing, and replacement FnCpf1 with

$Cas9_{Sth1}$. This facilitated genome editing in greater than 80 % of recovered transformants, with deletions of between 1 and 324 bp being introduced [83], [84]. CRISPRi illustrated in Figure 2.

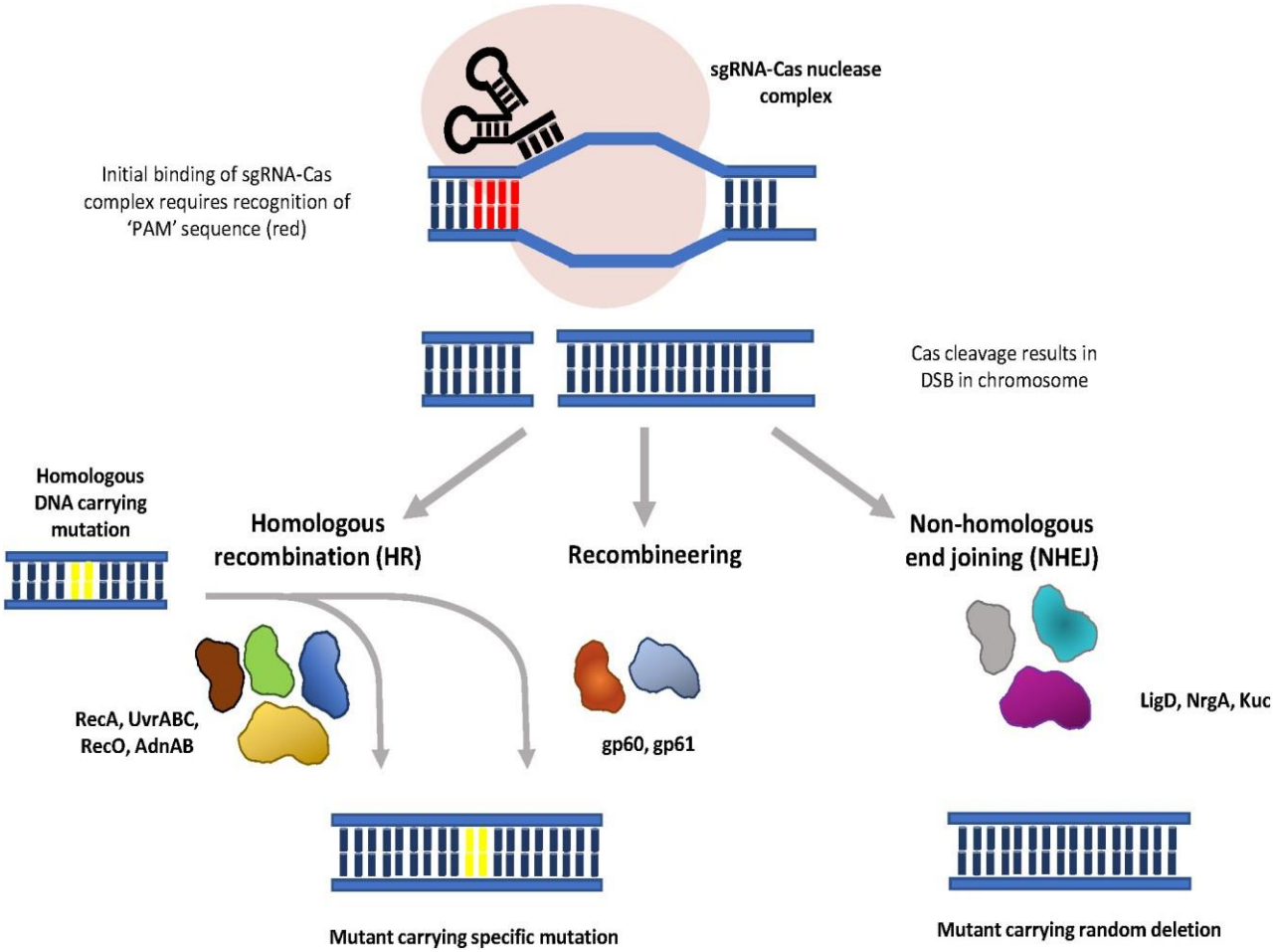

Figure 2: Graphical representation of CRISPR/ Cas mutagenesis.

Synthetic sgRNAs (black) direct binding of the Cas nuclease (pink) to a specific gene through Watson-Crick base paring between the sgRNA and the target sequence. Initial binding of the sgRNA-Cas complex is dependent on the recognition of an adjacent PAM sequence (red). Nuclease cleavage results in a double strand break in the chromosome, which is repaired either through homologous recombination, in the presence of a homologous substrate, or non-homologous end joining. The error-prone nature of NHEJit results in random mutations at the site of repair. Phage proteins gp60 and gp61 are proposed to function in DSB repair with ssDNA and dsDNA substrates (CRISPR/Cas-mediated recombineering). Taken from review article by (*Chimukuche* and *Williams., 2021*) **[55]**.

1.4 Background to this study

Iron-sulfur clusters (FeS) are the most versatile inorganic cofactors; proteins containing these cofactors are involved in basic biological functions such as photosynthesis, nitrogen fixation, respiration, and DNA repair [85]. FeS clusters are assembled by multi-protein systems in vivo [86]. The five main components of the FeS cluster biosynthetic machinery are of a cysteine desulfurase, an iron donor, an electron transfer mechanism, a scaffold, and FeS cluster transfer proteins [87]. Iron (ferric or ferrous) and sulfide are required for the basic process of FeS biogenesis [86]. Sulfur is provided by the cysteine desulfurase enzyme, which employs L-cysteine as a stable sulfur source, while the source of iron is unknown [88].

The nitrogen-fixing (NIF), iron–sulfur cluster (ISC), and Sulfur utilization factor (SUF) are the 3 main systems identified to be involved in the formation of FeS clusters. These three systems all follow the same biosynthetic process whereby the two components, iron and sulfide, come together on a scaffold protein or complex, and is then transferred either directly to the apo-protein or through a series of carrier proteins that mediate FeS protein trafficking and targeting [4]. The NIF system was discovered in *Azotobacter vinelandii* as the first FeS cluster biosynthesis route, and its function is specific to the assembly of FeS clusters for the nitrogenase in NIF species [89]. The ISC system was discovered in *A. vinelandii* and is proposed to play a regulatory role in FeS cluster assembly and are found in practically all life forms [90]. The SUF system was the third FeS cluster system to be discovered, it is less common and occurs exclusively in archaea, most gram-positive bacteria, plant chloroplasts, and green algae [91].

According to a previous working model based on phylogenetic and biochemical research, DUF59-containing proteins found in eukaryotes, bacteria, and archaea, play a role in the maturation of FeS proteins, [92]. *sufT* in *Staphylococcus aureus* is made up entirely of the DUF59 domain, and the *sufT* and *sufBC* genes, which encode for the scaffold proteins, are colocalized [92]. Phylogenetic analysis suggests that *sufT* was recruited to the same chromosomal position as *sufBC* in *S. aureus*, leading to the idea that *sufT*

functions in SUF-mediated FeS cluster assembly [92]. The assembly of FeS proteins was deficient in a *sufT* mutant of *S. aureus*. The role of the *sufT* homologue was investigated in *M. smegmatis* and the ∆*sufT* mutant was unable to grow in the absence of iron, indicating that *sufT* is necessary for growth in iron limiting conditions [93]. Furthermore, the *M. tuberculosis* DUF59 protein, Rv1466, partially complemented the phenotype of the *M. smegmatis sufT* mutant, suggesting conservation of function in mycobacteria [92].

Clustered Regularly Interspaced Short Palindromic Repeats (CRISPR)/ CRISPR associated proteins (Cas) is a bacterial system of acquired resistance to phages and plasmids which has been harnessed for genome editing [94], [95]. The system has further been modified to prevent the transcription of specific gene targets, termed CRISPR interference (CRISPRi), and it is now commonly used to mediate the knockdown of essential and non-essential genes [96]. Two major components are required for the CRISPRi system: a deactivated CRISPR associated protein-9 endonuclease (dCas9), and a single guide RNA (sgRNA) made of approximately 20 nucleotides which are complementary to the target sequence [97]. The protospacer adjacent motif (PAM) sequence (5'-NNAGAA-3'), and Watson-Crick base pairing of the sgRNA to the target DNA, determines the specificity of the system by directing the binding of the dCas9 enzyme [98]. The Cas9 endonuclease activity is deactivated (dCas9) by targeted point mutations on the HNH (H840A) and RuvC (D10A) nuclease domains [99]. This prevents cleavage of the target region, and it promotes transcriptional inhibition via steric hindrance rather than gene editing.

CRISPRi was found to be highly efficient in *E. coli* and *B. subtilis*, resulting in a thousand-fold reduction in gene expression, whereas testing in mycobacteria produced just a four-fold reduction in gene expression using dCas9 from *streptococcus pyogenes*. Rock *et al*., 2017 subsequently optimized the mycobacterial CRISPRi system by using the *Streptococcus thermophilus* dCas9 enzyme and generating CRISPRi backbone variants that limit leaky expression in the absence of the inducer, while maintaining high levels of expression following induction [20]. The degree of the Tet repressor expression differs between these backbones, for *M. smegmatis*, the CRISPRi backbone is pLJR962 is recommended, and the current backbone for *M. tuberculosis* is pLJR965.

1.4.1 Rationale of this study

To date, the FeS cluster assembly system has not been investigated in *M. abscessus*. The process is important to study in *M. abscessus* to understand what function it plays in *M. abscessus* pathogenesis. The FeS cluster assembly system is encoded by the *sufR-sufB-sufD-sufC-csd-nifU-sufT* (*suf* operon) in mycobacteria. Previous work characterised the protein encoded by the last gene in the *suf* operon in *M. smegmatis*, *sufT*, and demonstrated that it is required for growth under conditions of iron limitation [100]. During infection, mycobacteria are thought to experience iron limitation, and therefore the genes required for under these conditions could be important for survival within the host. Transcriptional repression using CRISPRi has been successfully employed in both *M. smegmatis* and *M. tuberculosis*, however at the time of initiating thisstudy it had not been used in *M. abscessus* [79].

We therefore aimed to investigate the utility of the mycobacterial CRISPRi system developed by Rock *et. al.* (2017) in *M. abscessus* to explore the function of the SufT protein as a component of the FeS cluster assembly system.

1.4.2 Hypothesis

The mycobacterial CRISPRi system has utility in *M. abscessus* and can be used to study the role of SufT in the survival of *M. abscessus* under iron limiting conditions.

1.4.3 Specific Aims

1. To evaluate the utility of the mycobacterial CRISPRi system for transcriptional repression in *M. abscessus*.
2. To investigate the role of *sufT* in the survival of *M. abscessus* under conditions of iron limitation.

1.4.4 Objectives:

1. Generate CRISPRi vectors for silencing *sufT* expression in *M. abscessus* using the system developed by *(Rock et al., 2017).*

2. Generate *M. abscessus sufT* knock-down strains and evaluate transcriptional repression in these strains.
3. Evaluate the impact of *sufT* knock-down on the survival of *M. abscessus*, under iron-limiting conditions.

2.1 Bacterial strains and standard growth conditions

E. coli (*DH5α*) was grown in Luria Bertani (LB) broth (1 % tryptone, 0.5 % yeast extract, 0.5 % sodium chloride (NaCl) at 37 ºC for 24 hours with shaking or plated on LB broth supplemented with 1.2 % agar and incubated overnight at 37 ^{o}C. When required kanamycin and ampicillin (amp) were added to a final concentration of 25 µg/ ml and 100 µg/ ml respectively.

All procedures involving *M. abscessus* were conducted in a biosafety level 2 laboratory. *M. abscessus ssp. abscessus* (ATCC 19977) wild-type and mutants were grown in Middlebrook 7H9 media supplemented with 0.05 % Tween 80 and 10 % Oleic Albumin Dextrose Catalase (OADC) (8.5 % sodium chloride, 20 % dextrose, 0.03 % catalase, 50 % bovine albumin fraction V, and 0.6 % oleic acid). For solid media, Middlebrook 7H10 was supplemented with 0.5 % glycerol and 10 % glucose salt (0.85 % NaCl, 2 % glucose) for solid growth. For iron limitation studies, Chelex® 100 resin treated Sauton's media (0.05 % Potassium phosphate monobasic (KH_2PO_4), 0.1 % Magnesium sulfate ($MgSO_4$), 0.4 % L-asparagine, 0.22 % citric acid, 5.7 % glycerol and 1 % zinc sulphate ($ZnSO_4$), pH 7.4) was prepared by stirring media with 1 % Chelex for 24 hours at room temperature. Filtration was used to remove the Chelex and sterilize the media. When required, kanamycin was added to a final concentration of 50 µg/ ml. For growth studies, starter cultures were diluted to a starting OD at 600 nm (OD_{600}) of 0.05 in 25 ml 7H9 OADC at 37 ^{o}C with shaking at 100 revolutions per minute (rpm). The growth was monitored over a period of 2 days by reading OD_{600} and plating for colony forming units at selected time points.

2.2 Preparation of freezer stocks

M. abscessus cultures were started by resuspending single colonies in 5 ml 7H9 OADC. For large colonies, 1 in 10 dilution was also prepared and grown at 37 ^{o}C shaking. The starter cultures were grown to an OD of approximately 1 and sub-cultured into 25 ml 7H9 OADC to a starting OD_{600} of 0.05 and grown for 24 hours under the same conditions.

Stocks were prepared once cultures reached an OD_{600} above 1. The cells were centrifuged at 3 220 x gravity (*g*) for 5 minutes and resuspended in 25 ml sterile storage media (0.47 % Middlebrook 7H9 media, 90 % of 50 % glycerol, 10 % OADC and 0.25 % of 20 % tween 80), and frozen at -80ºC for long-term storage. All the *E. coli* strains were stored by adding glycerol to a final concentration of 50 % and placing at -80 ºC.

2.3 Iron limitation growth curves

M. abscessus wild-type and mutants were grown as indicated in 5 ml 7H9 OADC. The cultures were washed by centrifuging at 1788.8 g and resuspended in 10 ml of chelated Sauton's media to remove the 7H9 OADC. Resuspended cells were used to inoculate cultures to a staring OD_{600} of 0.05. The cultures were grown at 37 ºC with shaking at 100 rpm for 24 hours to deplete intracellular iron stored. A second subculture at a starting OD_{600} of 0.05 was made into chelated Sauton's media with and without supplemental iron. The growth was monitored over a period of 2 days by reading OD_{600} at 0, 24, 27, 30,33, 48 and 51 hours respectively.

2.4 Spotting Assay

The *M. abscessus* mutants were cultured for 24 hours in 7H9 OADC to an OD of approximately 1. A dilution series from 10^{-1} to 10^{-6} was made and 10 µl of each dilution was plated on solid media containing 0, 50, 100, 200 or 500 nanogram (ng)/ µl anhydrotetracycline (ATc) and incubated for a period of 3 to 7 days.

2.5 Biofilms

M. abscessus mutant stocks were grown as indicated and sub-cultured for 24 hours using chelated Sauton's media with tween. The cultures were diluted to an OD_{600} of 0.05 in 30 ml Sauton's media without tween and a volume of 2 ml of the diluted culture was aliquoted into 24 well plates. ATc (final concentration 50 ng/ ml) and iron (final concentration of 2 µM) to the appropriate wells. Parafilm was used to wrap the plates to maintain a fixed air-liquid ratio. The biofilms were grown over a period of 3 weeks at 37 °C in an incubator without shaking.

2.6 General cloning methods

All the cloning experiments and DNA manipulations were performed according to standard protocols.

2.6.1 Plasmid DNA extraction from *E. coli*

The E.Z.N.A ® Plasmid DNA Mini Kit 1 was used according to the manufacturer's instructions to carry out plasmid DNA extraction using a culture volume of 5 ml. The plasmid DNA was eluted using a volume of 30 µl E.Z.N.A ® Plasmid DNA Mini Kit buffer. The NanoDrop (ND)-1000 Spectrophotometer was used to quantify the plasmid DNA, which was stored at -20 ºC.

2.6.2 Restriction Enzyme Digests

Bacterial restriction enzymes cleave dsDNA at specific sites, they recognize specific short sequences and create DNA fragments with blunt end or 3' and 5' overhangs. Restriction enzyme digests were set up according to the manufacturer's instructions. For cloning purposes, 200 - 500 ng plasmid DNA was digested with 2 units of enzyme in a total volume of 50 µl for 24 hours. For restriction enzyme mapping, approximately 100 ng plasmid DNA was digested with 2 units of enzyme in a total volume of 10 µl for 1 - 2 hours. BsmBI digests were incubated at 55 ºC, while all other digests were incubated at 37 ºC.

2.6.3 Agarose gel Electrophoresis

Agarose gel electrophoresis was performed to separate DNA fragments following plasmid DNA digests and to check the size of PCR amplicons. A 1 % gel was used to separate intermediate to high molecular weight fragments and 2 % gels were used to separate low molecular weight fragments (< 1 kb). Agarose gels were prepared in 1X Tris-acetate-Ethylenediamine tetra-acetic acid (EDTA) (TAE) buffer (40 mM Tris-acetate and 1 mM EDTA, at pH 8.3). For DNA visualization, a final concentration of 0.5 µg/ ml of ethidium bromide was added prior to solidification. The molecular weight marker GeneRuler 1 kilobyte (Kb) DNA ladder (Thermo) was used for size estimation. The gels were

electrophoresed at 100V for 60 minutes. The fragments were visualized by ultraviolet (UV) light using a Gel Viewer (BioRad).

2.6.4 Purification of the DNA fragments from agarose gels

The desired DNA fragments was excised from the agarose gel after electrophoresis and purified using the Wizard® SV Gel and PCR Clean-Up System according to the manufacturer's instructions. The DNA was eluted using 30 µl of nuclease free water. The NanoDrop ND-1000 Spectrophotometer was used to quantify the DNA. The DNA was visualized using UV light in the long wavelength range to reduce the chance of introducing mutations.

2.6.5 Ligations

T4 DNA ligase (NEB; 2, 000, 000 units/ ml) and 1 x buffer were used to ligate 50 ng of the digested purified plasmid DNA and DNA inserts. Ligation reactions were incubated at room temperature for 3 - 4 hours or at 4 ºC overnight. The ligations were inactivated at 65 ºC for 10 minutes (min) prior to transformation. A molar ratio of 1:3 vector to insert was used to increase the chances of getting positive clones.

2.6.6 Transformation of *E. coli*

For cloning procedures, either commercial Thermo Sensitive™ DH10B competent cells or competent cells were prepared in-house using the $CaCl_2$ or rubidium chloride methods were used.

2.6.6.1 Transformation of E. coli DH10B competent cells

A volume of 20 µl competent cells was added to 2 µl of the ligation mixture and incubated on ice for 30 minutes. A positive PUC19 control (0.01 ng) and a negative no DNA control were included. After incubation, the cells were heat shocked for 30 s at 42 ºC to allow DNA transformation then immediately placed on ice for 2 minutes. A volume of 900 µl of LB broth was added to the transformation mix and incubated at 37 ºC for 1 hour to facilitate cellular transcription and translation of proteins involved in resistance. Following cell recovery, 50 µl of the cells were spread on LB plates containing the appropriate

antibiotic and incubated further at 37 ºC overnight. The plates were then checked for bacterial colony growth.

2.6.6.2 Preparation and transformation of *E. coli* $CaCl_2$ chemical competent cells

A 5 ml *E. coli* culture was grown overnight at 37 ºC up to stationary phase of (OD_{600}= 0.9 - 1). The culture was diluted 1 in 10 with LB broth in a total volume of 50 ml and cultured at 37 ºC with shaking. The cells were collected by centrifugation at 3 220 x *g* for 5 mins at 4 ºC at early log phase (OD_{600}= 0.5). The subsequent steps were all performed on ice. The pellet was resuspended in 50 ml of 0.1 M magnesium chloride ($MgCl_2$) and incubated on ice for a minute. The cells were harvested as before and then resuspended in 25 ml of 0.1 M $MgCl_2$. Following incubation for 30 minutes on ice, cells were harvested and resuspended in 1/ 10th of the culture volume (5 ml) of 0.1 M calcium chloride ($CaCl_2$). A volume of 100 µl competent cell was mixed with 3 µl of the ligation reaction, left on ice for 10 minutes. The cells were heat shocked at 42 ºC for 2 minutes, cooled for 2 minutes on ice before adding 900 LB broth to allow recovery at 37 ºC for 1 hour, then plated as described above.

2.6.6.3 Preparation and transformation of *E. coli* rubidium chloride chemical competent cells

A 5 ml *E. coli* starter culture was grown overnight at 37 ºC up to stationary phase of (OD_{600}= 0.9-1) then sub-cultured to a starting OD of 0.05 in 100 ml LB. The *E. coli* culture was grown to an OD_{600} of 0.5 in LB broth. The cultures were cooled for 15 mins on ice then harvested by centrifugation at 5000 rpm for 10 mins at 4 ºC. The bacterial pellet resuspended in 60 ml TfbI (100 mM rubidium chloride (RbCl), 50 mM manganese chloride, 30 mM potassium acetate, 10 mM calcium chloride ($CaCl_2$) and 15 % glycerol) and cooled on ice for 15 mins. The cells were harvested by centrifugation at 3 220 x *g* for 5 mins at 4 ºC. The cells were resuspended using 6 ml TfbII (10 mM 3- (N-morpholino) propanesulfonic acid (MOPS), 10 mM RbCl, 75 mM CaCl2 and 15 % glycerol). Aliquots of 150 µl were made and stored at -80 ºC until required. The transformation procedure was the same as for $CaCl_2$ competent cells.

2.7 Polymerase Chain Reaction (PCR)

The Phusion® High-Fidelity DNA polymerase (Thermo Fisher Scientific) was used to amplify DNA templates, for cloning purposes since the enzyme reactivates at very high temperatures. It was also used because it has a 50-fold lower error rate than Taq and produces higher yields with low amount of enzyme (0.02 units (U) / ul). The KAPA Taq DNA polymerase (5 U/ µl) was used to confirm positive clones before sequencing. The KAPA 10 µl PCR mix contained KAPA Taq 10 x buffer A (1.5 mM Mg) at a final concentration of 1 x, 0.2 mM dNTPs, 0.4 µM primers, KAPA Taq polymerase (5U/ µl) using a final concentration of 0.5 U/ µl and 50 ng template DNA. The following cycling conditions were used: initial denaturation 95 °C for 3 min, followed by 30 cycles of denaturation 95 °C for 15 s, annealing 50 °C for 30 s and elongation 72 °C for 2 mins, with a final elongation step 72 °C for 5 mins. The Phusion® Hot Start II PCR mix contained 5 x Phusion HF buffer at final concentration of 1 x, 200 µM dNTPs, 0.5 µM primers, 0.02 U/ ul Phusion® Hot Start II and 50 ng template DNA. The PCR amplification conditions were initial denaturation 98 °C for 1 min, followed by 35 cycles of denaturation 98 °C for 15 s, annealing 60 °C for 30 s and elongation 72 °C for 2 mins, with a final elongation step 72 °C for 7 mins. Table 3 shows a list of all the primers used in this study.

Table 3: Table 3: List of primers generated in this study

All the primers used in the study were designed using Primer3 software.

Primer Name	Primer Sequence	Gene/ Region	Positions were primers bind	Expected product sizes
CRISPRi reverse sequencing primer	TTTCCTGCGTTATCCCCTGA	pLJR962 vector	186 bp from the Bsmbi enzyme start site of the PLJR962 vector	
MAB_2744c qPCR F1	GAATGTCGAGGAGAGCGAGAG	*MAB_2744c*	117 - 138 bp from the start of the *MAB_2744c* gene	137
MAB_2744c qPCR R1	TGATCTCTTTGACAAGTCCCGC		232 - 254 bp from the start of the *MAB_2744c* gene	
MAB_2744c qPCR F2	CCCAGAGCTCGGTATCAACG		69 - 89 bp from the start of the *MAB_2744c* gene	136
MAB_2744c qPCR R2	ACGTGAGGGTCATGTCGATG		153 - 173 bp from the start of the	

			MAB_2744c gene	
Sig A qPCR F1	GGTTACAAGTTCTCGACGTACG	*sigA*	906 - 928 bp from the start of the *sigA* gene	116
Sig A qPCR R1	TTGTTGATGACCTCGACCATGT		1000 - 1022 bp from the start of the *sigA* gene	
Sig A qPCR F2	TTACAAGTTCTCGACGTACGCC		908 - 930 bp from the start of the *sigA* gene	114
Sig A qPCR R2	TCCATTTCCTTGGCCAGCTCTT		1078 - 1100 bp from the start of the *sigA* gene	
AphF	CCACTGTTACAACCAATTAACCAAT	Kanamycin backbone on the pLJR962 vector	7849 - 8664 bp from the start of the PLJR962 vector	816
AphR	CATCATGAACAATAAAACTGTCTGCT			
2744stdF	CGTCGATTCGGCATAGCG	*MAB_2744c*	439 - 1435 bp bp from the start of the *MAB_2744c* gene	997
2744stdR	GTCCGGAAACCTGCAAGC			
SigAstdF	CAGGTTCTGCACTCTTGTCG	*sigA*	19 – 1589 bp from the	1676
SigAstdF	AAAGGGAACGGCTTAGTCCA			

			start of the *sigA* gene	

2.8 Generation of *M. abscessus* knock-down strains by CRISPRi

2.8.1 sgRNA design for CRISPRi

Published PAM sequences (*Rock et al*., 2017) were identified in the *M. abscessus* (ATCC 19977) genes *MAB_2744c* and *MAB_2745c* by inspection using Snap Gene Software. This allowed for the determination of the adjacent sgRNA sequences (20 bp) on the template strand. To investigate whether the sgRNA sequences bind anywhere else in the genome, an Ensemble BLAST was performed for each sgRNA. A cut-off of less than 4 mismatches was used. The sequence of the cleaved BsmBI restriction enzyme site was added to the 5' end of the two complementary sgRNA sequences to create compatible ends for cloning; the sequence GGGA was added to the sgRNA sequence running in the 5'-3' direction and the sequence AAAC-was added to the complementary sequence. Table 4 shows the sgRNA sequences and their position in the two genes.

Table 4: Showing sgRNA oligonucleotide sequences, the target gene, and locations that they bind.

Oligonucleotide name	Sequence (5'-3')	Gene	Sequence (5'-3')
sg2744F1	GGGAGCATCGCCTCCTCGACATCTT-	*MAB_2744c*	35 bp -56 bp from the start of *MAB_2744c*
sg2744R1	AAACAAGATGTCGAGGAGGCGATGC-		
sg2744F2	GGGAGATCTTGTCCGGGCCCCACG		278 bp - 298 bp from the start of *MAB_2744c*
sg2744R2	AAACCGTGGGGCCCGGACAAGATC		
sg2745F1	GGGAGTACATCTGCTCCAGACGCATTATGA	*MAB_2745c*	1 bp – 21 bp from the start of *MAB_2745c*
sg2745R1	AAACTCATAATGCGTCTGGAGCAGATGTAC		
sg2745F2	GGGAGTGCGGATGCTTGTAGTGAT -		37 bp – 48 bp from the start of *MAB_2745c*
sg2745R2	AAACATCACTACAAGCATCCGCAC-3'		

*Underlined sequences indicate bases added to create compatible ends for cloning into the BsmBI site in pLJR962.

2.8.2 sgRNA cloning

The complementary sgRNAs were annealed by adding 4 µl of a 100 µM stock of each oligonucleotide and annealing buffer (50 mM Tris pH 7.5, 1 M NaCl, 0.5 M EDTA) in a 50 µl reaction. The oligonucleotides were denatured 95 ºC for 2 minutes, and then annealed by reducing the temperature by 0.1 ºC/ sec until a temperature 25 ºC was reached. The BsmBI restriction enzyme was used to excise the insert from the pLJR962 and allow insertion of the annealed oligonucleotides. The ligation was performed using 50 ng of linearized PLJR962 vector and 0.5 µl of the annealed oligos. Plasmid DNA was extracted from the resulting clones as described in (Section 2.6.1). The presence of the insert was confirmed by PCR using 2744F1, 2745F1 and CRISPRi primers and Sanger sequencing performed by Central Analytical Facilities (CAF) at Stellensoch University. The resulting plasmids are indicated in Table 5.

Table 5: Bacterial vectors and derivatives used in this study

Vector	**Description**	**Source**
pLJR962	CRISPRi backbone plasmid. Expresses the dCas9 protein. Contains Kanamycin resistance gene, and the BsmBI restriction enzyme site forsgRNA cloning.	Addgene
pLJR962-*2744c*-a	pLJR962 derivative containing the sgRNA that targets the *MAB_2744c* gene 35 bp from thestart codon.	This study
pLJR962-*2744c*-b	pLJR962 derivative. Contains the sgRNA that targets the *MAB_2744c* gene 278bp from thestart codon.	This study
pLJR962-*2745c*-a	pLJR962 derivative. Contains the sgRNA thattargets the *MAB_2745c* gene 1bp from the start codon	This study
pLJR962-*2745c*-b	pLJR962 derivative. Contains the sgRNA that targets the *MAB_2745c* gene 37 bp from thestart codon	This study

PJET	Blunt end cloning vector, ampicillin resistant, contains a restriction enzyme fragment disrupted by ligation into the cloning site.	This study
PUV	It contains an origin of replication, that was usedfor generating q PCR standards.	

2.8.3 Preparation of electrocompetent *M. abscessus*

A preculture was made by inoculating 5 ml of 7H9 with 100 µl of a *M. abscessus* glycerol stock and incubating at 37°C with shaking. In late log phase i.e., actively growing cells, the pre-culture was used to inoculate a larger culture volume using 1ml of culture in 40 ml of 7H9 OADC. The culture was grown until it reached an OD_{600nm} ~1 or slightly above. The cells were harvested by low-speed centrifugation 3 220 x *g* for 10 min using two 50 ml Falcon tubes at 4 ºC. The cells were kept cold for the rest of the procedure. The pellet was resuspended in 3 ml of 10 % glycerol containing 0,05 % Tween 80 using a 2 ml disposable pipette. After resuspending the cells, the volume was made up to 25 ml and the harvesting procedure was repeated. The washing procedure was repeated by resuspending the cells in the following volumes: 12.5 ml (2^{nd} wash), 6.25 ml (3^{rd} wash), 6.25 ml (final wash). After the final wash the cells were resuspended in the minimum volume required for the electroporations i.e., 400 ul / electroporation.

2.8.4 Electroporation of *M. abscessus*

Electrocompetent *M. abscessus* electrocompetent cells (400 µl) were placed in a 0.2 cm Gene Pulser electroporation cuvette (Bio-Rad) and mixed with 500 ng of purified plasmid DNA. The electroporation was done in the Gene Pulser Xcell™ (Bio-Rad) at 2.5 kV, 25 µF and 1000 Ω. After each electroporation, 800 µl of 7H9 OADC was added to each cuvette and incubated at 37 ºC overnight for cell recovery. The cells were plated on 7H10 plates containing kanamycin (50 µg/ ml). For integrating plasmids, 10^{-1} and 10^{-2} dilutions were made and 100 ul of undiluted cells, and of each of the dilutions was plated. Once all

the liquid was absorbed the plates were sealed the plates in a secondary container and incubated at 37 °C for 4 - 5 days. A positive vector control using pLJR962 and a no DNA control was also included. The strains generated in this study are indicated in Table 6.

Table 6: **The bacterial strains used in this study.**

Strains	**Description**	**Source**
E. coli DH5α	Genotype- Δ (argF-lac) 169	Lab stock
E. coli DH10B	Competent Cells, Genotype- F⁻*mcr*A Δ(*mrr-hsd*RMS-*mcr*BC) φ80*lac*ZΔM15 Δ*lac*X74 *rec*A1 *ara*Δ139 Δ(*ara-leu*)7697 *gal*U *gal*K *rps*L (Str^R) *nup*G	NEB
E. coli DH10B (pJET1.2)	DH10B carrying the PJET1.2 cloning vector containing the PUV Origin of replication	
E. coli DH10B (pLJR962-*2744c*-a	DH10B carrying the pLJR962 derivative	This study
E. coli DH10B (pLJR962-*2744c*-b	DH10B carrying the pLJR962 derivative	This study
E. coli DH10B (pLJR962-*2745c*-a	DH10B carrying the pLJR962 derivative	This study

E. coli DH10B (pLJR962-*2745c*-b	DH10B carrying the pLJR962 derivative	This study
M. abscessus (ATCC19977)	Reference strain isolated by Gupta *et al.* (2018)	ATCC
M. abscessus attB:: pLJR962	ATCC 19977 strain carrying the pLJR962 vector	This study
M. abscessus attB:: pLJR962-2744c-a	ATCC 19977 strain carrying CRISPRi plasmid pLJR962-*2744c*-a	This study
M. abscessus attB:: pLJR962-2744c-b	ATCC 19977 strain carrying CRISPRi plasmid pLJR962-*2744c*-b	This study
M. abscessus attB:: pLJR962-2745c-a	ATCC 19977 strain carrying CRISPRi plasmid pLJR962-*2745c*-a	This study
M. abscessus attB:: pLJR962-2745c-b	ATCC 19977 strain carrying CRISPRi plasmid pLJR962-*2745c*-b	This study

2.9 Gene expression analysis

2.9.1 RNA extraction and purification

The *M. abcessus* strains were grown to an OD_{600} of approximately 1.5 at 33 hours, and were harvested by centrifugation at 12 000 × g for 5 minutes and the pellet was resuspended in 1 ml of Pro-Blue solution, and transferred to blue cap tubes for storage at -80 ºC. The *M. abscessus* cells were disrupted by ribolyzing for 10 minutes at 50 hertz(H/ z), with 1 minute cooling on ice, and this was repeated 3 times. Cellular debris was cleared by centrifuging the lysate at 12 000 × g for 15 minutes. Approximately 700 µl of clear cell lysate was transferred to a 1.5 ml microcentrifuge tube. The tubes were incubated at room temperature for 5 minutes to promote dissociation of nucleoprotein complexes. Next, a volume of 300 µl chloroform was added to the samples, and the tubeswere centrifuged at 12 000 × g for 5 minutes. The top layer was separated from the bottomlayer by transferring into a new 2 ml tube. The samples were moved to the BSL1 on ice.

RNeasy^{R} Mini Kit was used for RNA purification. The RNeasy spin column was setup, an equal volume of 70 % ethanol was added to the samples, mixed and immediately 700 µl of the lysate including any precipitate that may have formed was transferred to the RNeasy spin column. The samples were centrifuged at 8000 × g for 15 sec. The collection tube was reused, and a volume of 350 µl of Buffer RW1 was added to the RNeasy spin column and the tubes were centrifuged at 8000 × g for 15 sec.

DNA contamination was removed by an on-column DNAse digest. A volume of 10 µl DNAse I stock solution (50mg/ ml) was added to 70 µl of ribosomal DNA (rDNA) Buffer, gently mixed by inverting the tube. The DNAse I incubation mix (80 µl) was added directly to the RNasy spin column membrane, for all the samples. The tubes were incubated at room temperature for 15 minutes before proceeding.

A volume of 350 µl of Buffer RW1 was added directly on to the RNeasy spin column, and the tubes were centrifuged at 8000 × g for 15 sec. The flow through was discarded and the RNeasy spin column was placed in a new 2 ml collection tube. A volume of 500 µl of Buffer RPE was added then centrifuged at 8000 × g for 15 sec. Another 500 µl of Buffer RPE was added directly onto the RNeasy spin column and centrifuged at 8000 × g for 1

minute to wash the spin column. The spin column was placed in a new Eppendorf tube and centrifuged at 8000 × g for 1 minute to ensure no ethanol carried over during the elution. The RNeasy spin column was placed in a new 1.5 ml collection tube and a volume of 30 µl of RNase-free water was added directly to the spin column membrane and the tubes were centrifuged at 8000 × *g* for 1 minute to elute the RNA. The RNA samples were sent for TapeStation analysis at the Central Analytical Facility at Stellenbosch University to obtain the RNA integrity number (RIN) values, which were expected to be 8 and above if the RNA was of good quality and integrity.

The denaturing RNA gels (formaldehyde method) was used for running RNA gels. The gel was first prepared by heating 0.5 g agarose using 36 ml water and cooled to 60 ºC., followed by the addition of 5 ml 10 x 3-(N-morpholino) propanesulfonic acid (MOPS) running buffer (0.4 g MOPs (contains ethidium bromide), pH 7.0, 0.1 M sodium acetate, 0.01 M EDTA) and another 9 ml of 37 % fomaldehyde (stock concentration 12.3 M). A volume of 5 µl of the RNA sample was mixed with 15 µl formaldehyde loading dye. The samples were heated and denatured between 65 ºC for 15 minutes. The gel was loaded, and electrophoresis occurred at 70 V for 90 minutes before visualization.

2.9.2 Turbo DNase Treatment

The Turbo DNase treatment was used to remove any residual DNA that could have been contaminating the RNA. The reaction mix was prepared in 200 µl PCR tubes. The Turbo DNase Treatment was performed in 10 µl and contained 1111 ng RNA, Turbo DNase buffer 1 x, Turbo DNase at a final concentration of 0.04 U/ µl. Only half of the Turbo DNase was applied at first, followed by a 30- minute incubation at 37 °C in a PCR machine, and then the remaining Turbo DNase was added and incubated for another 30 minutes. A volume of 1 µl resuspended DNase Inactivation Reagent was added and mixed well. The samples were incubated for 5 minutes at room temperature, mixing occasionally. This was followed by centrifuging at 10,000 × g for 1.5 minutes to pellet the DNase Inactivation Reagent. The RNA was carefully transferred to a fresh tube.

2.9.3 Transcriptor First Strand CDNA synthesis

The RNA samples were placed on ice and the cDNA Transcriptor First Strand components were thawed and centrifuged before setting up the reactions. The reaction mixture was performed in 200 µl PCR tubes. Initially, the RNA (final concentration between 500 and 2000 ng and 10 µM of the RT primers: *sigA* (5'-CTCACGCGCGTACTGCTGGATT) and *MAB_2744c* (5'-GAGCTGCTCCCGACCATCGT) were added in a volume of 20 µl. The samples were mixed, and the template-primer mixture was denatured by heating the tube for 10 minutes at 65 °C in a PCR block cycler and immediately cooled on ice. The remaining components of the RT mix were added in the following order: the transcriptor reverse transcriptase reaction buffer at a final concentration of 1 ×, 20 U/ µl protector RNase inhibitor, 10 µM deoxynucleotides, 10 U/ µl transcriptor reverse transcriptase (volume of 0.5 µl. The RT negative controls had no Transcriptor reverse transcriptase added. The reagents were mixed and briefly centrifuged then placed in a PCR block cycler with a heated lid to minimize evaporation. The RT primers were sequence specific therefore the samples were incubated at 55 °C for 30 minutes. Following, the Transcriptor reverse transcriptase was inactivated by heating to 85 °C for 5 minutes then cooled to 4 °C. The complimentary DNA (cDNA) was stored at -20 °C prior to qPCR analysis.

2.9.4 Generation of qPCR standards

The qPCR standards were generated by cloning the *sigA* and *mab2744c* genes into the pJET1.2 plasmid. The genes were amplified by PCR (section 2.7) using primers (2744stdF and 2744stdR, SigAstdF and SigAstdR indicated in Table 1. Purified PCR products were cloned into pJET1.2 using the CloneJet kit. Using the DNA concentration obtained from plasmid extraction, a stock of each plasmid containing 10^7 molecules/µl for both *mab2744c* and *sigA* was prepared. A 10-fold dilution series from 10^6 to 10^2 molecules/ µl was used to generate a standard curve for qPCR

2.9.5 Quantitative PCR (qPCR)

The KAPA SYBR® FAST qPCR Kit Master Mix (2X) Universal was used to perform real-time quantitative PCR (qPCR). Each reaction contained 2X KAPA SYBR® FAST qPCR

Master Mix Universal at final concentration of 1 X, 200 nanomolar (nM) forward and reverse primers (indicated in Table 1) The cDNA for the reactions was reversed transcribed from the extracted RNA samples, described in (Section 2.9.3). Reactions were placed in a cooling block during set-up, and the block was wrapped in foil to shield from light prior to loading in the instrument. The qPCR was performed on a Rotor-Gene® Q 6000 62HO-100 instrument, and a run profile was set up using the Rotor-Gene Q software. The qPCR program included a 95 °C activation step for 3 minutes, followed by 40 cycles of 95 °C for 5 s, 60 °C for 15 s, and 72 °C for 5 s and measurement of the fluorescein SYBR green was measured using an excitation of 470 ± 10 nm and a detected at 510± 10 nm for 40 cycles, although the first 10 cycles can be ignored since there will not be any amplification observed.

Amplification was monitored by measurement of the Synergy Brands Inc (SYBR) green fluorescence (59 nm). Following the last cycle, the Rotor-Gene® Q 6000 62HO-100 generates standard curve and melting curve permitted temperature was between 35 and 99 ºC. When performing a normal melt, the temperature is increased by 1 ºC increments, with a 5-second delay between each acquisition. The minimum temperature step hold time varies depending on the number of degrees between each step. The cycle number at which the amplification curve crosses a detection threshold is referred to as the CT value. The standard curve is plotted by using CT values against Concentration. A scatter plot and a line of best fit are drawn, the best fit line depicts the data and can either pass through some, all, or none of the points. The CT value for each sample is determined by setting a threshold line and calculating the intersection with each curve. The machine automatically calculates the CT values and the concentration from the given standards. The standard curve generates the reaction efficiency of the run. The R^2 value is the percentage of data that supports the hypothesis that the standards form a standard curve. If the R^2 is low, the standards will be difficult to fit onto the best fit line. This implies that the reaction outcomes are (the calculated concentrations) may not be accurate. A good R^2 value is around 0.999 percent. To get the relative expression of each CRISPRi strain,

the copy number of the *mab2744c* gene is expressed relative to the copy number of the reference gene *sigA*.

3.1 Design of sgRNA for transcriptional silencing by CRISPRi

A mycobacterial CRISPRi system was developed by Rock *et al.* (2017) and has been used in *M. smegmatis* and *M. tuberculosis*. In this study we investigated if the system could be used for transcriptional silencing in *M. abscessus*. To do this, PAM sequences were identified on the template strand of the *sufT* gene (*MAB_2744c*), and the upstream gene (*MAB_2745c*). Using the published predicted PAM sequence silencing efficiencies [102], 4 single guide RNAs (sgRNA) were designed, two located in *MAB_2744c* and two located in *MAB_2745c* (Figure 3.1). The CRISPRi system was previously shown to silence downstream genes located in the same operon. Since *MAB_2745c* and *MAB_2744c* are operonic, the sgRNAs targeting *MAB_2745c* were designed to evaluate the efficiency of silencing the downstream *MAB_2744c* gene. Only a small fragment of *MAB_2745c* was targeted because the PAM sequence was located at the end of the gene. The position of the sgRNA is determined by the presence of a PAM sequence.

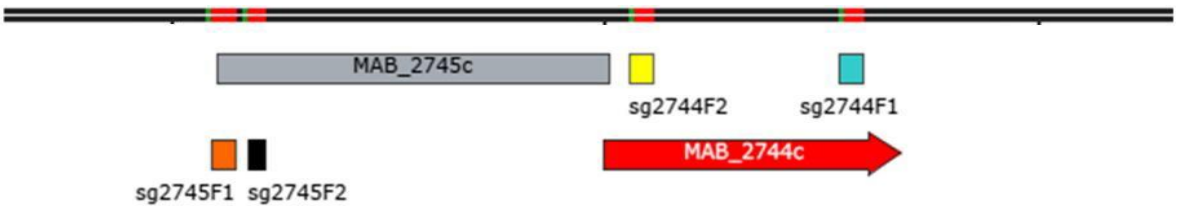

Figure 3. 1: Design of sgRNA.

(A) A Snap-Gene Viewer map showing the positions of the PAM sequences (green) and 4 sgRNA (red) present on the *M. abscessus* genome. The locations of the sgRNA on *MAB_2744c* (red) and the upstream gene, *MAB_2745c* (grey). The sgRNA are represented by squares that are highlighted in different colours, sg2745F1 – orange, sg2745F2 – black, sg2744F2 – yellow and sg2744F1 – blue.

3.2 Generation of knock-down vectors

To construct knock-down vectors for *MAB_2744c* and the upstream gene *MAB_2745c*, the CRISPR interference pLJR962 vector was used. The pLJR962 vector encodes a

catalytically dead Sth1 dCas9 nuclease under the control of a tetracycline-inducible promoter and the BsmBI restriction enzyme cloning sites for sgRNA insertion. Restriction enzyme digestion with BsmBI was performed on the pLJR962 vector, creating sticky ends for directional sgRNA oligo cloning (Figure 3.2). The undigested plasmid gives multiple bands, which appears as a less defined band, and the digested is shown by a single sharp band indicating the linear form.

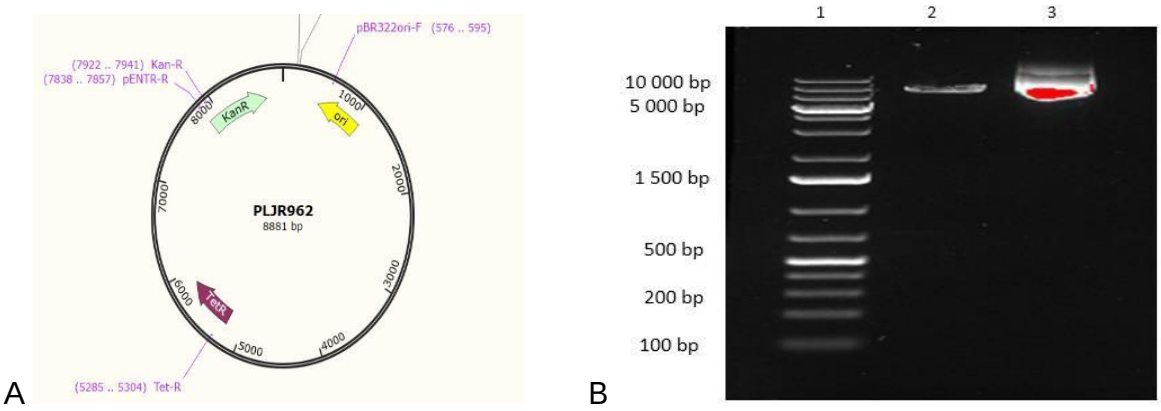

Figure 3. 2: Restriction map and restriction enzyme digestion of pLJR962.

(A). Map of the pLJR962 vector used for co-expression of dCas9 and sgRNAs, showing the positions of BsmBI restriction enzyme cut sites at 163 and 188 bp. (B). Agarose gel electrophoresis of pLJR962 after restriction enzyme digestion with the BsmBI enzyme. Lane 1 showing the 1 KB Plus DNA Ladder, lane 2 showing the digested pLJR962 vector-expected band size 8906 bp, lane 3 undigested pLJR962 vector.

Following annealing of the sgRNA oligonucleotides, ligation into the BsmBI digested pLJR962 vector was performed. *E. coli* transformed with the ligation reactions were selected on plates containing kanamycin. The resulting transformants were screened by colony PCR to verify the presence of the sgRNA insert (264 bp) (Figure 3.3). Agarose gel electrophoresis gels show the result of colony PCR performed on competent *E. coli* cells that contained pLJR962 plasmids cloned with 264 bp inserts. The forward primers used were the sgRNA oligo sg2744F1, which binds from 35 bp to 56 bp from the start of *MAB_2744c*, and the oligo sg2744F2, which binds from 1 bp to 21 bp from the start of *MAB_2745c*, and the CRISPRi reverse sequencing primer, which binds 186 bp from the Bsmbi enzyme start site of the pLJR962 vector was used. If the insert had been

successfully cloned into the plasmid, colony PCR using the reverse sequencing primer would amplify the insert fragment size (264 bp) as shown on the resultant gels in Figure 3.3. All positive clones were sent for Sanger sequencing (Figure 3.4).

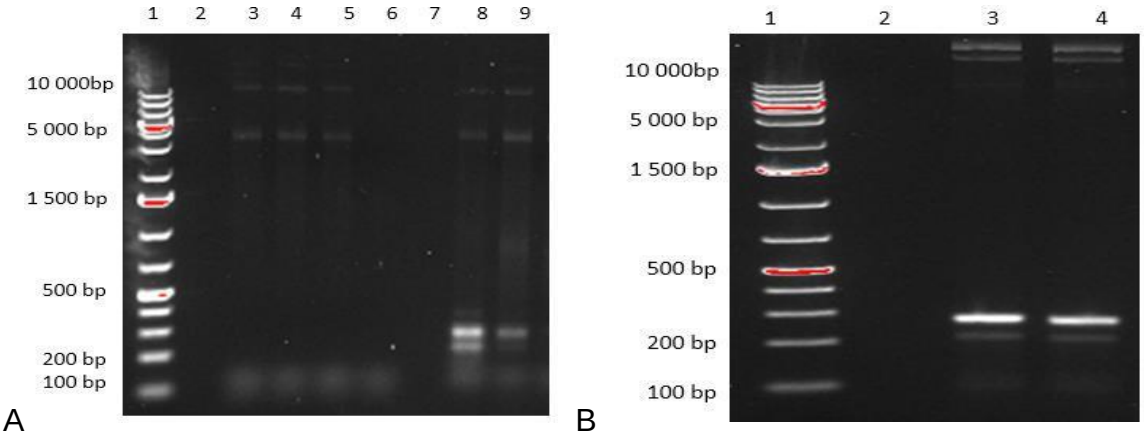

Figure 3. 3: Colony PCR screening of CRISPRi vectors targeting *MAB_2744c* and *MAB_2745c*

The 2 gels highlight the different inserts present in the different *M. abcessus* strains i.e., gel (A) Lane 1 showing the 1 KB Plus DNA Ladder, lanes 2 – 6 had no expected bands observed, lane 7 had no template control, lane 8 showing the screening of pLJR962-*2744c*-a and lane 9 showing the screening of pLJR962-*2744c*-b. (B) Lane 1 showing the 1 KB Plus DNA Ladder, lanes 2 had the no template control, lane3 showing the screening of pLJR962-*2745c*-a, and lane 4 showing the screening of pLJR962-*2745c*-b.

Following identification of the sgRNA insert in the pLJR962 vector, the sequencing was performed at CAF using the CRISPRi sequencing primer (Table 3).

A

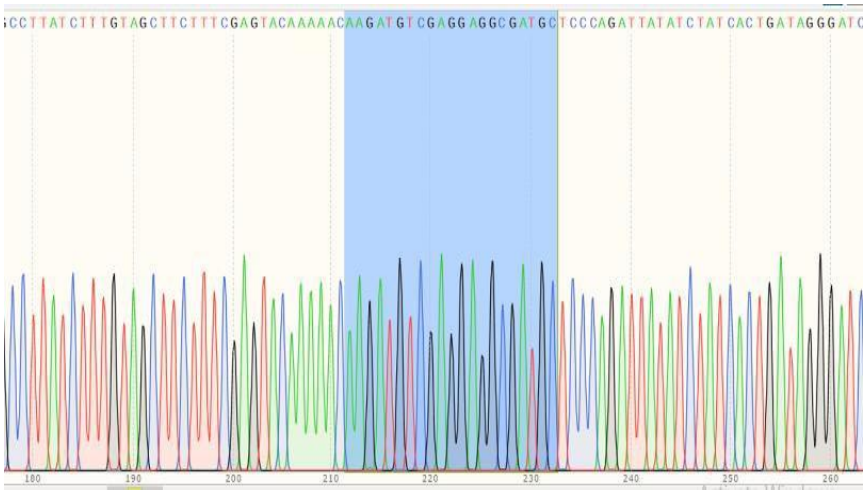

B

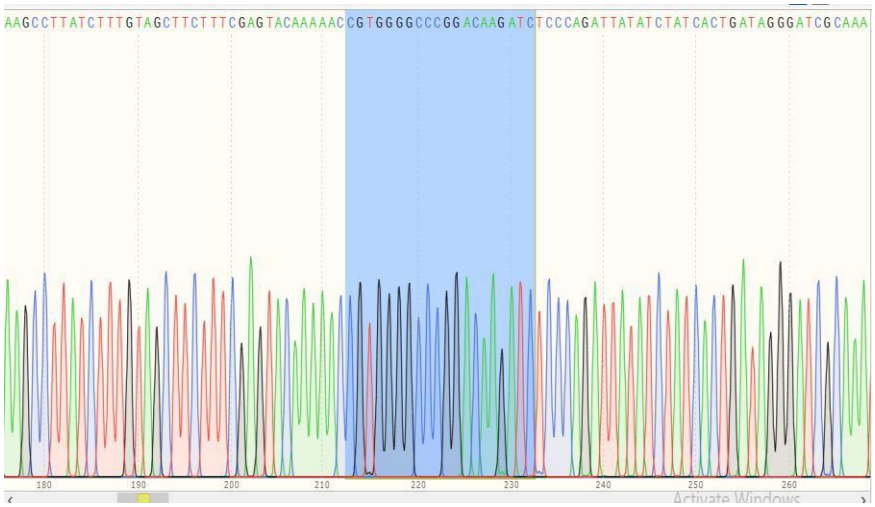

C

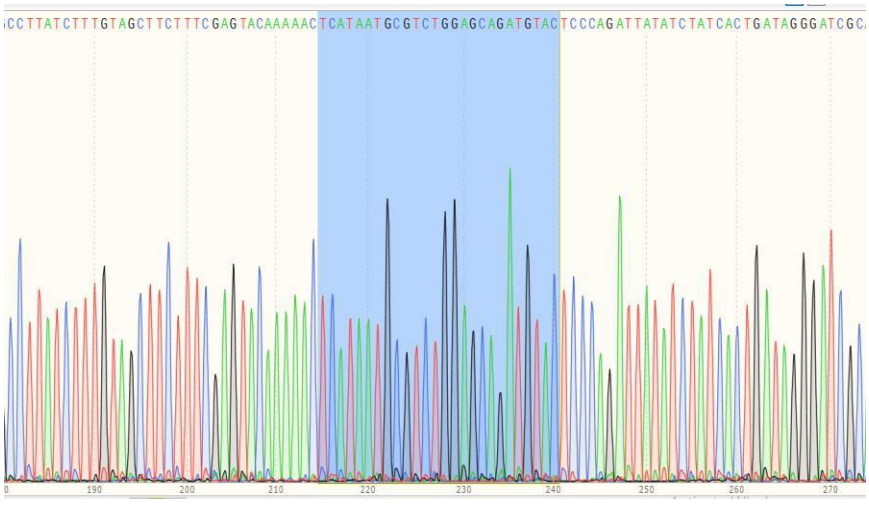

D

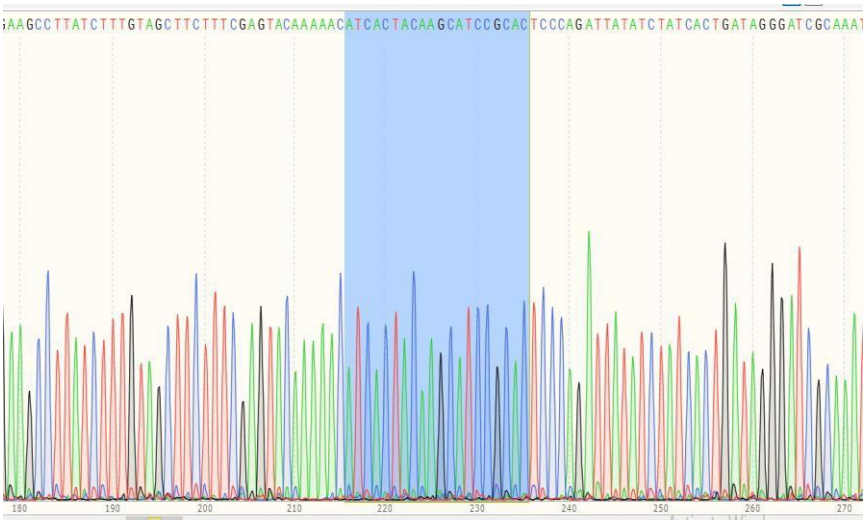

Figure 3. 4: Sanger sequencing results for CRISPRi vectors.

pLJR962 mutiple cloning site showing BsmBI restriction site on either side of the cloned sgRNA sequences highlighted in blue. (A) Confirming the presence of sg2744F1 (5'-GCATCGCCTCCTCGACATCTT-3') in pLJR962-*2744c*-a. (B) Confirming the presence of sg2744F2 (5'- GATCTTGTCCGGGCCCCACG-3' in pLJR962-*2744c*-b. (C) Confirming the presence of sg2745F1 (5'- GTACATCTGCTCCAGACGCATTATGA-3') in pLJR962-*2745c*-a. (D) Confirming the presence of sg2745F2 (5'- GTGCGGATGCTTGTAGTG AT-3') in pLJR962-*2745c*-b.

3.3 Generation of *M. abscessus* knock-down strains

To create knockdown mutants in *M. abcessus* (ATCC 19977), we employed electroporation to transform *M. abscessus* with the generated CRISPRi vectors, and the pLJR962 vector as a control. To confirm the presence of the plasmids in the transformants, colony PCR was performed on the clones using primers targeting the kanamycin resistance gene in backbone of pLJR962. The expected band product size of 900 bp (Figure 3.5) was observed for all strains (Table 6)

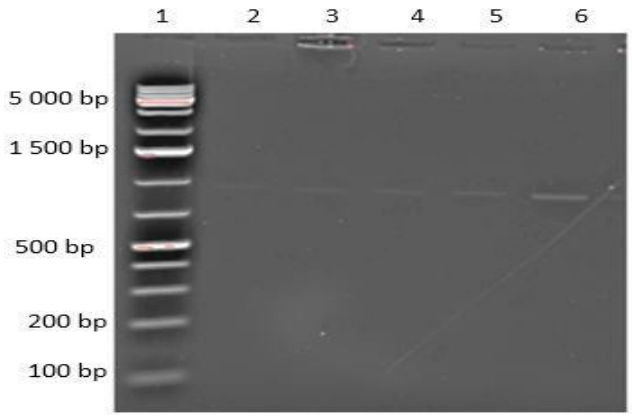

Figure 3. 5: Confirmation of the *M. abscesus* knock-down strains.
Agarose gel of colony PCR of the *M. abcessus* tranformants. Lane 1 showing the 1 KB Plus DNA ladder, lane 2 showing *M. abscessus attB*::, lane 3 showing *M. abscessus attB*:: pLJR962-*2744c*-a, lane 4 showing *M. abscessus attB*:: pLJR962-*2744c*-b, lane 5 showing *M. abscessus attB*:: pLJR962-*2745c*-a and lane 6 showing *M. abscessus attB*:: pLJR962-*2745c*-b. Positive amplification for the *M. abcessus* strains confirmed the presence of the kanamycin gene (816 bp).

3.4 Growth of *M. abscessus* CRISPRi strains under standard conditions

After successfully generating the *M. abscessus* CRISPRi strains, *M. abscessus attB*:: pLJR962, *M. abscessus attB*:: pLJR962-*2744c*-a, *M. abscessus attB*:: *pLJR962-2744c*-b, *M. abscessus attB*:: pLJR962-*2745c*-a and *M. abscessus attB*:: pLJR962-*2745c*-b, their growth phenotype was compared under standard growth conditions in 7H9 OADC media supplemented with 0.05 % Tween 80 (Figure 3.6 A). The growth curve was in lag phase for the first 24 hours, reaching an OD between 1 and 2, while exponential phase occurred between 27 and 48 hours, reaching an OD of between 8 and 9 at 48 hours. No difference between the growth of the different CRISPRi mutants or the control strain (pLJR962) was observed without sgRNA induction.

Simultaneously, colony forming units (CFUs) were plated at 0, 24 and 48 hours (Figure 3.6 B). This was done in order to estimate the cell densities in the liquid cultures. The CFUs for all strains ranged between 1 x $10^{7}$and 1x 10^{8} at 0 hours, then steadily grew to

between 1 x 10^{10} and 1 x 10^{11} at 24 hours, and finally plateaued remaining around 1 x 10^{11} at 48 hours, indicating that the cells had achieved stationary phase.

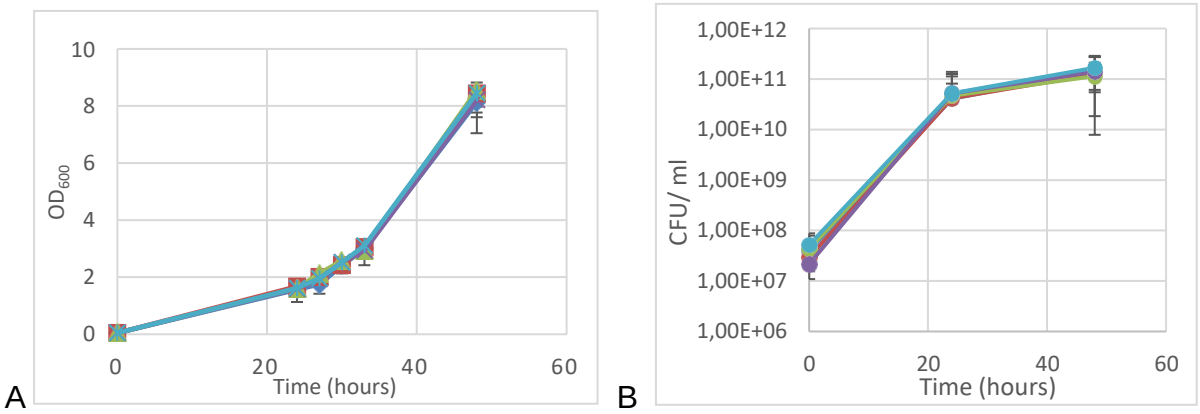

Figure 3. 6: Growth of M. abscessus CRISPRi strains under standard conditions.

(A) Growth of the *M. abscessus* CRISPRi strains in 7H9 media supplemented with 0.05 % Tween 80 and 10 % OADC was monitored by optical density at 600 nm. *M. abscessus attB*:: pLJR962 (blue), *M. abscessus attB*:: pLJR962-*2744c*-a (orange), *M. abscessus attB*:: *pLJR962-2744c*-b (grey), *M. abscessus attB*:: pLJR962-*2745c*-a (yellow) and *M. abscessus attB*:: pLJR962-*2745c*-b (light blue). The data represents the mean and standard deviation of three biological replicates. (B) Colony forming units per milliliter (CFU/ ml) were used to assess bacterial growth. The data represents the mean and standard deviation of three biological replicates.

3.5 Determination optimal anhydrotetracycline (ATc) concentration

When induced with ATc, the CRISPRi system enables gene knockdown by sterically preventing transcription of a gene of interest through binding of the sgRNA and a catalytically inactive Cas9 endonuclease. The CRISPRi strains were individually assessed to determine the effect of CRISPRi on cell growth and viability by spotting cells on rich 7H10 medium with and without anhydrotetracycline (ATc) (Figure 3.7). Three ATc concentrations were tested (0, 100 and 500 µg/ µl) and no difference was observed between the 3 concentrations. Therefore, 100 ng/ µl ATc was used for all subsequent experiments.

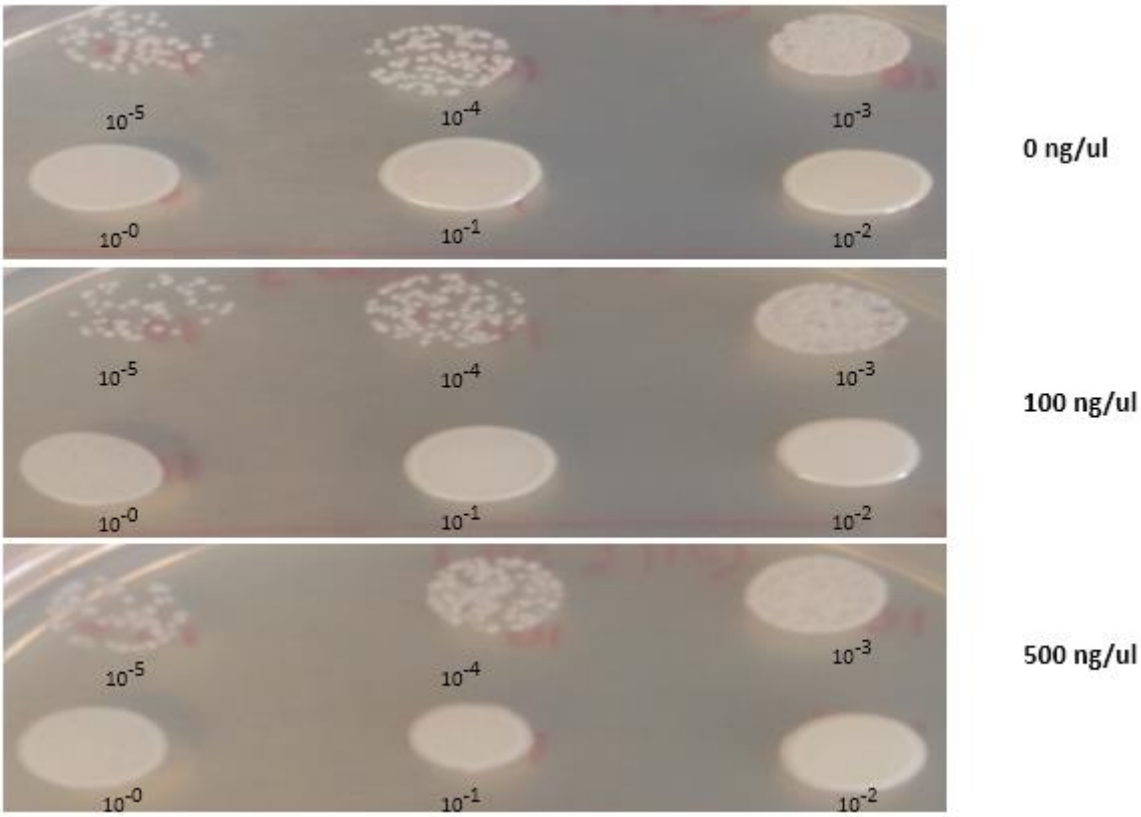

Figure 3. 7: **Determination optimal anhydrotetracycline (ATc) concentration.**

Growth of CRISPRi strains on solid media containing different ATc concentrations. Showing the *M. abscessus attB*:: pLJR962-*2744c*-a strain. The assay was done in 3 biological replicates for all strains. Image show representative result and no difference in growth was observed at the three concentrations.

3.6 Growth of *M. abscessus* CRISPRi strains in defined media with and without iron

A *sufT* mutant was previously created in *M. smegmatis* to examine the effect of the loss of *sufT* under iron limitation. The authors showed the *sufT* mutant was unable to grow under conditions of iron deprivation. To determine if *sufT* plays a similar role in *M. abscessus*, the CRISPRi strains were subjected to growth in chelated Sauton's media with and without ATc (iron limitation) and in the presence of 2 µM and 200 µM Fe, with and without ATc. At 48 hours, the cultures containing 200 µM Fe curves reached a maximum OD_{600} of 2, while at 24 hours the OD_{600} was about 0.5. When compared to the cultures containing 2 µM Fe, these also grew to a maximum OD_{600} of 2 with an OD_{600} of 0.3 to 0.5 at 24 hours. This suggests that 2 µM Fe meets the cellular requirements for

planktonic growth of *M. abscessus*. When comparing the growth in the absence of supplemental iron to cultures with 2 µM Fe, there was no difference observed up to 33 hours. At 48 hours, cultures without supplemental iron reached an OD about 0.5 lower than cultures containing iron. In strains, the addition of ATc had no effect on the growth either in the presence or the absence of iron. Taken together, the data suggests that either i) *sufT* has no role in the survival of the CRISPRi strains under iron limiting conditions or that ii) transcriptional silencing is not occurring. To differentiate between these possibilities, expression analysis was performed.

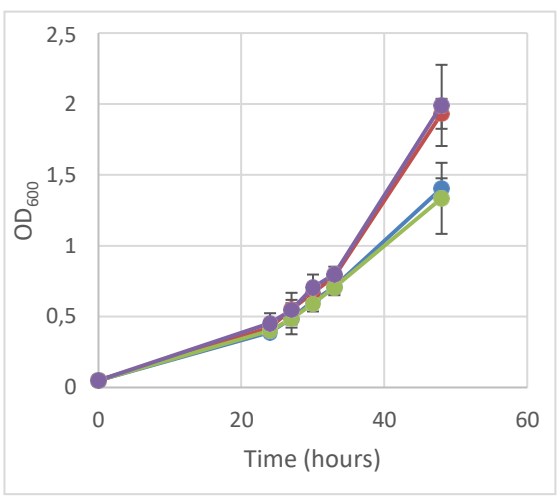

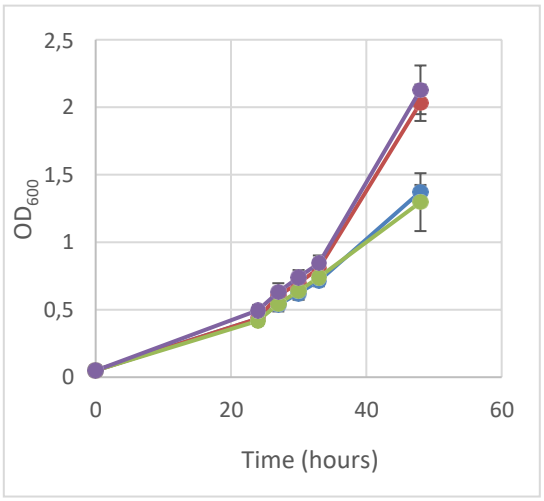

C

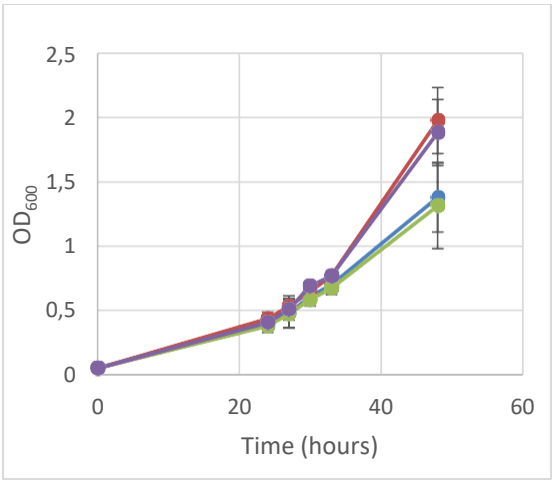
2,5
2
1,5
1
0,5
0
OD600
0
20
40
60
Time (hours)

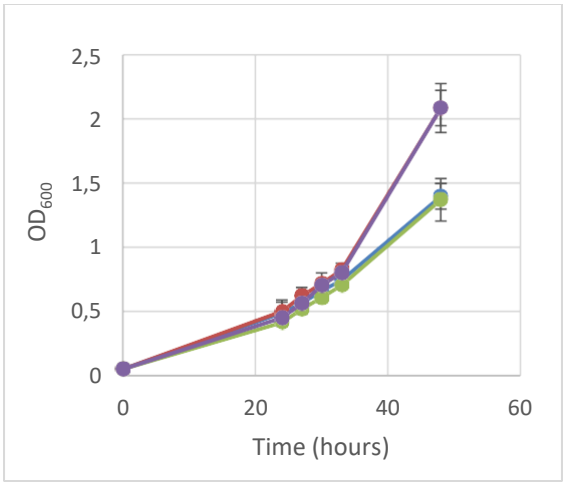
2,5
2
1,5
1
0,5
0
OD600
0
20
40
60
Time (hours)

D

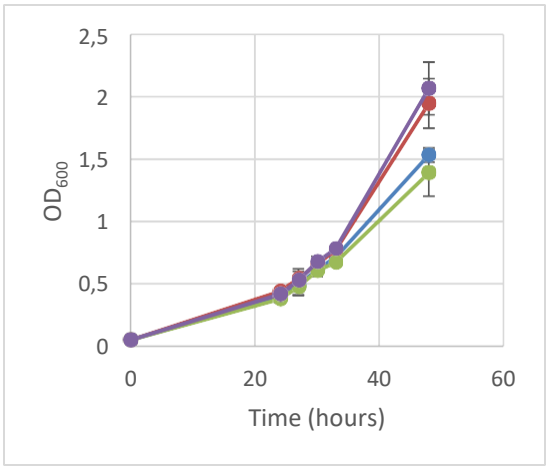
2,5
2
1,5
1
0,5
0
OD600
0
20
40
60
Time (hours)

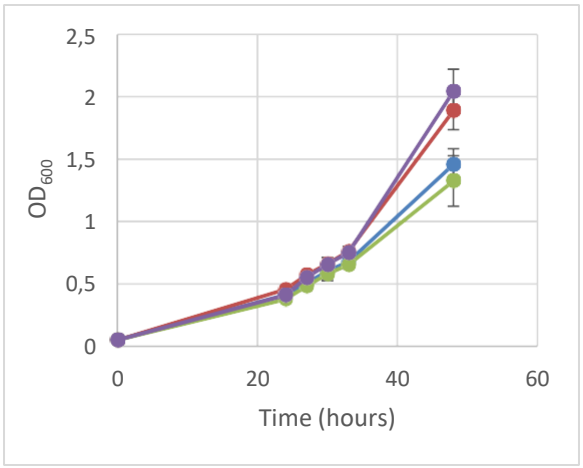
2,5
2
1,5
1
0,5
0
OD600
0
20
40
60
Time (hours)

E

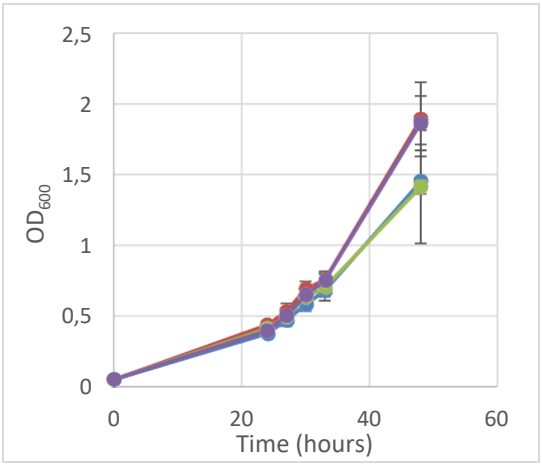
2,5
2
1,5
1
0,5
0
OD600
0
20
40
60
Time (hours)

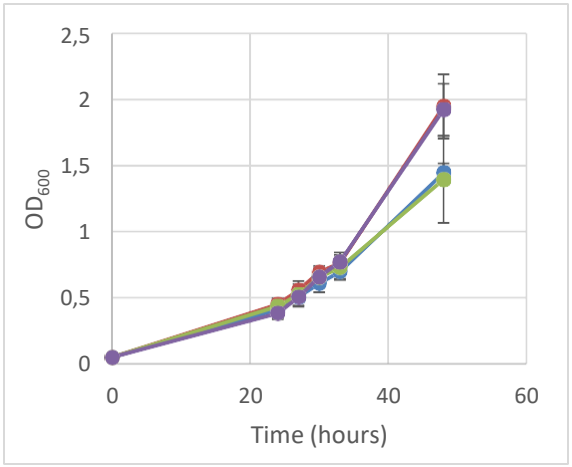
2,5
2
1,5
1
0,5
0
OD600
0
20
40
60
Time (hours)

Figure 3. 8: Growth of *M. abscessus* CRISPRi strains in defined media with and without iron.

Left panel showing the growth of (A) *M. abscessus attB:* pLJR962 (B) *M. abscessus attB::* pLJR962-*2744c*-a, (C) *M. abscessus attB::* pLJR96*2-2744c*-b, (D) *M. abscessus attB::* pLJR962-*2745c*-a and (E) *M. abscessus attB::* pLJR96*2-2745c*-b in Sauton's media with 0.05 % Tween 80, in the presence of 200 µM Fe. Right panel showing the growth of (A) *M. abscessus attB:* pLJR962 (B) *M. abscessus attB::* pLJR962-*2744c*-a, (C) *M. abscessus attB::* pLJR96*2-2744c*-b, (D) *M. abscessus attB:: pLJR962-2745c*-a and (E) *M. abscessus attB::* pLJR96*2-2745c*-b in Sauton's media with 0.05 % Tween 80, in the presence of 2 µM Fe. Green represents cultures grown in no Fe and no ATc, red represents cultures grown in either 200 µM or 2 µM Fe and no ATc, blue represents cultures grown in no Fe and 100 ng/ µl ATc and purple represents cultures grown in either 200 µM of 2 µM Fe and 100 ng/ µl ATc. The mean and standard deviation of three biological replicates is represented.

3.7 Determination of the level of transcriptional silencing in knock-down strains

We sought to determine the level of transcriptional silencing of *MAB_2744c* by using RT-qPCR to estimate the amount of RNA transcript in the presence and absence of ATc inthe 5 strains. To investigate the expression of the *MAB_2744c* and *sigA* we created qPCRstandards for both genes. The gene regions were amplified by PCR from *M. abscessus*genomic DNA (Figure 3.1) and cloned into the pJET 1.2 vector (Table 5). The presenceof the inserts was confirmed by restriction enzyme digestion (Figure 3. 2)) and Sangersequencing (Figure 3.4). Two qPCR primer sets were designed for each gene (Table 3).The qPCR primers were tested by creating 10-fold serial dilutions of the plasmidstandards (10^2 - 10^6 copies/ reaction), and their efficiency as well as the linear range ofamplification determined (Figure 3.9) Melt curve analysis was used to confirm primerspecificity. For every run, a standard curve was generated and R^2 values of above 0.99 %
were used. An example of the standard curves can be seen in Appendix 1.

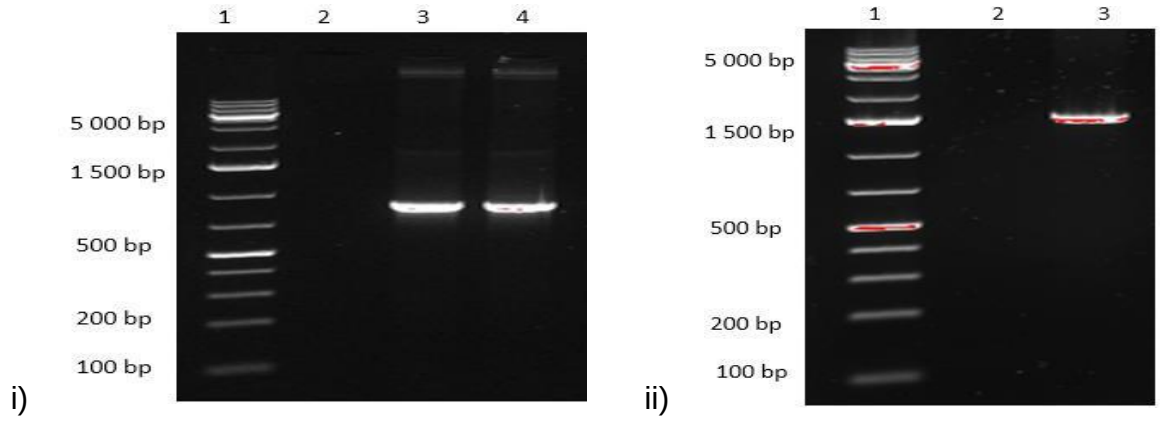

Figure 3. 9: Generation of DNA standards for qPCR

Amplification of the *MAB_ 2744c* and *MAB_2745c* (997 bp) region, and *sigA* (1676 bp) by Phusion HS using the MAB_2744cstdF1 and MAB_2744cstdR1; and SigAstdF1 and SigAstdR1 respectively. Figure 3.9 (i) Lane 1 shows the 1KB Plus DNA ladder, lane 2 shows the no template control, lane 3 shows the amplification of *MAB_ 2744c* and the upstream gene *MAB_2745c* (997 bp) total size, lane 4 shows the amplification of *MAB_ 2744c* and the upstream gene *MAB_2745c* (997 bp) total size. Figure 3.9 (ii) lane 1 shows the 1KB Plus DNA ladder, lane 2 has the no template control lane 3 shows the amplification *sigA* gene (1676 bp) total size.

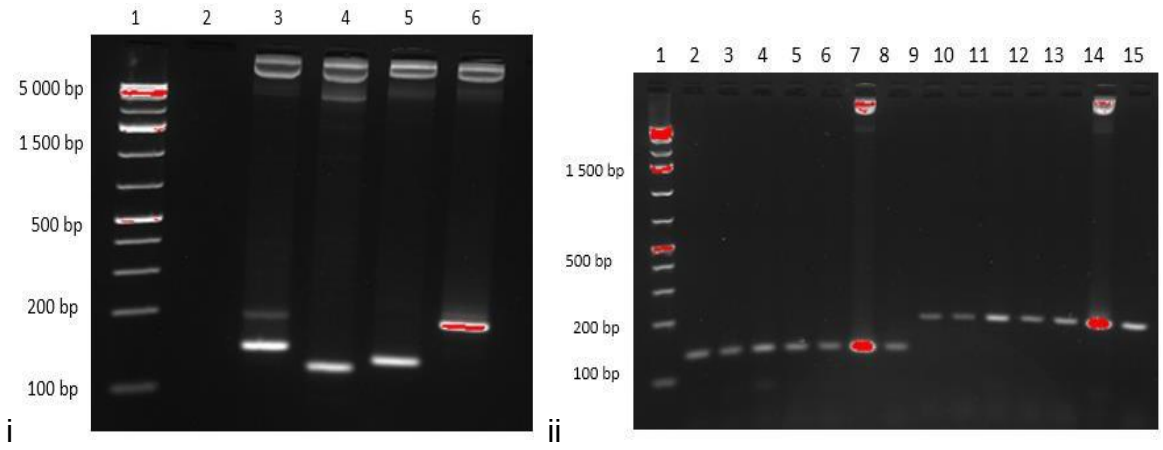

Figure 3. 10: Testing of primers for qPCR.

The DNA qPCR standards for *sigA* and *MAB_2744c* genes were used to test qPCR primer sets. (i) the lane 1 shows the 1KB Plus DNA ladder, lane 2 has the no template control, lane 3 shows the 136bp qPCR amplicon obtained using MAB_2744c qPCR F2 and *MAB_2744c* qPCR R2, lane 4 shows the 114 bp qPCR amplicon obtained from using Sig A qPCR F2 and SigA qPCR R2, lane 5 shows the 116 bp qPCR amplicon obtained from using SigA qPCR F1 and SigA qPCR R1, lane 6 shows the 137bp qPCR fragment obtained from using *MAB_2744c* qPCR F1 and *MAB_2744c* qPCR R1. (B) (ii) the *sigA* and *MAB_2744c* DNA templates were diluted from the 10^7 copies/ ul DNA stock to 10^2 copies/ ul. Lane 1 shows the 1KB Plus DNA ladder, lanes 2-7 show the amplification when 10^7, 10^6, 10^5, 10^4, 10^3 and 10^2 copies of sigA DNA were included in the reaction. Lane 8 shows amplification of the positive control. Lane 9 to 14 shows amplification when 10^7, 10^6, 10^5, 10^4, 10^3 and 10^2 copies of *MAB_2744c* DNA was included in the reaction. Lane 15 shows amplification of the positive control.

3.8 RNA quality analysis

All the *M. abcessus* CRISPRi cultures were grown with and without 50 ng/ µl ATc for 32 hours to an OD_{600} of approximately 1.5. The cells were immediately harvested, resuspended in RNA Pro-Blue solution then stored temporarily at -80 ºC. Following extraction and purification, the RNA was visualised by denaturing agarose gels using the High range RNA ladder using the 16s and 23s genes as an indication of integrity. Examples of gels are shown in Figure 3.11. For samples where 16s and 23s bands were

visible, the RNA samples were sent for TapeStation RNA analysis at CAF to obtain the RNA integrity number (RIN). These allowed us to evaluate the quality of the RNA produced. For high quality RNA we expected a RIN value of 8 and above. From the results obtained, all the RIN values were above 8. Upon completion, the RNA was reverse transcribed into cDNA using the cDNA synthesis kit. A no-RT control was included, and qPCR on these samples were used to confirm the absence of DNA contamination. The knockdown of CRISPRi targets was then quantified by quantitative real-time PCR using SYBR green dye.

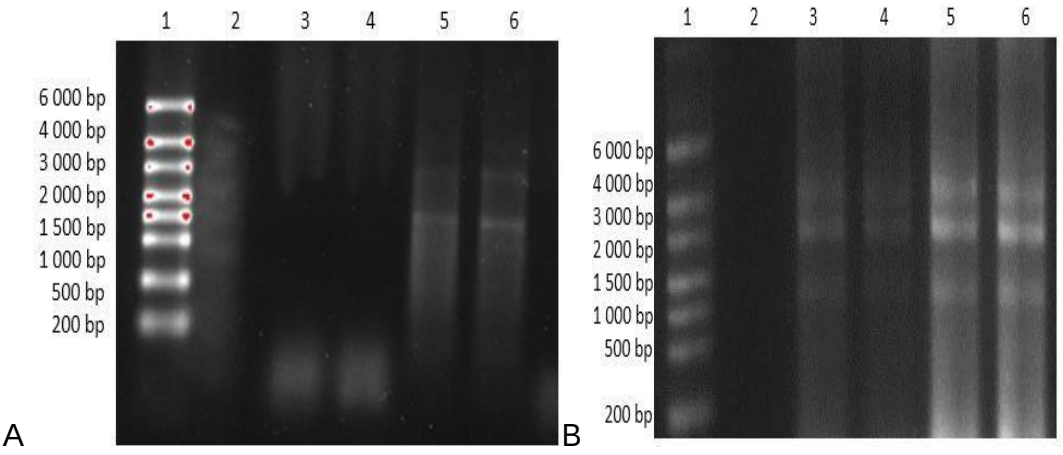

Figure 3. 11: Denaturing RNA agarose gel to confirm RNA integrity.

(A) lane 1 shows the High Range RNA ladder, lanes 2, 3 and 4 had no RNA observed, lane 5 shows the expected RNA 16s and 23s bands for RNA extracted from *M. abscessus attB*:: pLJR962 and lane 6 shows *M. abscessus attB*:: pLJR962-*2744c*-a strain, without ATc addition. (B) lane 1 shows the High Range RNA ladder, lane 2 has no amplification, lane 3 shows *M. abscessus attB*:: pLJR962, lane 4 shows *M. abscessus attB*:: pLJR962-*2744c*-a and lane 5 shows *M. abscessus attB*:: *pLJR962-2744c*-b and lane 6 shows *M. abscessus attB*:: pLJR962-*2745c*-a, all with the addition of ATc.

Further, the real time experiments were done in 3 replicates for both *MAB_2744c* and *sigA* DNA. The expression was determined by dividing the concentration values of *MAB_2744c*

with the reference gene *sigA* concentrations. The samples are shown in (Table 7), however no difference was observed between all the strains. In each run, a standard curve was done to determine the cycle threshold and the concentration in each of the samples. Table 7 also shows the replicates concentrations and the mean concentration values ± SD.

Table 7: RT qPCR expression data and t-test values. The average concentrations for 3 replicates are shown. A statistical t-test was done, and the p-values are highlighted in the table.

Strains		**Replicate 1**	**Replicate 2**	**Replicate 3**	**Mean ± SD**	**P - value**
M. abscessus attB:: pLJR962	+ATc	4.91	1.81	9.65	5.46 ± 3.95	0.234915
	-ATc	2.69	1.95	2.13	2.25 ± 0.38	
M. abscessus attB:: pLJR962-*2744c-a*	+ATc	1.81	1.31	1.99	1.71 ± 0.36	0.803606
	-ATc	3.66	6.06	1.58	1.95 ± 1.56	
M. abscessus attB:: pLJR962-*2744c-b*	+ATc	5.30	1.28	3.73	3.44 ± 2.03	0.760298
	-ATc	1.34	5.57	1.64	2.85 ± 2.36	
M. abscessus	+ATc	7.34	3.60	1.78	4.24 ± 2.83	0.358052

attB:: pLJR962-*2745c-a*	-ATc	0.90	4.42	1.22	2.18 ± 1.95	
M. abscessus attB:: pLJR962-*2745c-b*	+ATc	4.73	2.26	2.68	3.22 ± 1.32	0.761397
	-ATc	5.60	4.92	0.793	3.77 ± 2.60	

3.9 Growth of *M. abscessus* CRISPRi strains as biofilms

Mycobacteria are known to clump together at air and media interface creating pellicle biofilms [95]. Since iron was previously discovered to be essential for biofilm maturation in *M. smegmatis*, we sought to investigate if it was also required for biofilm maturation in *M. abscessus*. In the present study, the ability of the *M. abscessus* attB:: pLJR962, *M. abscessus* attB:: pLJR962-*2744c*-a, *M. abscessus* attB:: pLJR962-*2744c*-b, *M. abscessus* attB:: pLJR962-*2745c*-a and *M. abscessus* attB:: pLJR962-*2745c*-b strains to form biofilms was determined in defined media with and without iron, in the presence and absence of ATc. When the strains were grown in static liquid culture without Tween 80, the cells settled at the bottom of the wells. They had a thick rigid structure which was difficult to disrupt, although some of the wells also had cells in suspension (Figure 3.12).

Crystal violet staining was used to quantify biofilm formation. The highest absorbance values were observed in the ATCC1997 the parent strain and the *M. abscessus* attB:: pLJR962 control strain. When comparing the CRISPRi strains for one condition (i.e., no supplemental iron or 2 µM Fe) the average ODs differed by less than 1, while the standard deviations for the replicated ranged from 0.20 to 0.92. There was no significant difference observed when samples with and without ATc were compared, consistent with the lack of transcriptional silencing observed in the qPCR data. However, a significant difference was observed for several of the strains when samples with no supplemental Fe and 2 µM were compared. This was consistent with what was observed visually in the wells (Figure3.13).

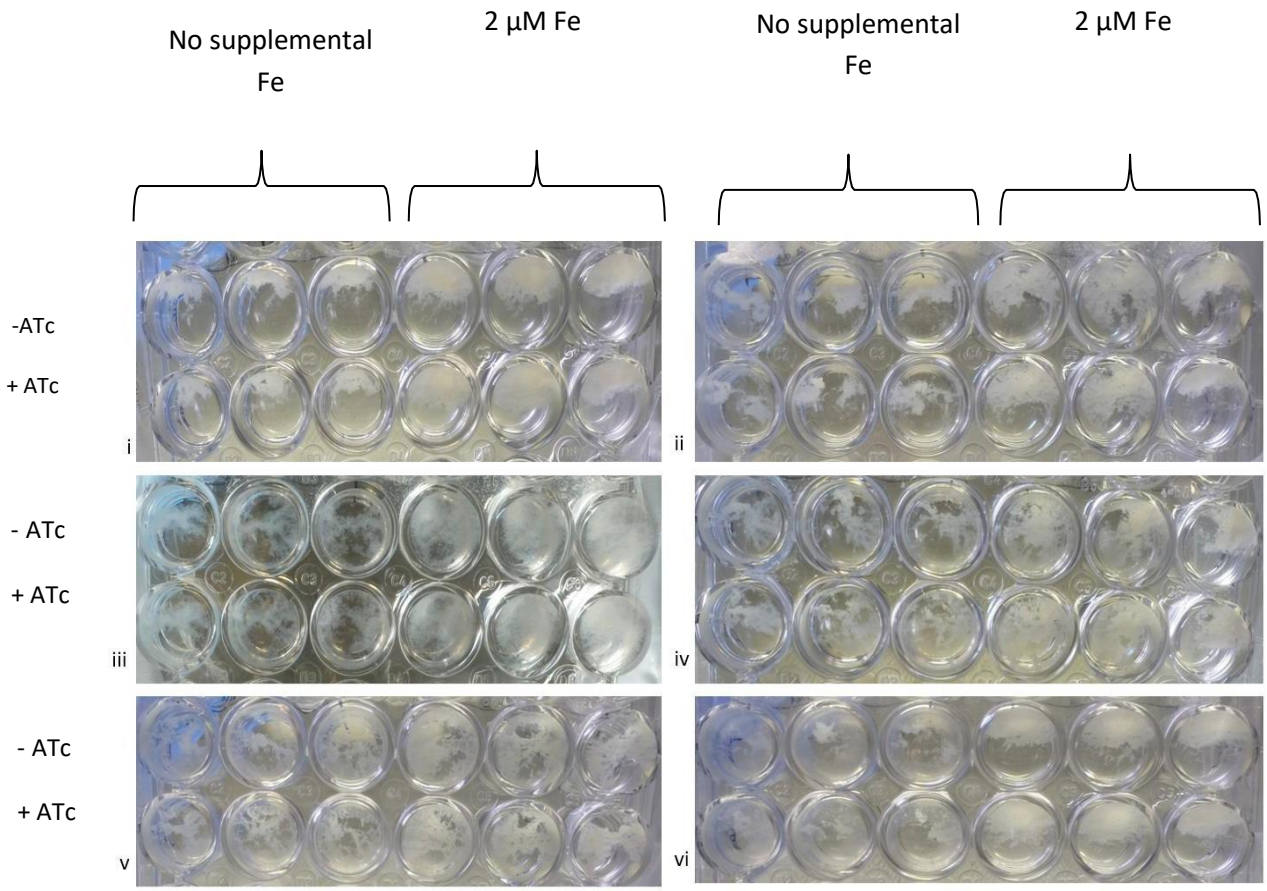

Figure 3. 12: Showing the biofilms obtained by

(i) *M. abscessus* (ATCC1997), (ii) *M. abscessus* attB:: pLJR962, (iii) *M. abscessus attB:: pLJR962-2744c*-a, (iv) *M. abscessus attB:: pLJR962-2744c*-b, (v) *M. abscessus attB:: pLJR962-2745c*-a and (iv) *M. abscessus attB:: pLJR962-2745c*-b strains in the absence and presence of Fe (2 µM). The biofilms were grown over a period of 3 weeks and the images show one of the 3 biological replicates.

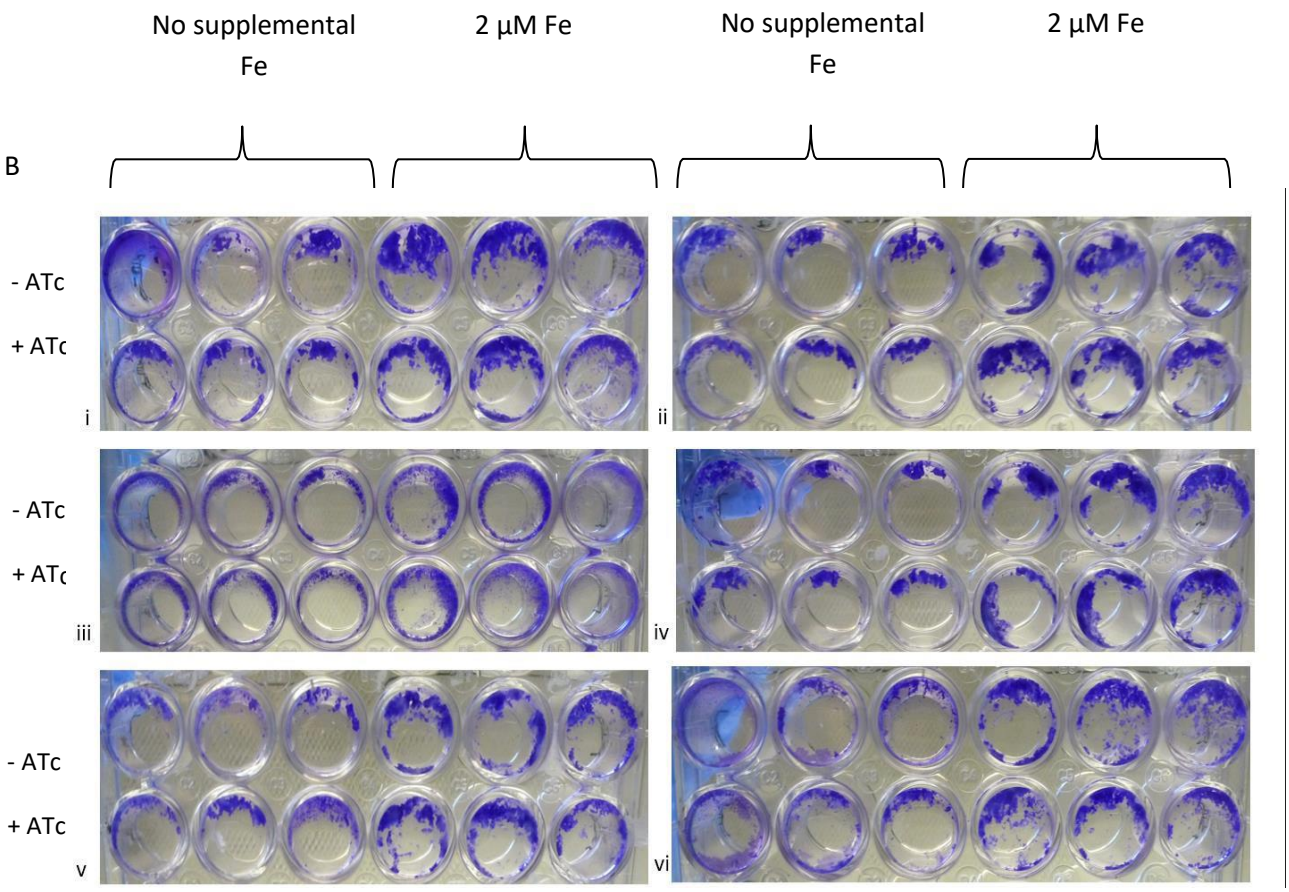

Figure 3. 13: Crystal violet quantitation of the CRISPRi strains.

After 3 weeks the biofilms quantified using the crystal violet method. (i) *M. abscessus* (ATCC1997), (ii) *M. abscessus* attB:: *pLJR962*, (iii) *M. abscessus attB:: pLJR962-2744c*-a, (iv) *M. abscessus attB:: pLJR962-2744c*-b, (v) *M. abscessus attB:: pLJR962-2745c*-a and (iv) *M. abscessus attB:: pLJR962-2745c*-b strains in the absence and presence of Fe (2 µM).

In the Crystal Violet experiment (Figure 3.13), the standard deviation of all the CV strained strains ranged from 0.20 to 0.92, indicating that the samples were not dispersed but rather grouped around the mean. When no Fe vs (+ ATc and – Atc) were compared, the highest mean was 2.932 in *M. abscessus attB:: pLJR962-2744c*-a and the lowest was 0.844 in *M. abscessus attB:: pLJR962-2745c*-b, the small differences suggested that there was variance between the samples. Further, the t- test results displayed the p- values to be 0.75, 0.23, 0.84, 0.79, 0.27, 0.878 and this shows us that there was no significant

difference between all the strains (Table 8 and 9). When 2 µM Fe vs (+ ATc and – ATc) were compared the highest mean was 3.676 in *M. abscessus* ATCC1997 and the lowest was 1.702 in *M. abscessus attB:: pLJR962-2745c*-a, the small differences suggested that there was also variance between the samples. Further, the t- test p-value resultsdisplayed that there was no significant difference between all the strains (Table 8 and 9).

When no ATc vs (+ 2 µM Fe and – Fe) were compared, the t- test showed that *M. abscessus* (ATCC1997), *M. abscessus attB:: pLJR962, M. abscessus attB:: pLJR962-2744c*-b and *M. abscessus attB:: pLJR962-2745c*-a p-values were significant (Table 8 and 9). This is coinciding with what is observed in (Figure 3.10). When + ATc vs (+ Fe and - 2 µM Fe) were compared using a t- test, it was observed that *M. abscessus attB:: pLJR962*, *M. abscessus attB:: pLJR962-2744c-b, M. abscessus attB:: pLJR962-2745c-a* and *M. abscessus attB:: pLJR962-2745c-b* all had significant p-values according to the t-test (Table 8 and 9). This data corresponds to what is shown in Figure 3.12. The CV quantitation reflects that iron is necessary for growth of the *M. abscessus* strains.

Table 8: Mean OD600 values obtained following crystal violet staining

Strains		**No Fe**			**Ave ± SD**	**2µM**			**Ave ± SD**
M. abscessus (ATCC1997)	-ATc	1.684	2.532	2.366	2.194 ± 0.45	2.986	3.676	3.144	3.27 ± 0.36
	+ATc	1.962	2.358	2.584	2.301 ± 0.32	3.064	3.648	1.842	2.85 ± 0.92
M. abscessus	-ATc	2.062	2.592	2.498	2.384 ±	3.028	3.348	3.892	3.42 ±

					0.28				0.44

attB:: pLJR962	+ATc	2.448	1.61	1.852	1.97 ± 0.43	3.11	3.362	3.498	3.32 ± 0.20
M. abscessus attB:: pLJR962-*2744c*-a	-ATc	2.932	2.638	2.056	2.542 ± 0.45	2.692	2.658	2.158	2.50 ± 0.30
	+ATc	2.382	2.8	2.242	2.47 ± 0.29	2.7	1.976	2.316	2.33 ± 0.36
M. abscessus attB:: pLJR962-*2744c*-b	-ATc	2.036	1.494	1.918	1.816 ± 0.29	2.664	3.28	3.522	3.16 ± 0.44
	+ATc	2.186	1.566	1.452	1.73 ± 0.40	2.622	3.086	3.724	3.14 ± 0.55
M. abscessus attB:: pLJR962-*2745c*-a	-ATc	0.844	1.226	1.302	1.124 ± 0.25	1.762	1.702	2.438	1.97 ± 0.41
	+ATc	1.134	1.364	1.778	1.42 ± 0.33	2.538	1.986	2.176	2.23 ± 0.28
M. abscessus	-ATc	1.614	1.85	2.216	1.89 ±	2.236	2.414	2.906	2.52 ±

attB::					0.30				0.35

pLJR962-*2745c*-b	+ATc	2.016	1.758	2.002	1.93 ± 0.15	2.448	2.338	3.144	2.64 ± 0.44

Table 9: **T-test results of the crystal violet quantitation**

Strains	**no Fe (ATC vs no ATC)**	**Fe (ATC vs no ATC)**	**no ATC (no Fe vs Fe)**	**ATC (no Fe vs Fe)**
	P - values			
M. abscessus (ATCC1997)	0.751798	0.505746	0.032057	0.383376
M. abscessus attB:: pLJR962	0.236773	0.73768	0.025883	0.007793
M. abscessus attB:: pLJR962-2744c-a	0.837215	0.560348	0.905131	0.61956
M. abscessus attB:: pLJR962-2744c-b	0.786793	0.97922	0.011617	0.022947
M. abscessus attB:: pLJR962-*2745c*-a	0.270333	0.405243	0.037517	0.031302
M. abscessus attB:: pLJR962-2745c-b	0.877066	0.718529	0.078527	0.054068

3.10 Growth of *M. abscessus* (ATCC1997) strain under iron limiting conditions

Iron is necessary for mycobacterial growth and infection [95]. In the iron limiting experiments described in section 3.6.2, the *M. abscessus* strains were cultured for two growth cycles in chelated Sauton's media. Despite this, the strains were able to grow in the absence of iron in the second growth cycle. To further investigate the importance of iron for the growth of *M. abscessus* (ATCC1997) strain, the strain was cultured in the presence of the metal chelator deferoxamine (DFO). Consistent with previous results, bacterial growth was shown to be substantially higher in the presence of high concentrations of iron (2 µM) than in the absence of the metal. (Figure 3.8). After 3 days, a maximum OD of above 3.5 was observed in the presence of 2 µM Fe, compared to the no supplemental Fe culture which reached an OD of ~2.5. Inclusion of DFO in the culture was able to significantly inhibit growth, with the culture reaching an OD ~ 0.5 after 3 days.

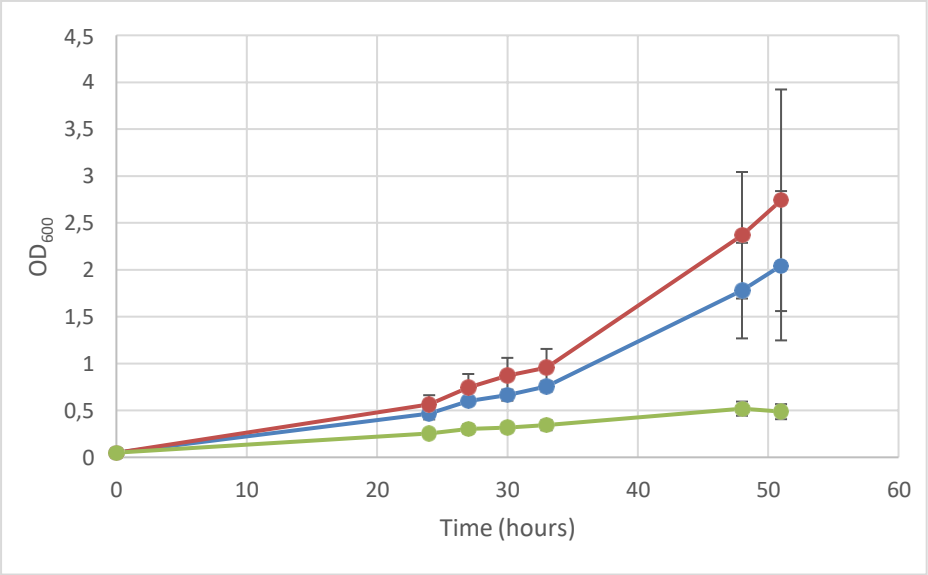

Figure 3. 14: Growth of *M. abscessus* (ATCC1997) strain under iron limiting conditions.

Showing the growth and survival of *M. abscessus* (ATCC1997) in chelated Sauton's media with (red) and without 2 µM Fe supplementation (blue) and in the presence of 1.25 mM DFO (green). The standard deviation indicates the results of three biological replicates. CFUs were alsodone to determine the bacterial culture concentration.

Chapter 4: Discussion

The current study investigated the role of *sufT* homologue in *M. abscessus* (*MAB_2744c*) using CRISPRi. Understanding *M. abscessus* pathogenesis requires knowledge of the essential mycobacterial pathways. This involves employing novel techniques to identify and characterize *M. abscessus* genes that are involved in important mycobacterial processes, such as iron-sulphur (FeS) cluster formation, which represents a crucial process in mycobacterial metabolism. Mycobacteria require FeS clusters which is the most primitive, diverse, and vital prosthetic group and are required for growth and infection [85]. Siderophores are high affinity iron chelators synthesized and secreted by mycobacteria, and these are utilized as siderophore iron complexes [101]. Some mycobacteria, such as *M. smegmatis*, produce two distinct siderophores: exochelin, a pentapeptide derivative, and two salicylate-derived mycobactin; an acylated intracellular cell form and an extracellular carboxymycobactin [101]. Other mycobacteriasuch as *M. tuberculosis* can only synthesize mycobactins which are important for growth in iron-limiting conditions [101]. Furthermore, mutants that lack siderophores are defective for intracellular growth and survival in animal models, highlighting the importance of iron during infection. In mycobacteria, iron limitation causes *suf* operon induction, implying that this is a state of increased FeS cluster production or demand [100]. Previously, a study in *M. smegmatis* using a Δ*sufT* mutant showed that deletion of *sufT* had no effect on growth under standard culture conditions, while the Δ*sufT* mutant showed a growth deficiency in iron-limited conditions and a required higher iron concentrations for biofilm formation [100].

In this current study, a CRISPRi-based system was used to knock-down *M. abcessus* (ATCC1997) *sufT* gene expression to determine the impact on survival during iron limitation. Single sgRNAs (Figure 3.1) were designed to target the *sufT* (*MAB_2744c*), and the upstream gene (*MAB_2745c*) for comparison purposes. For each gene, two sgRNAswere designed in different locations to compare the knockdown efficiency. It was proposed that since the CRISPRi system is polar, it would knock off both genes at the same time (Figure 3.1). The mycobacterial CRISPRi system is designed to use tetracycline-inducible co-expression to control expression of the sgRNA and dCas9

enzyme in the generated CRISPRi knock-down strains (Table 6), using anhydrotetracycline (ATc) as the inducer [82].

In the experiment of growth of *M. abscessus* CRISPRi strains under standard conditions (Figure 3.6 A), the 7H9 OADC growth curves were partially sigmoidal, and no differences was observed amongst all the *M. abscessus* CRISPR interference strains. The *M. abscessus* CRISPRi strains are suggested to have been synthesizing RNA, enzymes and necessary metabolites (growth factors and macromolecules) during the lag phase, which lasted from 0 to 24 hours. In (Figure 3.6 B), following dilution into fresh media, bacteria grew exponentially because they were responding to changing conditions such as changes in nutrients, temperature, or pH. The CFUs were between 1 x 10^{7} and 1 x 10^{10} CFUs / ml and increase in cell number led to an increase in optical density. The lag phase data showed that the number of viable cells was increasing (Figure 3.6 B). The lack of compatibility between the OD and CFU at 20 hours could be because cell clumping can impact optical density readings when using the spectrophotometer approach, resulting in an underestimation of *M. abscessus* cells due to CFU's emerging from more than one cell.

Following that, from 24 to 48 hours, the standard curves exponential phase showed a rise in the curves for all *M. abscessus* CRISPRi strains however, the exponential phase data did not correspond with the CFUs data (Figure 3. 6 B) whereby between 24 - 48 hours the cell density did not increase and was ranging between 1 x 10^{10} and 1 x 10^{11} CFUs / ml. At this stage, the CFUs data showed that the cells were no longer growing and multiplying only up to 1 x 10^{11} CFUs / ml, this suggests that the cells were already reaching the stationary phase. It is suggested that the increase in growth of the CRISPRi strains (Figure 3.6 A), could have been caused by cells that were dying, the OD_{600} could have been rising because the cell volume was increasing, or the cells were lysing, this is displayed by the steep slope observed in (Figure 3.6 A) [102], [103]. In (Figure 3.6 A), the OD_{600} at 48 hours was between 8 and 9, this is abnormally high compared to most studies of *M. abcessus*, however there are also studies that highlight higher OD_{600} values in mycobacteria, the variation might be the growth media used or the spectrophotometer used to read the OD values. The increase in the OD could also be explained by the conditions that stimulate morphotype switching in vitro. In a previous study, *M. abscessus*

grown in MB media had the S morphotype and that grown in LB media had the R morphotype, the varied morphotypes caused the abnormal increase in OD values [104], [105]. The 7H9 OADC curves stationaryphase was observed after 48 hours where all the CRISPRi strains ceased growing.

In the experiment of growth of *M. abscessus* CRISPRi strains using defined media with (2 µM Fe, 200 µM) Fe and without iron (iron limitation) (Figure 3.8), there was a no difference observed in planktonic growth of all CRISPRi strains grown in fold-higher concentrations > 200 µM Fe, and 2 µM iron, they all reached a maximum OD_{600} of 2 at 48 hours. Likewise at 24 hours the OD_{600} was 0.5 for all strains. This suggests that 2 µMFe is sufficient for *M. abscessus* to grow planktonically. Therefore, the growth of the 2 µMFe was compared to growth in the absence of supplementary iron, it was observed that up to 33 hours there was no difference in the growth of all strains. The cultures without supplementary iron had an OD_{600} of approximately 0.5 lower than cultures with iron after 48 hours (Figure 3.8) The results demonstrate that varying iron concentrations had no impact on the growth of all CRISPRi strains. It was proposed in this study that ATc induction would significantly decrease the growth of the *M. abscessus* CRISPRi strains by repressing both the *sufT MAB_2744c* and the upstream *MAB_2745c* genes, but the results showed that the addition of ATc had no effect on the growth of all strains in both the presence and absence of iron. The study shows that either *sufT* plays no role in the survival of CRISPRi strains in the presence of no iron, or transcriptional silencing somehow did not occur.

To further investigate the impact of iron limitation on *M. abscessus* (ATCC1997) growth (Figure 3.14), we investigated growth in no iron, 2 µM iron and in the presence of deferoxamine. The results indicate that use of chelated media and an iron chelator such as deferoxamine resulted in growth inhibition, although the cells are still viable up to an OD_{600} of 0.5. When the DFO cultures were compared to the culture with no iron, the cultures grew up to and OD_{600} of 2 and this suggested that there could be residual iron in the media, that is promoting growth or that the DFO not only chelates iron but also chelates the supplemented magnesium and zinc metals. This experiment clearly demonstrates the importance of iron in mycobacterial growth and survival.

A similar study was done in *M. Massiliense*, were they evaluated two genes *mycma_0076* and *MYCMA_0077* required for iron storage [106]. They showed that *M. massiliense* growth wasunaffected by various iron concentrations, ranging from very low to very high, such as 450 mM [106]. The growth of mycobacteria was seriously affected when iron was fully eliminated (using deferoxamine) meaning that *M. massiliense* has iron homeostasis mechanisms that allow it to grow in high iron conditions. Surprisingly, high iron concentrations increased the expression of the *MYCMA_0076* 50- fold not the *MYCMA_0077* gene [106]. As a result, it appeared that only the *MYCMA_0076* gene had a positive association between iron levels and expression [106].

The extraction of RNA is a critical step in ensuring that RNA quantitation is accurate. Most of the RIN values obtained in this study from RNA analysis were above 8, indicating that the RNA used was of good quality, as evidenced by the visibility of 16s and 23s rRNA bands on denaturing gels (Figure 3.11) and TapeStation analysis (Appendix 1). In the validation of the level of transcriptional silencing in knock-down strains experiment (Figure 3.10), the RT-qPCR results showed no silencing. The *sigA* was used as a mycobacterial reference to compare the transcriptional expression of *MAB_2744c*. Although the precision may deteriorate at very low target numbers, real-time polymerase chain reaction-based DNA quantification is usually recognized as a sensitive and trustworthy technique [107]. The evidence of no silencing suggests that either the different sgRNA locations might have not been able to allow successful gene silencing or the sgRNA-dCas9 complex had poor access to the target DNA [108].

The RT-qPCR experiments all had optimal reaction conditions, as shown by their near 100 % efficiency (Appendix 1). However, the *M. abscessus sigA* and *MAB_2744c* DNA qPCR replicates were inconsistent, which could be due to the sample dilutions used, i.e., the cDNA samples were not diluted in the first replicate for *MAB_2744c* and *sigA*, but in replicates 2 and 3. A 1 in 2 dilution of the sample was done before performing the qPCR. The RT qPCR results show that there was no difference in the growth.

A recent study by (*Akusobi et al*., 2021) used CRISPRi to effectively inhibit gene expression in *M. abscessus* [109]. They showed that CRISPRi can generate strong gene repression by targeting genes using numerous sgRNAs per gene, allowing for the study of essential genes, an alternative to gene knockouts. Using a single sgRNA construct showed no detectable impact on *M. abscessus* growth, while the growth of *M. abscessus* was decreased when *pbp-lipo* was targeted with either 2 or 3 sgRNAs, demonstrating that PBP-transpeptidase lipo's activity is essential for *M. abscessus* to grow optimally. They also showed that the extent of *pbp-lipo* knockdown, as determined by RT-qPCR, could be fine-tuned utilizing single sgRNAs had 0- fold knock-down whereas 2 and 3 sgRNA constructs had 1000-fold knockdown [109]. Therefore, improving gene knock- down of *MAB_2744c* may be achieved by using 2 or 3 sgRNA that target a single gene. PBP-lipo knockdown strains with 0, 1, 2, and 3 sgRNA and PBP-lipo complement strains

were generated by transforming the pCT296 vector with an empty sgRNA to create the 0 sgRNA (empty sgRNA) *M. abscessus* strain.

This system differed with the current study system because they used different vectors and a different method i.e., to create the 1, 2, and 3 sgRNA strains, individual CRISPRi plasmids harboring single PBP-lipo-targeting sgRNAs were used (cr25, cr26, and cr56) plasmids. Then, using Golden Gate cloning, the inserts were combined into one vector by amplifying the sgRNA targeting region with the necessary flanking sequences.For the 1 sgRNA (cr25) was transformed into the ATCC1997 strain. For 2 sgRNA, the vector pCRC1 containing the (cr25 and cr26) sgRNAs on one backbone were transformed into *M. abscessus*. Finally, they transformed pCRC2 which contained the (cr25, cr26, and cr56) sgRNAs on 1 single backbone into the *M. abscessus* (3 sgRNA) strain. In addition to this system, the authors complemented the PBP-lipo knockdown growth phenotype and the *PBP-lipo* target gene was recoded with the protospacer adjacent motif (PAM) sequence that had been altered. This prohibited sgRNAs from binding to the integrated plasmid's inserted PBP-lipo copy. They showed that the PBP- lipo recovered growth of the original *PBP-lipo* knockdown when produced constitutively. A recoded and catalytically- dead mutant of *PBP-lipo*, on the other hand, did not rescue growth. Unlike *M. abscessus*, when the gene expressing PBP-lipo was removed in *M. tuberculosis* (Rv2864c) the knockout and wild-type strains grew indistinguishably. In *M. smegmatis* (2584c) the *PBP-lipo* homolog grew identically to wildtype with no growth impairment when knocked out [109]. Taken together this study demonstrates a CRISPRi system that could be applied in the current study, that could allow efficient knockdown ofthe CRISPRi strains.

Our findings can also be improved by using the recent CRISPRi approaches used by (*Bosch et al.,* 2021) on *M. tuberculosis*, whereby the authors improved the experiment by modifying the length of the sgRNA targeting sequence to control the degree of complementarity between the sgRNA and the DNA target, with initially testing and removing mismatched sgRNAs [110]. In the *M. tuberculosis* study, for identified essential genes, the length of the sgRNA targeting sequence was varied from 15 to 26 nucleotides; for identified non-essential genes, sgRNAs with lengths of 21-26 nucleotides were

chosen. No longer length variants were included in any gene class if an sgRNA for a single targeted PAM of length R 22 nucleotides was created [110]. The non-template strand of ORFs and non-coding RNAs was chosen as a target for sgRNAs. The overlap of the sgRNA targeting sequence with an ORF or non-coding RNA was specified by the sgRNA targeting sequence's 30 base [110]. The selection criteria were carefully defined, in contrast to the current investigation, in which the lengths of the target *sufT* sgRNA sequences were not varied and only 20 ± 2 bp were employed. On average, sgRNAs targeting essential genes depleted more than sgRNAs targeting non-essential genes and non-targeted controls. They observed no evidence of fitness problems in the absence of ATc compared to the presence of ATc, showing that the ATc-inducible system had a tight regulation. To test the different sizes of sgRNA strength, they determined how effectively they suppressed expression of a luminous reporter gene (Renilla luciferase) in *M. smegmatis* and showed that the anticipated sgRNA strength and Renilla knockdown had a high association ($R^2 = 0.74$). This suggested CRISPRi knockdown efficacy is influenced by biophysical characteristics of the dCas9-sgRNA-DNA interaction. This different CRISPRi system can be applied to the current study for quantitation analysis.

Pellicle biofilm in mycobacteria has different phases that include cell aggregation, substratum attachment, spreading, as well as maturation [101], [97]. When compared to their planktonic counterparts, mycobacterial cells in biofilms have very distinct phenotypic features. The experiment of growing *M. abscessus* CRISPRi strains as biofilms (Figure 3.12) revealed that with 2 µM iron, increased cell numbers and biofilm thickness were observed after three weeks, indicating that the biofilms were at an advanced stage of maturation, and thus 2 µM iron was required for full biofilm formation.

In the current study, the presence of no iron slowed biofilm formation suggesting that iron is important for growth in *M. abscessus* strains. The current study is comparable to what was previously shown in *M. smegmatis* [101] where the iron required for biofilm production was higher than the iron requirements for planktonic growth. In addition, the authors demonstrated a link between iron availability and the production of mycolic acid C56–C68 matrix components, which is likely a primary metabolic demand for biofilm maturation [101]. These biofilms differ from *M. smegmatis* whose biofilms mature in a

short space of time, the stages commence with the creation of a thin layer at the liquid–air interface three days after inoculation, followed by the appearance of mature biofilm structures, and final maturation seven days later [100]. The *M. smegmatis* study was similar to what was observed in *M. avium* which grew biofilms in a period of 7 days. Biofilm production is linked to the early phases of infection in *M. ulcerans'* insect host (Naucoris cimicoids) [111]. Biofilm formation in *M. marinum* is linked to a cordingmorphology and the biofilms grew in a period of 14 days [112].

In the previous study they investigated whether morphological differences in the *M. smegmatis sufT* mutant were linked to biofilm formation and discovered that the *sufT* mutant exhibited a shorter cell morphology than the wildtype strain during both planktonic and biofilm growth [100]. This demonstrated that the phenotype of the *sufT* mutant was not confined to cells developing in a biofilm, but rather was linked to iron availability [100]. This implied that the absence of *sufT* has no effect on *M. smegmatis* ability to generate pellicle biofilms, but rather raises the iron concentration required for biofilm formation [101]. However, since *sufT* knockdown was not achieved in this study, its role in biofilm formation in *M. abscessus* could not be investigated

Pseudomonas aeruginosa biofilm formation also requires increased iron concentrations [113] and in the presence of lactoferrin, a *fur* (iron regulatory protein) mutant of the *P. aeruginosa* developed mushroom-like biofilm formations, demonstrating that iron is primarily involved in biofilm growth regulation. This was also supported with what was observed in *M. tuberculosis* [114], where they investigated the variables that regulate biofilm formation and three models of *M. tuberculosis* biofilm formation were developed; pellicle biofilms that generated at the liquid-air interface of cultures, leukocyte lysate-induced biofilms, and thiol reductive stress-induced biofilms are all examples of these models. Pellicle biofilm production took 5 weeks, and this made making *M. tuberculosis* biofilm research time-consuming. The thiol reductive stress-induced biofilms differed from pellicle biofilms in that they were a thick cottony biomass when grown without Tween 80 and a thin but tightly adhering matt of biomaterial encapsulating bacteria when formed with Tween 80 [115].

It is suggested that mycobacterium glycopeptidolipids (GPLs) are involved in cell motility and biofilm spread and help to prevent cell aggregation and temporal differences in gene expression support the specific requirements for each step of pellicle biofilm development [116].

Figure 3.10 tested and optimized the qPCR primer sets that were previously generated for use in (Figure 9), the expected band sizes were shown which indicated that the qCR primers were working efficiently. Therefore, it was expected that the use of qPCR standards for both *MAB_2744c* and *sigA* to investigate expression would be efficient.

In the RT qPCR experiment, the ATCC1997 parent strain and the *M. abscessus* attB:: pLJR962 control strain had the greatest concentration values obtained from the standard curves (Appendix 1). The sample concentrations were taken from the line of best fit of the standards (Appendix 1). An efficient qPCR run had R^2 value of 0.99. When the concentration values of the three CRISPRi replicates were compared, the highest concentration was 9.65 and the lowest was 0.793. The concentrations were inconsistent between all the 3 replicates, having a difference of less than one between all 3 replicates. When the t- test was performed on the RT qPCR concentrations, the standard deviation ranged between 0.36 and 5.46, which was considerable, however the t-test revealed that the differences across the strains were not significant, with values of 0.23, 0.80, 0.76, 0.36, and 0.76 for all strains.

CRISPRi can efficiently silence gene expression and the effectiveness is inversely proportional to the distance between the target region and the transcription start point [25]. However, the CRISPRi designed sgRNA can influence downstream gene expression. The selected target gene and binding site could profoundly influence the downstream genes and outcome proteins hence underlining the importance of the sgRNA design [117]. For most phenotypic changes, confirmation of protein level changes is an important validation step. This is because the protein translated from the gene of interest that leads to downstream signalling and phenotypes. Western blot method is used to obtain information on protein translation [117]. However, it requires particular antibodies and depending on the target, finding high-quality antibodies that detect a region of the protein 5′ to the sgRNA binding site may be difficult. Target validation can be supplemented with downstream gene biological pathway analyses. Once the requisite

validation assays have been completed to ensure that the CRISPRi screen resulted in changes to the gene, mRNA, and protein being targeted [117]. More research is needed to determine and characterize the role that the identified protein performs in mycobacteria. In this study, the use of qPCR was not the best method to use in testing the efficacy of the expression. These proteins can be tested for by using techniques such as mass spectrometry and edman degradation [118]. These could have helped check the expression levels of the *M. abscessus* strains.

In the cystal violet quantitation, a t- test was also performed and the results were successful in quantifying the cultures grown in iron against those grown without iron. It displayed that iron is necessary for the growth of the *M. abcessus* CRISPRi strains and coincides with what was observed in the biofilms experiment and iron limitation experiment. Therefor CV quantitation can be used to quantitate growth efficiently.

This study showed that when a single sgRNA is employed, the previously disclosed mycobacterial CRISPRi system does not function efficiently in *M. abscessus*, and that the system needs to be further optimized for usage in this mycobacterium. Future work involves exploring the other CRISPRi systems that have been utilized in other studies as well as the vectors utilized.

References

[1] "Nontuberculous Mycobacteria (NTM) Infections | HAI | CDC," *Cdc*, Aug. 12, 2019. https://www.cdc.gov/hai/organisms/nontuberculous-mycobacteria.html (accessed Apr. 29, 2020).

[2] M. M. Johnson and J. A. Odell, "Nontuberculous mycobacterial pulmonary infections," *J. Thorac. Dis.*, vol. 6, no. 3, pp. 210–220, Mar. 2014, doi: 10.3978/j.issn.2072-1439.2013.12.24.

[3] J. E. Stout, W.-J. Koh, and W. W. Yew, "Update on pulmonary disease due to non-tuberculous mycobacteria," *Int. J. Infect. Dis.*, vol. 45, pp. 123–134, Apr. 2016, doi: 10.1016/j.ijid.2016.03.006.

[4] D. R. Prevots and T. K. Marras, "Epidemiology of human pulmonary infection with nontuberculous mycobacteria: a review," *Clin. Chest Med.*, vol. 36, no. 1, pp. 13–34, Mar. 2015, doi: 10.1016/j.ccm.2014.10.002.

[5] K. L. Winthrop, E. Chang, S. Yamashita, M. F. Iademarco, and P. A. LoBue, "Nontuberculous mycobacteria infections and anti-tumor necrosis factor-alpha therapy," *Emerg. Infect. Dis.*, vol. 15, no. 10, pp. 1556–1561, Oct. 2009, doi: 10.3201/eid1510.090310.

[6] R. Thomson, C. Tolson, R. Carter, C. Coulter, F. Huygens, and M. Hargreaves, "Isolation of Nontuberculous Mycobacteria (NTM) from Household Water and Shower Aerosols in Patients with Pulmonary Disease Caused by NTM," *J. Clin. Microbiol.*, vol. 51, no. 9, pp. 3006–3011, Sep. 2013, doi: 10.1128/JCM.00899-13.

[7] H. Kunst, M. Wickremasinghe, A. Wells, and R. Wilson, "Nontuberculous mycobacterial disease and Aspergillus-related lung disease in bronchiectasis," *Eur. Respir. J.*, vol. 28, no. 2, pp. 352–357, Aug. 2006, doi: 10.1183/09031936.06.00139005.

[8] L.-O. Larsson *et al.*, "Pulmonary disease by non-tuberculous mycobacteria – clinical management, unmet needs and future perspectives," *Expert Rev. Respir. Med.*, pp. 1–13, Oct. 2017, doi: 10.1080/17476348.2017.1386563.

[9] D. E. Griffith *et al.*, "An Official ATS/IDSA Statement: Diagnosis, Treatment, and Prevention of Nontuberculous Mycobacterial Diseases," *Am. J. Respir. Crit. Care Med.*, vol. 175, no. 4, pp. 367–416, Feb. 2007, doi: 10.1164/rccm.200604-571ST.

[10] Y.-S. Kwon and W.-J. Koh, "Diagnosis and Treatment of Nontuberculous Mycobacterial Lung Disease," *J. Korean Med. Sci.*, vol. 31, no. 5, pp. 649–659, May 2016, doi: 10.3346/jkms.2016.31.5.649.

[11] A. H. Shahraki *et al.*, "'Multidrug-resistant tuberculosis' may be nontuberculous mycobacteria," *Eur. J. Intern. Med.*, vol. 26, no. 4, pp. 279–284, May 2015, doi: 10.1016/j.ejim.2015.03.001.

[12] S. Kahkouee *et al.*, "Multidrug resistant tuberculosis versus non-tuberculous mycobacterial infections: a CT-scan challenge," *Braz. J. Infect. Dis.*, vol. 17, no. 2, pp. 137–142, Mar. 2013, doi: 10.1016/j.bjid.2012.10.011.

[13] P. Tabarsi *et al.*, "Nontuberculous Mycobacteria Among Patients Who are Suspected for Multidrug-Resistant Tuberculosis—Need for Earlier Identification of Nontuberculosis Mycobacteria," *Am. J. Med. Sci.*, vol. 337, no. 3, pp. 182–184, Mar. 2009, doi: 10.1097/MAJ.0b013e318185d32f.

[14] K. Borgers, K. Vandewalle, N. Festjens, and N. Callewaert, "A guide to *Mycobacterium* mutagenesis," *FEBS J.*, vol. 286, no. 19, pp. 3757–3774, Oct. 2019, doi: 10.1111/febs.15041.

[15] M. Jankute, J. A. G. Cox, J. Harrison, and G. S. Harrison, "Assembly of the Mycobacterial Cell Wall," *Annu. Rev. Microbiol.*, vol. 69, pp. 405–423, 2015, doi: 10.1146/annurev-micro-091014-104121.

[16] C. Hoffmann, A. Leis, M. Niederweis, J. M. Plitzko, and H. Engelhardt, "Disclosure of the mycobacterial outer membrane: cryo-electron tomography and vitreous sections reveal the lipid bilayer structure," *Proc. Natl. Acad. Sci. U. S. A.*, vol. 105, no. 10, pp. 3963–3967, Mar. 2008, doi: 10.1073/pnas.0709530105.

[17] C. Asselineau, J. Asselineau, G. Lanéelle, and M.-A. Lanéelle, "The biosynthesis of mycolic acids by Mycobacteria: current and alternative hypotheses," *Prog. Lipid Res.*, vol. 41, no. 6, pp. 501–523, Nov. 2002, doi: 10.1016/S0163-7827(02)00008-5.

[18] D. Hanahan, J. Jessee, and F. R. Bloom, "[4] Plasmid transformation of Escherichia coli and other

bacteria," in *Methods in Enzymology*, vol. 204, Academic Press, 1991, pp. 63–113. doi: 10.1016/0076-6879(91)04006-A.
[19] B. J. Wards and D. M. Collins, "Electroporation at elevated temperatures substantially improves transformation efficiency of slow-growing mycobacteria," *FEMS Microbiol. Lett.*, vol. 145, no. 1, pp. 101–105, Nov. 1996, doi: 10.1111/j.1574-6968.1996.tb08563.x.
[20] S.-H. Lee *et al.*, "Optimization of electroporation conditions for Mycobacterium avium," *Tuberc. Edinb. Scotl.*, vol. 82, no. 4–5, pp. 167–174, 2002, doi: 10.1054/tube.2002.0335.
[21] N. Wu, K. Matand, B. Kebede, G. Acquaah, and S. Williams, "Enhancing DNA electrotransformation efficiency in Escherichia coli DH10B electrocompetent cells," *Electron. J. Biotechnol.*, vol. 13, no. 5, pp. 0–0, Sep. 2010, doi: 10.2225/vol13-issue5-fulltext-11.
[22] S. B. Snapper, R. E. Melton, S. Mustafa, T. Kieser, and W. R. Jacobs, "Isolation and characterization of efficient plasmid transformation mutants of Mycobacterium smegmatis," *Mol. Microbiol.*, vol. 4, no. 11, pp. 1911–1919, Nov. 1990, doi: 10.1111/j.1365-2958.1990.tb02040.x.
[23] E. M. Foley-Thomas, D. L. Whipple, L. E. Bermudez, and R. G. Barletta, "Phage infection, transfection and transformation of Mycobacterium avium complex and Mycobacterium paratuberculosis," *Microbiology*, vol. 141, no. 5, pp. 1173–1181, May 1995, doi: 10.1099/13500872-141-5-1173.
[24] F. A. Khattak, A. Kumar, E. Kamal, R. Kunisch, and A. Lewin, "Illegitimate recombination: An efficient method for random mutagenesis in Mycobacterium avium subsp. hominissuis," *BMC Microbiol.*, vol. 12, p. 204, Sep. 2012, doi: 10.1186/1471-2180-12-204.
[25] A. Viljoen, A. V. Gutiérrez, C. Dupont, E. Ghigo, and L. Kremer, "A Simple and Rapid Gene Disruption Strategy in Mycobacterium abscessus: On the Design and Application of Glycopeptidolipid Mutants," *Front. Cell. Infect. Microbiol.*, vol. 8, 2018, doi: 10.3389/fcimb.2018.00069.
[26] B. P. Cormack, R. H. Valdivia, and S. Falkow, "FACS-optimized mutants of the green fluorescent protein (GFP)," *Gene*, vol. 173, no. 1 Spec No, pp. 33–38, 1996, doi: 10.1016/0378-1119(95)00685-0.
[27] S. Bardarov *et al.*, "Conditionally replicating mycobacteriophages: A system for transposon delivery to Mycobacterium tuberculosis," *Proc. Natl. Acad. Sci. U. S. A.*, vol. 94, no. 20, pp. 10961–10966, Sep. 1997.
[28] J. Otero, W. R. Jacobs, and M. S. Glickman, "Efficient Allelic Exchange and Transposon Mutagenesis in Mycobacterium avium by Specialized Transduction," *Appl. Environ. Microbiol.*, vol. 69, no. 9, pp. 5039–5044, Sep. 2003, doi: 10.1128/AEM.69.9.5039-5044.2003.
[29] M. S. Dragset *et al.*, "Global Assessment of Mycobacterium avium subsp. hominissuis Genetic Requirement for Growth and Virulence," *mSystems*, vol. 4, no. 6, Dec. 2019, doi: 10.1128/mSystems.00402-19.
[30] K. T. Park *et al.*, "Demonstration of Allelic Exchange in the Slow-Growing Bacterium Mycobacterium avium subsp. paratuberculosis, and Generation of Mutants with Deletions at the pknG, relA, and lsr2 Loci," *Appl. Environ. Microbiol.*, vol. 74, no. 6, pp. 1687–1695, Mar. 2008, doi: 10.1128/AEM.01208-07.
[31] W. H. Pope *et al.*, "Cluster K Mycobacteriophages: Insights into the Evolutionary Origins of Mycobacteriophage TM4," *PLoS ONE*, vol. 6, no. 10, Oct. 2011, doi: 10.1371/journal.pone.0026750.
[32] M. K. Lehman, J. L. Bose, and K. W. Bayles, "Allelic Exchange," in *The Genetic Manipulation of Staphylococci: Methods and Protocols*, J. L. Bose, Ed. New York, NY: Springer, 2016, pp. 89–96. doi: 10.1007/7651_2014_187.
[33] S. Bardarov *et al.*, "Specialized transduction: an efficient method for generating marked and unmarked targeted gene disruptions in Mycobacterium tuberculosis, M. bovis BCG and M. smegmatis," *Microbiology,* vol. 148, no. 10, pp. 3007–3017, 2002, doi: 10.1099/00221287-148-10-3007.
[34] M. N. Alonso *et al.*, "Efficient method for targeted gene disruption by homologous recombination in Mycobacterium avium subspecie paratuberculosis," *Res. Microbiol.*, vol. 171, no. 5–6, pp. 203–210,

Sep. 2020, doi: 10.1016/j.resmic.2020.04.001.
[35] Vinicius Calado Nogueira de Moura, Sara Gibbs, Mary Jackson, “Gene Replacement in Mycobacterium chelonae: Application to the Construction of Porin Knock-Out Mutants.”
[36] E. Mahenthiralingam, B.-I. Marklund, L. A. Brooks, D. A. Smith, G. J. Bancroft, and R. W. Stokes, “Site-Directed Mutagenesis of the 19-Kilodalton Lipoprotein Antigen Reveals No Essential Role for the Protein in the Growth and Virulence of Mycobacterium intracellulare,” *Infect. Immun.*, vol. 66, no. 8, pp. 3626–3634, Aug. 1998.
[37] P. Jain *et al.*, “Specialized Transduction Designed for Precise High-Throughput Unmarked Deletions in Mycobacterium tuberculosis,” *mBio*, vol. 5, no. 3, Jul. 2014, doi: 10.1128/mBio.01245-14.
[38] X.-J. Mao, M.-Y. Yan, H. Zhu, X.-P. Guo, and Y.-C. Sun, “Efficient and simple generation of multiple unmarked gene deletions in Mycobacterium smegmatis,” *Sci. Rep.*, vol. 6, no. 1, Art. no. 1, Mar. 2016, doi: 10.1038/srep22922.
[39] K. Borgers *et al.*, “Use of a counterselectable transposon to create markerless knockouts from a 18,432-clone ordered *M. bovis* BCG mutant resource,” Microbiology, preprint, Oct. 2019. doi: 10.1101/817007.
[40] H. Song, F. Wolschendorf, and M. Niederweis, “Construction of Unmarked Deletion Mutants in Mycobacteria,” in *Mycobacteria Protocols: Second Edition*, T. Parish and A. C. Brown, Eds. Totowa, NJ: Humana Press, 2009, pp. 279–295. doi: 10.1007/978-1-59745-207-6_19.
[41] E. Krzywinska, S. Bhatnagar, L. Sweet, D. Chatterjee, and J. S. Schorey, “Mycobacterium avium 104 deleted of the methyltransferase D gene by allelic replacement lacks serotype-specific glycopeptidolipids and shows attenuated virulence in mice,” *Mol. Microbiol.*, vol. 56, no. 5, pp. 1262–1273, Jun. 2005, doi: 10.1111/j.1365-2958.2005.04608.x.
[42] V. R. Irani, S.-H. Lee, T. M. Eckstein, J. M. Inamine, J. T. Belisle, and J. N. Maslow, “Utilization of a ts-sacB selection system for the generation of a Mycobacterium avium serovar-8 specific glycopeptidolipid allelic exchange mutant,” *Ann. Clin. Microbiol. Antimicrob.*, vol. 3, p. 18, Sep. 2004, doi: 10.1186/1476-0711-3-18.
[43] S. A. Gregoire, J. Byam, and M. S. Pavelka, “galK-based suicide vector mediated allelic exchange in Mycobacterium abscessus,” *Microbiology*, vol. 163, no. 10, pp. 1399–1408, Oct. 2017, doi: 10.1099/mic.0.000528.
[44] M. Dal Molin, M. Gut, A. Rominski, K. Haldimann, K. Becker, and P. Sander, “Molecular Mechanisms of Intrinsic Streptomycin Resistance in Mycobacterium abscessus,” *Antimicrob. Agents Chemother.*, vol. 62, no. 1, pp. e01427-17, Dec. 2017, doi: 10.1128/AAC.01427-17.
[45] Halima Medjahed, Jean-Marc Reyrat, “Construction of Mycobacterium abscessus Defined Glycopeptidolipid Mutants: Comparison of Genetic Tools.”
[46] Q. Zhang *et al.*, “EsxA membrane-permeabilizing activity plays a key role in mycobacterial cytosolic translocation and virulence: effects of single-residue mutations at glutamine 5,” *Sci. Rep.*, vol. 6, p. 32618, 07 2016, doi: 10.1038/srep32618.
[47] A. Rominski, A. Roditscheff, P. Selchow, E. C. Böttger, and P. Sander, “Intrinsic rifamycin resistance of Mycobacterium abscessus is mediated by ADP-ribosyltransferase MAB_0591,” *J. Antimicrob. Chemother.*, vol. 72, no. 2, pp. 376–384, 2017, doi: 10.1093/jac/dkw466.
[48] K. C. Murphy, “Use of Bacteriophage λ Recombination Functions To Promote Gene Replacement in Escherichia coli,” *J. Bacteriol.*, vol. 180, no. 8, pp. 2063–2071, Apr. 1998.
[49] J. C. van Kessel, L. J. Marinelli, and G. F. Hatfull, “Recombineering mycobacteria and their phages,” *Nat. Rev. Microbiol.*, vol. 6, no. 11, pp. 851-, Nov. 2008.
[50] J. C. V. Kessel and G. F. Hatfull, “Efficient point mutagenesis in mycobacteria using single-stranded DNA recombineering: characterization of antimycobacterial drug targets,” *Mol. Microbiol.*, vol. 67, no. 5, pp. 1094–1107, 2008, doi: 10.1111/j.1365-2958.2008.06109.x.
[51] T. Parish, E. Mahenthiralingam, P. Draper, E. O. Davis, and M. J. Colston, “Regulation of the inducible acetamidase gene of Mycobacterium smegmatis,” *Microbiol. Read. Engl.*, vol. 143 (Pt 7), pp. 2267–2276, Jul. 1997, doi: 10.1099/00221287-143-7-2267.
[52] J. C. van Kessel and G. F. Hatfull, “Recombineering in Mycobacterium tuberculosis,” *Nat. Methods*,

vol. 4, no. 2, pp. 147–152, Feb. 2007, doi: 10.1038/nmeth996.
[53] M. Kenan, “Mycobacterial Recombineering | Springer Nature Experiments,” 2015. https://experiments.springernature.com/articles/10.1007/978-1-4939-2450-9_10 (accessed Apr. 15, 2020).
[54] F. Khattak, A. Kumar, E. Kamal, R. Kunisch, and A. Lewin, “Illegitimate recombination: An efficient method for random mutagenesis in Mycobacterium avium subsp. hominissuis,” *BMC Microbiol.*, vol. 12, no. 1, p. 204, 2012, doi: 10.1186/1471-2180-12-204.
[55] N. M. Chimukuche and M. J. Williams, “Genetic Manipulation of Non-tuberculosis Mycobacteria,” *Front. Microbiol.*, vol. 12, p. 633510, 2021, doi: 10.3389/fmicb.2021.633510.
[56] K. C. Murphy, S. J. Nelson, S. Nambi, K. Papavinasasundaram, C. E. Baer, and C. M. Sassetti, “ORBIT: a New Paradigm for Genetic Engineering of Mycobacterial Chromosomes,” *mBio*, vol. 9, no. 6, Dec. 2018, doi: 10.1128/mBio.01467-18.
[57] T. R. Ioerger *et al.*, “Identification of new drug targets and resistance mechanisms in Mycobacterium tuberculosis,” *PloS One*, vol. 8, no. 9, p. e75245, 2013, doi: 10.1371/journal.pone.0075245.
[58] Beliaev, “Mutagenesis as a Genomic Tool for Studying Gene Function | Request PDF.” https://www.researchgate.net/publication/227986379_Mutagenesis_as_a_Genomic_Tool_for_Studying_Gene_Function (accessed Aug. 19, 2020).
[59] D. J. Lampe, B. J. Akerley, E. J. Rubin, J. J. Mekalanos, and H. M. Robertson, “Hyperactive transposase mutants of the Himar1 mariner transposon,” *Proc. Natl. Acad. Sci. U. S. A.*, vol. 96, no. 20, pp. 11428–11433, Sep. 1999, doi: 10.1073/pnas.96.20.11428.
[60] C. Martin, J. Timm, J. Rauzier, R. Gomez-Lus, J. Davies, and B. Gicquel, “Transposition of an antibiotic resistance element in mycobacteria,” *Nature*, vol. 345, no. 6277, Art. no. 6277, Jun. 1990, doi: 10.1038/345739a0.
[61] C. Guilhot, I. Otal, I. Van Rompaey, C. Martìn, and B. Gicquel, “Efficient transposition in mycobacteria: construction of Mycobacterium smegmatis insertional mutant libraries.,” *J. Bacteriol.*, vol. 176, no. 2, pp. 535–539, Jan. 1994.
[62] V. Pelicic, M. Jackson, J.-M. Reyrat, W. R. Jacobs, B. Gicquel, and C. Guilhot, “Efficient allelic exchange and transposon mutagenesis in Mycobacterium tuberculosis,” *Proc. Natl. Acad. Sci.*, vol. 94, no. 20, pp. 10955–10960, Sep. 1997, doi: 10.1073/pnas.94.20.10955.
[63] R. A. McAdam *et al.*, “In vivo growth characteristics of leucine and methionine auxotrophic mutants of Mycobacterium bovis BCG generated by transposon mutagenesis.,” *Infect. Immun.*, vol. 63, no. 3, pp. 1004–1012, 1995, doi: 10.1128/IAI.63.3.1004-1012.1995.
[64] J. Rybniker, M. Wolke, C. Haefs, and G. Plum, “Transposition of Tn5367 in Mycobacterium marinum, Using a Conditionally Recombinant Mycobacteriophage,” *J. Bacteriol.*, vol. 185, no. 5, pp. 1745–1748, Mar. 2003, doi: 10.1128/JB.185.5.1745-1748.2003.
[65] N. B. Harris, Z. Feng, X. Liu, S. L. G. Cirillo, J. D. Cirillo, and R. G. Barletta, “Development of a transposon mutagenesis system for Mycobacterium avium subsp. paratuberculosis,” *FEMS Microbiol. Lett.*, vol. 175, no. 1, pp. 21–26, Jun. 1999, doi: 10.1016/S0378-1097(99)00170-6.
[66] L.-Y. Gao, R. Groger, J. S. Cox, S. M. Beverley, E. H. Lawson, and E. J. Brown, “Transposon Mutagenesis of Mycobacterium marinum Identifies a Locus Linking Pigmentation and Intracellular Survival,” *Infect. Immun.*, vol. 71, no. 2, pp. 922–929, Feb. 2003, doi: 10.1128/IAI.71.2.922-929.2003.
[67] G. Rathnaiah *et al.*, “Analysis of Mycobacterium avium subsp. paratuberculosis mutant libraries reveals loci-dependent transposition biases and strategies for novel mutant discovery,” *Microbiology*, vol. 162, no. 4, pp. 633–641, Apr. 2016, doi: 10.1099/mic.0.000258.
[68] William C. Budell, “Transposon mutagenesis in Mycobacterium kansasii links a small RNA gene to colony morphology and biofilm formation and identifies 9,885 intragenic insertions that do not compromise colony outgrowth.”
[69] Eveline M Weerdenburg, “Genome-wide transposon mutagenesis indicates that Mycobacterium marinum customizes its virulence mechanisms for survival and replication in different hosts. | Sigma-Aldrich.” https://www.sigmaaldrich.com/catalog/papers/25690095 (accessed Sep. 03, 2020).

[70] Y. Tateishi *et al.*, “Genome-wide identification of essential genes in Mycobacterium intracellulare by transposon sequencing - Implication for metabolic remodeling,” *Sci. Rep.*, vol. 10, no. 1, p. 5449, 25 2020, doi: 10.1038/s41598-020-62287-2.
[71] G. A. Cangelosi, J. S. Do, R. Freeman, J. G. Bennett, M. Semret, and M. A. Behr, “The Two-Component Regulatory System mtrAB Is Required for Morphotypic Multidrug Resistance in Mycobacterium avium,” *Antimicrob. Agents Chemother.*, vol. 50, no. 2, pp. 461–468, Feb. 2006, doi: 10.1128/AAC.50.2.461-468.2006.
[72] R. K. Taylor, V. L. Miller, D. B. Furlong, and J. J. Mekalanos, “Use of phoA gene fusions to identify a pilus colonization factor coordinately regulated with cholera toxin.,” *Proc. Natl. Acad. Sci.*, vol. 84, no. 9, pp. 2833–2837, May 1987, doi: 10.1073/pnas.84.9.2833.
[73] P. Katoch, K. Gupta, R. M. Yennamalli, J. Vashistt, G. S. Bisht, and R. Shrivastava, “Random insertion transposon mutagenesis of Mycobacterium fortuitum identified mutant defective in biofilm formation,” *Biochem. Biophys. Res. Commun.*, vol. 521, no. 4, pp. 991–996, Jan. 2020, doi: 10.1016/j.bbrc.2019.11.021.
[74] Igor Y. Goryshin, “Insertional transposon mutagenesis by electroporation of released Tn5 transposition complexes | Nature Biotechnology.” https://www.nature.com/articles/nbt0100_97 (accessed Sep. 04, 2020).
[75] Collins DM, “Generation of attenuated Mycobacterium bovis strains by signature-tagged mutagenesis for discovery of novel vaccine candidates. - Abstract - Europe PMC.” http://europepmc.org/article/PMC/1087418 (accessed Sep. 04, 2020).
[76] T. Wilson, B. J. Wards, S. J. White, B. Skou, G. W. de Lisle, and D. M. Collins, “Production of avirulent Mycobacterium bovis strains by illegitimate recombination with deoxyribonucleic acid fragments containing an interrupted ahpC gene,” *Tuber. Lung Dis. Off. J. Int. Union Tuberc. Lung Dis.*, vol. 78, no. 5–6, pp. 229–235, 1997, doi: 10.1016/s0962-8479(97)90003-4.
[77] A. M. Talaat and M. Trucksis, “Transformation and transposition of the genome of Mycobacterium marinum,” *Am. J. Vet. Res.*, vol. 61, no. 2, pp. 125–128, Feb. 2000, doi: 10.2460/ajvr.2000.61.125.
[78] N. Baltes *et al.*, “Conferring resistance to geminiviruses with the CRISPR–Cas prokaryotic immune system,” *Nat. Plants*, vol. 1, p. 15145, Sep. 2015, doi: 10.1038/nplants.2015.145.
[79] M. H. Larson, L. A. Gilbert, X. Wang, W. A. Lim, J. S. Weissman, and L. S. Qi, “CRISPR interference (CRISPRi) for sequence-specific control of gene expression,” *Nat. Protoc.*, vol. 8, no. 11, pp. 2180–2196, Nov. 2013, doi: 10.1038/nprot.2013.132.
[80] J. Xiao *et al.*, “Application of the CRISPRi system to repress sepF expression in Mycobacterium smegmatis,” *Infect. Genet. Evol. J. Mol. Epidemiol. Evol. Genet. Infect. Dis.*, vol. 72, pp. 183–190, 2019, doi: 10.1016/j.meegid.2018.06.033.
[81] S. B, Y. J, Y. S, Y. Rd, C. D, and J. Y, “A CRISPR-Cpf1-Assisted Non-Homologous End Joining Genome Editing System of Mycobacterium smegmatis.,” *Biotechnol. J.*, vol. 13, no. 9, pp. e1700588–e1700588, Aug. 2018, doi: 10.1002/biot.201700588.
[82] Eira Choudhary, “Gene silencing by CRISPR interference in mycobacteria | Nature Communications.” https://www.nature.com/articles/ncomms7267 (accessed Oct. 05, 2020).
[83] M.-Y. Yan, S.-S. Li, X.-Y. Ding, X.-P. Guo, Q. Jin, and Y.-C. Sun, “A CRISPR-Assisted Nonhomologous End-Joining Strategy for Efficient Genome Editing in Mycobacterium tuberculosis,” *mBio*, vol. 11, no. 1, 28 2020, doi: 10.1128/mBio.02364-19.
[84] M.-Y. Yan, H.-Q. Yan, G.-X. Ren, J.-P. Zhao, X.-P. Guo, and Y.-C. Sun, “CRISPR-Cas12a-Assisted Recombineering in Bacteria,” *Appl. Environ. Microbiol.*, vol. 83, no. 17, Sep. 2017, doi: 10.1128/AEM.00947-17.
[85] M. Pandey, S. Talwar, S. Bose, and A. K. Pandey, “Iron homeostasis in Mycobacterium tuberculosis is essential for persistence,” *Sci. Rep.*, vol. 8, no. 1, p. 17359, Dec. 2018, doi: 10.1038/s41598-018-35012-3.
[86] J. Pérard and S. Ollagnier de Choudens, “Iron-sulfur clusters biogenesis by the SUF machinery: close to the molecular mechanism understanding,” *J. Biol. Inorg. Chem. JBIC Publ. Soc. Biol. Inorg. Chem.*, vol. 23, no. 4, pp. 581–596, Jun. 2018, doi: 10.1007/s00775-017-1527-3.
[87] A. D. Tsaousis, E. Gentekaki, L. Eme, D. Gaston, and A. J. Roger, “Evolution of the Cytosolic Iron-

Sulfur Cluster Assembly Machinery in Blastocystis Species and Other Microbial Eukaryotes," *Eukaryot. Cell*, Nov. 2013, Accessed: Feb. 04, 2022. [Online]. Available: https://journals.asm.org/doi/abs/10.1128/EC.00158-13

[88] C. A. Roberts *et al.*, "The Suf Iron-Sulfur Cluster Biosynthetic System Is Essential in Staphylococcus aureus, and Decreased Suf Function Results in Global Metabolic Defects and Reduced Survival in Human Neutrophils," *Infect. Immun.*, vol. 85, no. 6, pp. e00100-17, Jun. 2017, doi: 10.1128/IAI.00100-17.

[89] M. R. Jacobson, V. L. Cash, M. C. Weiss, N. F. Laird, W. E. Newton, and D. R. Dean, "Biochemical and genetic analysis of the nifUSVWZM cluster from Azotobacter vinelandii," *Mol. Gen. Genet. MGG*, vol. 219, no. 1–2, pp. 49–57, Oct. 1989, doi: 10.1007/BF00261156.

[90] R. Lill, "Function and biogenesis of iron-sulphur proteins," *Nature*, vol. 460, no. 7257, pp. 831–838, Aug. 2009, doi: 10.1038/nature08301.

[91] Y. Takahashi and U. Tokumoto, "A third bacterial system for the assembly of iron-sulfur clusters with homologs in archaea and plastids," *J. Biol. Chem.*, vol. 277, no. 32, pp. 28380–28383, Aug. 2002, doi: 10.1074/jbc.C200365200.

[92] A. A. Mashruwala, S. Bhatt, S. Poudel, E. S. Boyd, and J. M. Boyd, "The DUF59 Containing Protein SufT Is Involved in the Maturation of Iron-Sulfur (FeS) Proteins during Conditions of High FeS Cofactor Demand in Staphylococcus aureus," *PLOS Genet.*, vol. 12, no. 8, p. e1006233, Aug. 2016, doi: 10.1371/journal.pgen.1006233.

[93] T. Tamuhla, L. Joubert, D. Willemse, and M. J. Y. 2020 Williams, "SufT is required for growth of Mycobacterium smegmatis under iron limiting conditions," *Microbiology*, vol. 166, no. 3, pp. 296–305, doi: 10.1099/mic.0.000881.

[94] L. A. Marraffini and E. J. Sontheimer, "CRISPR interference limits horizontal gene transfer in staphylococci by targeting DNA," *Science*, vol. 322, no. 5909, pp. 1843–1845, Dec. 2008, doi: 10.1126/science.1165771.

[95] V. Faulkner *et al.*, "Re-sensitization of Mycobacterium smegmatis to Rifampicin Using CRISPR Interference Demonstrates Its Utility for the Study of Non-essential Drug Resistance Traits," *Front. Microbiol.*, vol. 11, p. 619427, 2020, doi: 10.3389/fmicb.2020.619427.

[96] B. D. Janssen, Y.-P. Chen, B. M. Molgora, S. E. Wang, A. Simoes-Barbosa, and P. J. Johnson, "CRISPR/Cas9-mediated gene modification and gene knock out in the human-infective parasite Trichomonas vaginalis," *Sci. Rep.*, vol. 8, no. 1, Art. no. 1, Jan. 2018, doi: 10.1038/s41598-017-18442-3.

[97] E. Deltcheva *et al.*, "CRISPR RNA maturation by trans-encoded small RNA and host factor RNase III," *Nature*, vol. 471, no. 7340, pp. 602–607, Mar. 2011, doi: 10.1038/nature09886.

[98] A. V. Wright, J. K. Nuñez, and J. A. Doudna, "Biology and Applications of CRISPR Systems: Harnessing Nature's Toolbox for Genome Engineering," *Cell*, vol. 164, no. 1, pp. 29–44, Jan. 2016, doi: 10.1016/j.cell.2015.12.035.

[99] D. Bikard, W. Jiang, P. Samai, A. Hochschild, F. Zhang, and L. A. Marraffini, "Programmable repression and activation of bacterial gene expression using an engineered CRISPR-Cas system," *Nucleic Acids Res.*, vol. 41, no. 15, pp. 7429–7437, Aug. 2013, doi: 10.1093/nar/gkt520.

[100] "SufT is required for growth of Mycobacterium smegmatis under iron limiting conditions. - PubMed - NCBI." https://www.ncbi.nlm.nih.gov/pubmed/31860439 (accessed Mar. 11, 2020).

[101] A. Ojha and G. F. Hatfull, "The role of iron in Mycobacterium smegmatis biofilm formation: the exochelin siderophore is essential in limiting iron conditions for biofilm formation but not for planktonic growth," *Mol. Microbiol.*, vol. 66, no. 2, pp. 468–483, Oct. 2007, doi: 10.1111/j.1365-2958.2007.05935.x.

[102] J. A. Gonzalez-y-Merchand *et al.*, "Evaluation of the cell growth of mycobacteria using Mycobacterium smegmatis mc2 155 as a representative species," *J. Microbiol.*, vol. 50, no. 3, pp. 419–425, Jun. 2012, doi: 10.1007/s12275-012-1556-0.

[103] M. B. Gochnauer and D. J. Kushner, "Growth and nutrition of extremely halophilic bacteria," *Can. J. Microbiol.*, vol. 15, no. 10, pp. 1157–1165, Oct. 1969, doi: 10.1139/m69-211.

[104] N. Nandanwar, J. E. Gibson, and M. N. Neely, "Growth medium and nitric oxide alter

Mycobacterium abscessus morphotype and virulence," *Microbiol. Res.*, vol. 253, p. 126887, Dec. 2021, doi: 10.1016/j.micres.2021.126887.
[105] S.-H. Tsai, H.-C. Lai, and S.-T. Hu, "Subinhibitory Doses of Aminoglycoside Antibiotics Induce Changes in the Phenotype of Mycobacterium abscessus," *Antimicrob. Agents Chemother.*, vol. 59, no. 10, pp. 6161–6169, Oct. 2015, doi: 10.1128/AAC.01132-15.
[106] F. M. Oliveira *et al.*, "Mycobacterium abscessus subsp. massiliense mycma_0076 and mycma_0077 Genes Code for Ferritins That Are Modulated by Iron Concentration," *Front. Microbiol.*, vol. 9, p. 1072, 2018, doi: 10.3389/fmicb.2018.01072.
[107] S. Rondini, E. Mensah-Quainoo, H. Troll, T. Bodmer, and G. Pluschke, "Development and Application of Real-Time PCR Assay for Quantification of Mycobacterium ulcerans DNA," *J. Clin. Microbiol.*, vol. 41, no. 9, pp. 4231–4237, Sep. 2003, doi: 10.1128/JCM.41.9.4231-4237.2003.
[108] X. Liu *et al.*, "High-throughput CRISPRi phenotyping identifies new essential genes in Streptococcus pneumoniae," *Mol. Syst. Biol.*, vol. 13, no. 5, p. 931, May 2017, doi: 10.15252/msb.20167449.
[109] C. Akusobi *et al.*, "High-density transposon mutagenesis in Mycobacterium abscessus identifies an essential penicillin-binding lipo-protein (PBP-lipo) involved in septal peptidoglycan synthesis and antibiotic sensitivity." bioRxiv, p. 2021.07.01.450732, Jul. 03, 2021. doi: 10.1101/2021.07.01.450732.
[110] B. Bosch *et al.*, "Genome-wide gene expression tuning reveals diverse vulnerabilities of M. tuberculosis," *Cell*, vol. 184, no. 17, pp. 4579-4592.e24, Aug. 2021, doi: 10.1016/j.cell.2021.06.033.
[111] L. Marsollier *et al.*, "Early trafficking events of Mycobacterium ulcerans within Naucoris cimicoides," *Cell. Microbiol.*, vol. 9, no. 2, pp. 347–355, 2007, doi: 10.1111/j.1462-5822.2006.00790.x.
[112] L. Hall-Stoodley, J. W. Costerton, and P. Stoodley, "Bacterial biofilms: from the Natural environment to infectious diseases," *Nat. Rev. Microbiol.*, vol. 2, no. 2, Art. no. 2, Feb. 2004, doi: 10.1038/nrmicro821.
[113] E. Banin, M. L. Vasil, and E. P. Greenberg, "Iron and Pseudomonas aeruginosa biofilm formation," *Proc. Natl. Acad. Sci. U. S. A.*, vol. 102, no. 31, pp. 11076–11081, Aug. 2005, doi: 10.1073/pnas.0504266102.
[114] J. J. De Voss, K. Rutter, B. G. Schroeder, H. Su, Y. Zhu, and C. E. Barry, "The salicylate-derived mycobactin siderophores of Mycobacterium tuberculosis are essential for growth in macrophages," *Proc. Natl. Acad. Sci. U. S. A.*, vol. 97, no. 3, pp. 1252–1257, Feb. 2000.
[115] P. Chakraborty and A. Kumar, "The extracellular matrix of mycobacterial biofilms: could we shorten the treatment of mycobacterial infections?," *Microb. Cell*, vol. 6, no. 2, pp. 105–122, doi: 10.15698/mic2019.02.667.
[116] "Defining a temporal order of genetic requirements for development of mycobacterial biofilms - PubMed." https://pubmed.ncbi.nlm.nih.gov/28628249/ (accessed Jan. 26, 2022).
[117] L. A. Miles, R. J. Garippa, and J. T. Poirier, "Design, execution, and analysis of pooled in vitro CRISPR/Cas9 screens," *FEBS J.*, vol. 283, no. 17, pp. 3170–3180, 2016, doi: 10.1111/febs.13770.
[118] S. H. Joo, Q. Xiao, Y. Ling, B. Gopishetty, and D. Pei, "High-Throughput Sequence Determination of Cyclic Peptide Library Members by Partial Edman Degradation/Mass Spectrometry," *J. Am. Chem. Soc.*, vol. 128, no. 39, pp. 13000–13009, Oct. 2006, doi: 10.1021/ja063722k.

4.2: Appendix 1

Table 10: The RIN values for RNA samples extracted for 3 biological replicates

Samples	ATc	Replicate 1	Replicate 2	Replicate 3
M. abscessus attB:: pLJR962 ATc	+ ATc	7.9	9.8	9.0
M. abscessus attB:: pLJR962-2744c-a ATc	+ ATc	9.9	9.5	9.1
M. abscessus attB:: pLJR962-2744c-b ATc	+ ATc	8.7	9.2	9.2
M. abscessus attB:: pLJR962-2745c-a ATc	+ ATc	8.4	9.9	9.0
M. abscessus attB:: pLJR962-2745c-b ATc	+ ATc	8.6	9.6	8.8
M. abscessus attB:: pLJR962 No ATc	- ATc	8.6	10	9.3
M. abscessus attB:: pLJR962-2744c-a No ATc	- ATc	9.6	9.7	8.8

M. abscessus attB:: pLJR962-2744c-b No ATc	- ATc	8.4	9.7	9.3
M. abscessus attB:: pLJR962-2745c-a No ATc	- ATc	8.5	9.2	9.2
M. abscessus attB:: pLJR962-2745c-b No ATc	- ATc	8.9	9	8.9

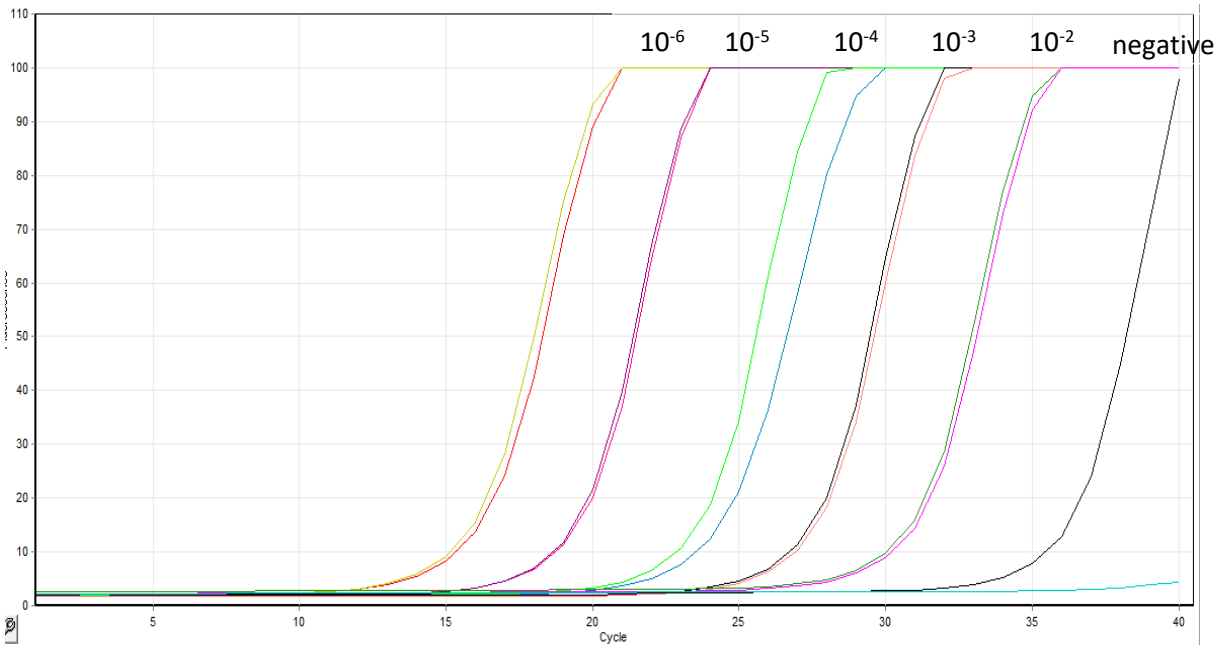

Figure 4. 1: **Showing PCR optimized standard curves for *sigA*.**

The standards were run as duplicate dilutions that ranged from 10^6 to 10^{2} The no template control showed no amplification.

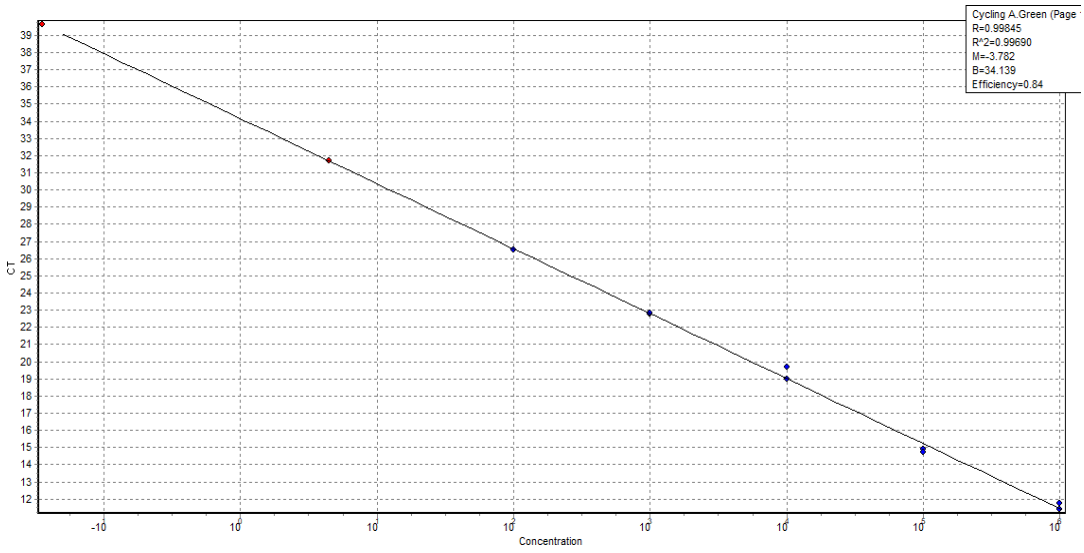

Figure 4. 2: Showing the optimal standard curve for the *sigA*.

The standards 10^{-6}, 10^{-5}, 10^{-4}, 10^{-3} and 10^{-2} were used, the cycle threshold was plotted against the concentration. The optimal R^2 value is 0.99 (2 decimal places).

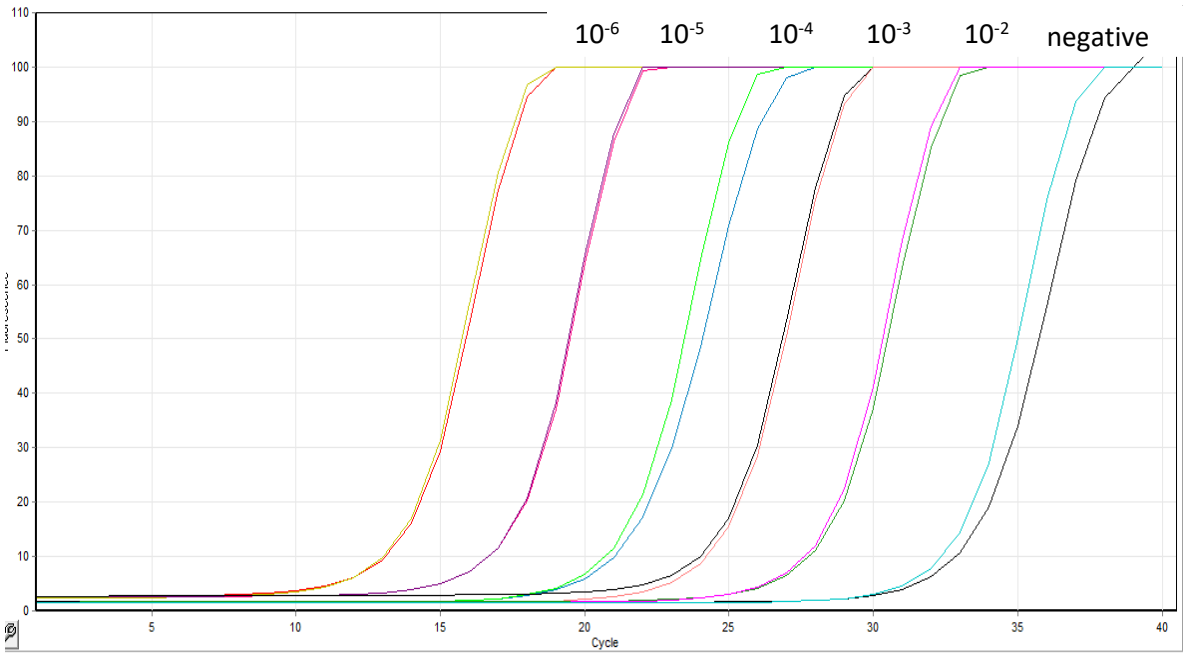

Figure 4. 3: Showing PCR optimized standard curves for *MAB_2744c*.

The standards were run as duplicate dilutions that ranged from 10^{6} to 10^{2}. The no template control showed no amplification.

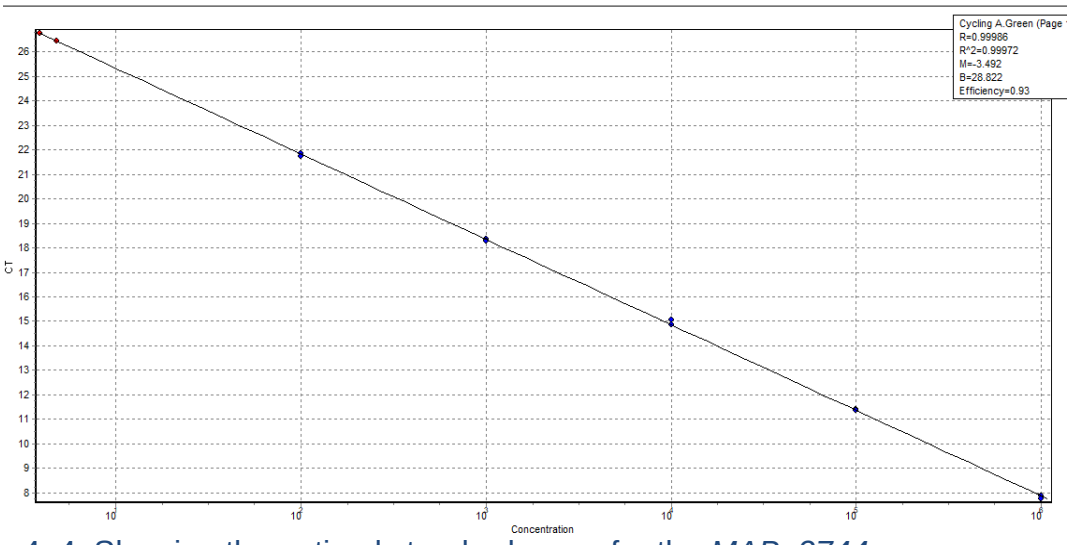

Figure 4. 4: Showing the optimal standard curve for the *MAB_2744c*.

The standards 10^{-6}, 10^{-5}, 10^{-4}, 10^{-3} and 10^{-2} were used and the cycle threshold was plotted against the concentration. The optimal R^2 value is 0.99 (2 decimal places).